Control and Optimization of Future Electric Grid Integrating Plug-In Electric Vehicles and Wind Power

by

Chiao-Ting Li

A dissertation submitted in partial fulfillment
of the requirements for the degree of
Doctor of Philosophy
(Mechanical Engineering)
in the University of Michigan
2013

Doctoral Committee:

Professor Huei Peng, Co-Chair
Professor Jing Sun, Co-Chair
Assistant Professor Branko Kerkez
Professor Jeffrey L. Stein
Professor Dawn M. Tilbury

ACKNOWLEDGMENTS

I would like to express my gratitude to both of my advisors, Professor Huei Peng and Professor Jing Sun. Their guidance and encouragement have been enormous to my research and the completion of this dissertation, and their patience and supports have never been absence especially when time was hard. I would also like to thank my other committee members, Professor Branko Kerkez, Professor Jeffrey Stein, and Professor Dawn Tilbury, for their advice. Their comments on my work will remind me to think wide, broad and holistic while attending the details.

I am indebted to the people, with whom I work together in the NSF EFRI-RESIN Project. They are Professor Ian Hiskens, Professor Greg Keoleian, Professor Mariesa Crow, Dr. Tulga Ersal, Dr. Jarod Kelly, Brandon Marshall, Dr. Joel Forman, Dr. Rakesh Patil, Dr. Changsun Ahn, and Dr. Tae-Kyung Lee. Their inputs and suggestions are helpful and have enriched my research. In addition, I would like to acknowledge the EFRI project for the financial supports for my graduate study.

Also, I would like to thank my colleagues in the Vehicle Dynamics Lab: Jong-Hwa Yoon, Byung-Joo Kim, William Smith, Xiaowu Zhang, Tianyou Guo, Ding Zhou, Ziheng Pan. I shall never forget their help, assistance, and all the good times we have had in the office.

Lastly, my deepest thanks go to my family. They grant me a strong mind to walk through storms, and they have companied me through my journey of perusing the Ph.D.

TABLE OF CONTENTS

LIST OF FIGURES

LIST OF TABLES

LIST OF APPENDICES

ABSTRACT

Control and Optimization of Future Electric Grid Integrating Plug-In Electric Vehicles and Wind Power

by

Chiao-Ting Li

Co-Chairs: Huei Peng and Jing Sun

This dissertation studies the integration and control problems that will arise when large numbers of plug-in electric vehicles (PEVs) and wind power are introduced to the electric grid. Various control and optimization techniques are developed in this dissertation to harnesses the synergy between PEVs and wind power to facilitate the grid operations.

First, a PEV charging control algorithm is developed to utilize the idle generating capacity in evening hours to charge of the newly introduced PEVs on the future Michigan grid. The control algorithm adopts a partially-decentralized structure, so that its implementation does not require excessive computation and communication. At the global level, a SOC threshold command is calculated and broadcasted to all PEVs as the basis of charging level. At each charger, two attributes of individual PEVs, the battery state of charge and plug-off time, are considered to calculate the final charging power. The proposed algorithm allows most PEVs to be fully charged. In the meantime, the grid-level objective "valley filling" is achieved. The algorithm also includes a feedback mechanism to regulate grid frequency to explore the potential of manipulating PEV charging to replace conventional reserves in the valley hours.

Secondly, this dissertation investigates means to mitigate wind power intermittency. Model predictive control (MPC) is used to control the charging and discharging of battery energy storage system (BESS) to provide reserves. Unlike existing MPC studies that focused on state tracking or output regulation, realistic objective

functions that capture the reserve costs to cover wind surplus or deficit are used. The effect of BESS capacity sizing is also investigated.

Thirdly, to accommodate both PEVs and wind power on the grid, a hierarchical control algorithm is proposed. The control algorithm has three levels. The top-level controller solves a scheduling optimization problem to minimize the grid-wide cost of electricity generation. The middle- and bottom-level controllers are based on the control algorithms previously developed for PEV charging and wind power scheduling. The hierarchical structure allows the features in the different control algorithms to be preserved.

Next, a carbon disincentive policy is proposed to promote the use of low-carbon power plants for electricity generation to reduce grid CO_2 emissions. The proposed policy can be used to adjust the carbon content in the generation mix, and the tradeoff between the generation costs and grid CO_2 emissions is investigated. Analyses show that introducing wind generation can significantly reduce the electricity generation costs, but not grid CO_2 emissions if no PEVs are available to mitigate wind intermittency. To address both the generation costs and CO_2 emissions, manipulations in both the supply and demand on the grid are needed.

Lastly, the generation planning problem is studied. A systematic methodology is proposed to evaluate the cost of constructing different types of generating capacities. The methodology considers the evolutions in both the supply and demand of the electric grid, including annual increases in the grid load and changes in the merit order when new power plants are commissioned. Furthermore, the renewable intermittency and reserve-related costs are also considered, which are new features not seen in the literature. Based on the used assumptions, the cost evaluation identifies the construction cost as the bottleneck that prevents wind power from entering the market, although the wind intermittency can be addressed by BESS or PEVs on the operation stage.

The modeling and optimization framework developed in this dissertation makes it possible to study the synergy between PEVs and wind power on the electric grid. Simulation results show that PEVs and wind power are complementary to each other, and a proper integration is needed to realize their full potential.

CHAPTER 1
Introduction

1.1 Motivation

Electricity generation and transportation are the two largest energy consumption sectors in the U.S. As can be seen from Figure 1.1, in 2011 alone, they are responsible for 68% of the total energy use. In addition, most of the energy used in these two sectors comes from non-renewable sources. Figure 1.1 shows that 87% of the energy used in electricity generation and 96% in the transportation sector are non-renewable. These non-renewable fossil fuels create significant carbon emissions. Figure 1.2 shows that, in 2010, transportation and electricity generation were responsible for 73% of CO_2 emissions in the U.S. Thus, there are urgent needs to find sustainable and cost-effective ways to reduce the energy consumption and environment impacts of these two sectors.

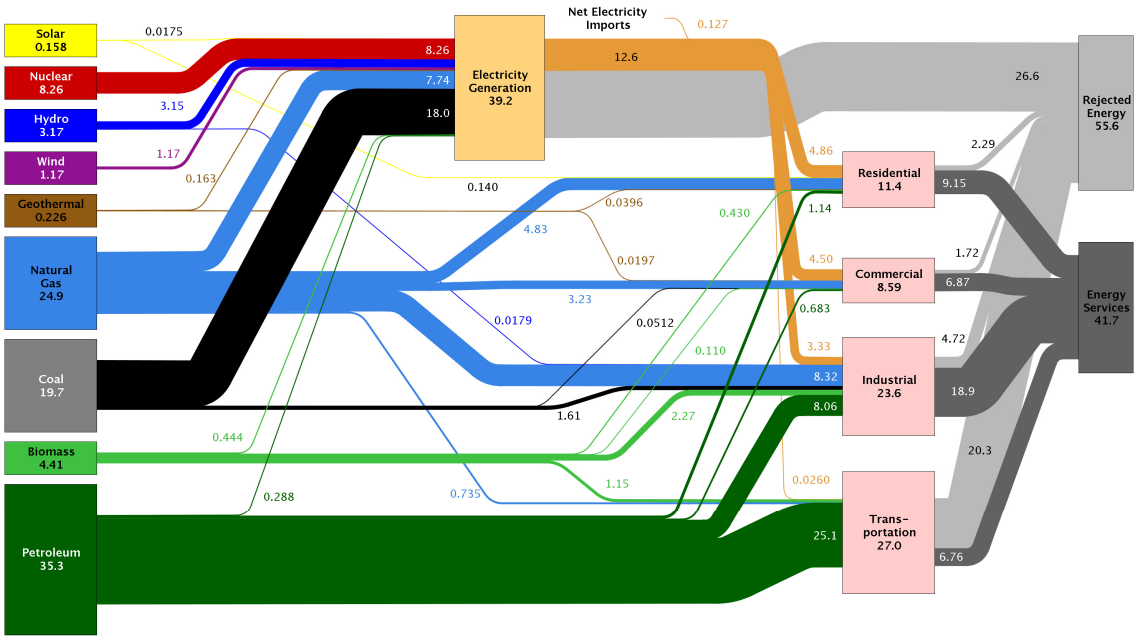

Figure 1.1 The U.S. energy use in 2011 (quadrillion BTU) [1]

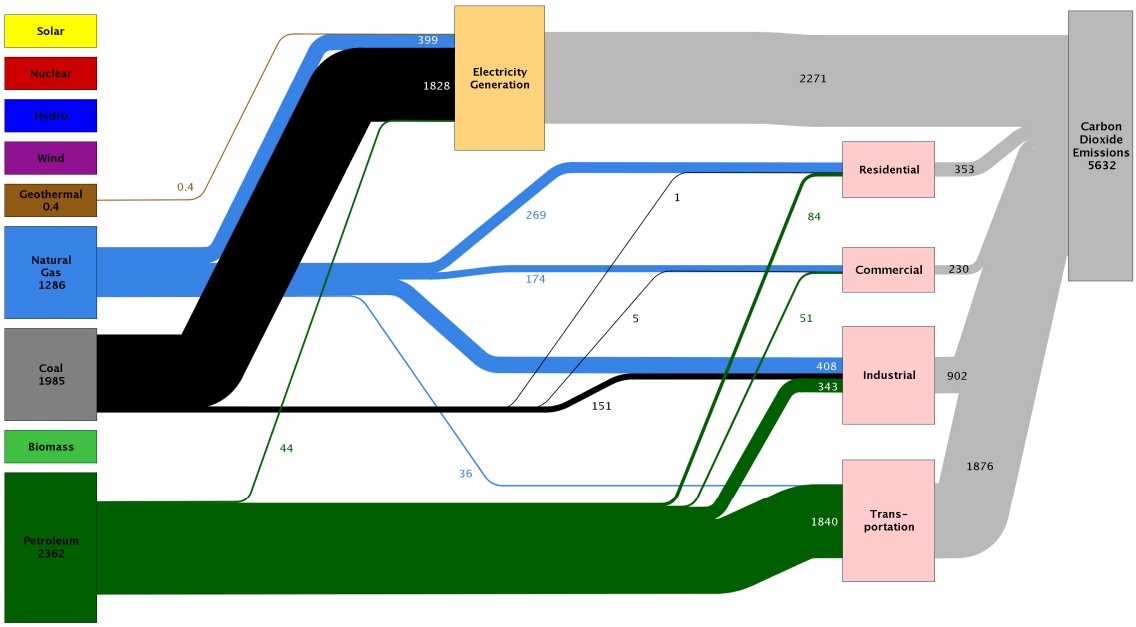

Figure 1.2 The U.S. energy-related CO_2 emissions in 2010 (million metric tons) [2]

In response to the growing demands of electricity usage and transportation, researchers are seeking solutions from many angles. There are legislations to require cleaner and more efficient operations of electric utility companies and automakers. For example, the American Clean Energy and Security Act of 2009 requires electric utilities to have 20% of their sales generated by renewable sources by 2020 [3] and the Obama Administrative announced the new CAFE standards in 2011 with the target to increase the automotive fleet fuel economy from 25.3 mpg to 54.5 mpg by 2025 [4]. In addition, many states in the U.S. have Renewable Portfolio Standards with targets of energy production from renewable sources (see Figure 1.3). In 2012, renewable energy accounted for 49.1% of all new U.S. electricity generating capacity installed, according to the latest update from the Federal Energy Regulatory Commission (FERC). Therefore, renewable sources now account for 15.4% of total installed U.S. generating capacity, which is more than nuclear (9.24%) and oil (3.57 %) combined [5]. Furthermore, electric utilities are initiating grid reform, such as variable pricing, advanced metering systems, and load-side controls to better accommodate renewable generation. Automakers are actively pursuing high-efficiency vehicle technologies, such as diesel engines, start-stop, alternative fuels, and hybrid vehicles. Plug-in electric vehicles (PEVs) in particular receive a lot of attention. PEVs are expected to leverage the electrified powertrain

technologies with larger battery packs to enable all-electric or blended driving so that less fossil fuel and more electric energy can be used in the transportation sector. The increased awareness from the public also stimulates the penetration of clean technologies into electricity generation and transportation.

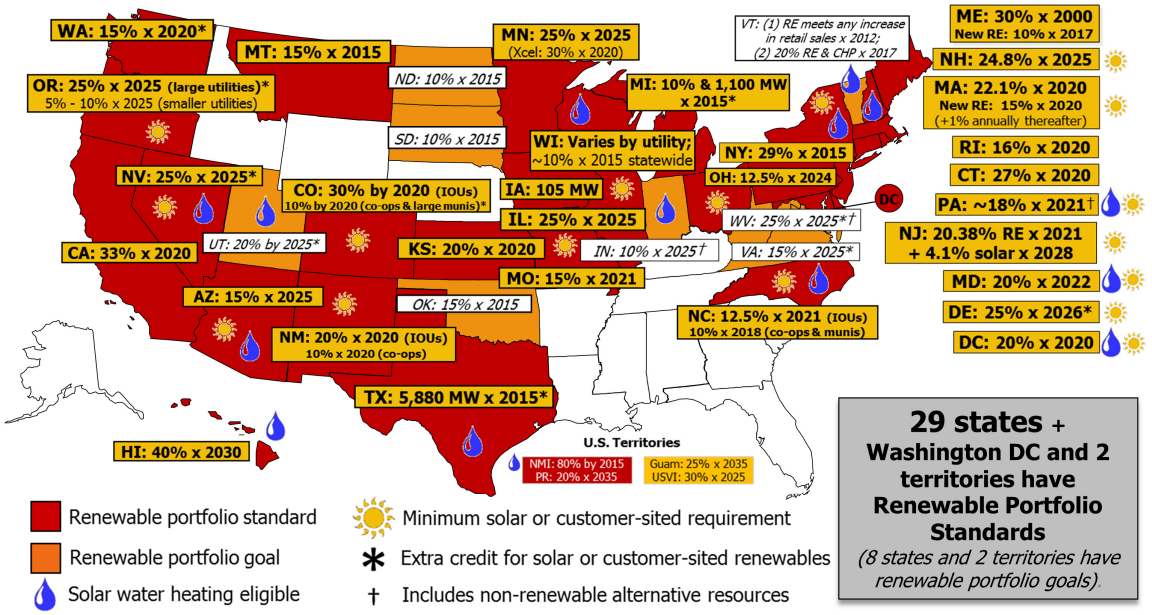

Figure 1.3 Renewable portfolio standards in the U.S. (adopted from [6])

With the favorable governmental and industry driving forces described above, PEVs and renewable energy sources are expected to gain popularity and drastically change the supply and demand on the electric grid. Although PEV charging will add additional load to the grid, if the charging is properly controlled, the presence of PEVs can have a positive impact to the grid. This dissertation focuses on studying wind power as the representative renewable energy source, as it is one of the fastest-growing renewable generating capacities on the grid and has the installation costs low enough to be comparable to coal-fired power plants [7, 8]. Furthermore, the fact that wind power sources are available overnight makes it more suitable than solar power for PEV charging. However, wind intermittency will increase electricity generation uncertainties, which needs to be properly addressed in the grid operation. In addition to their individual features, PEVs and wind power have significant synergy: PEVs can serve as a demand response to mitigate the intermittent wind generation, and wind power can provide low-

carbon electricity to PEVs. PEVs will also significantly change the ground transportation sector, but the focus of this dissertation will mainly be on the electric grid. This dissertation tackles challenges of incorporating large numbers of PEVs and wind power on the electric grid via control and optimization techniques. It also presents solutions to integrate PEV charging and wind power dispatch on the electric grid. Those solutions include charging control, grid frequency regulation, electricity generation costs minimization, and grid CO_2 emission reduction.

1.2 Background

This chapter summarizes background information on PEV charging, operation of the electricity market, attributes of renewable energy, and challenges associated with high penetrations of PEVs and wind power on the grid.

1.2.1 Plug-in Electric Vehicles

A key feature of PEVs is that they have much larger battery capacities than hybrid vehicles, which enables electric-only driving. The all-electric range (AER) is a main attribute of PEVs. Long AER is highly correlated to better fuel economy on the EPA label and lower tailpipe emissions. In addition to recovering kinetic energy through regenerative braking during driving, PEVs often need to plug into household outlets or designated chargers to recharge their batteries. Though there is an improvement in fuel economy and tailpipe emissions during the driving phase, reduction in carbon footprint is not guaranteed. PEVs might have higher carbon footprints if the electricity from the grid is produced by coal-firing plants. Therefore, the development of PEVs and the deployment of renewable energy should proceed simultaneously for PEVs to be a sensible and sustainable solution for future ground transportation.

Battery sizing and the onboard power management are aspects related to PEV charging. Sizing the battery capacity for PEVs is an important design problem because the battery capacity affects the AER. In addition, the battery is still fairly expensive, so the battery size significantly affects the vehicle cost. Furthermore, battery size and weight are important packaging issues in vehicle integration. Battery capacity also affects the charging time. As PEV penetration increases, the PEV charging demand will be more

substantial and influential to the grid operation. Table 1.1 is a list of recent PEV and electric vehicle models available in the U.S. They come in various battery capacities, and many studies have investigated battery sizing for PEVs [9-14]. With battery capacity significantly larger than non-plug-in hybrid vehicles, PEVs require different power management [15]. Several optimization methods have been used to solve the PEV power management problem, and it is generally recognized that the blending strategy is more efficient than the CDCS (charge-depletion, charge-sustaining) strategy [16-19] when the driving range is known *a priori*.

Despite of the fact that battery sizing is an important design decision, battery sizing and power management are not going to be studied in this dissertation. All PEVs are assumed to have a given size of 16kWh (the same size as the 2013 Chevrolet Volt) in this dissertation. In addition, instead of making assumptions on power management, the EPA rated fuel economy listed in Table 1.1 will be used to assess the battery use during driving.

Table 1.1 PEVs and EVs in the U.S. Market by January 2013 [20-22]

Vehicle	Year Model	Operating Mode	EPA Rated All-Electric Range	EPA Rated Fuel Economy	Battery Capacity
Chevrolet Volt	2012	Plug-in Hybrid	38 mi	98 mpg-e (34 kWh/100 mi)	16 kWh
Fisker Karma	2012	Plug-in Hybrid	20 mi	54 mpg-e (62 kWh/100 mi)	20 kWh
Ford C-Max Energi Plug-in Hybrid	2013	Plug-in Hybrid	21 mi	100 mpg-e (34 kWh/100 mi)	7.6 kWh
Ford Fusion Energi Plug-in Hybrid	2013	Plug-in Hybrid	21 mi	100 mpg-e (34 kWh/100 mi)	7.6 kWh
Toyota Prius Plug-in Hybrid	2012	Plug-in Hybrid	11 mi	95 mpg-e (35 kWh/100 mi)	4.4 kWh
Nissan Leaf	2011	All-electric	73 mi	99 mpg-e (34 kWh/100 mi)	24 kWh
Tesla model S	2012	All-electric	265 mi	89 mpg-e (38 kWh/100 mi)	85 kWh
Coda	2012	All-electric	88 mi	73 mpg-e (46 kWh/100 mi)	31 kWh

Ford Focus EV	2012	All-electric	76 mi	99 mpg-e (34 kWh/100 mi)	23 kWh
Mitsubishi i-MiEV	2013	All-electric	62 mi	99 mpg-e (34 kWh/100 mi)	16 kWh
Fiat 500e	2013	All-electric	87 mi	116 mpg-e (29 kWh/100 mi)	31 kWh
Honda Fit EV	2012	All-electric	82 mi	118 mpg-e (29 kWh/100 mi)	20 kWh
Scion iQ EV	2013	All-electric	38 mi	121 mpg-e (28 kWh/100 mi)	12 kWh
Smart ED	2013	All-electric	68 mi	107 mpg-e (32 kWh/100 mi)	17.6 kWh
Toyota Prius	2012	Hybrid	N/A	50 mpg	1.4 kWh
Average U.S. new car	2013	Gasoline only	N/A	24.5 mpg [23]	N/A

The charging infrastructure is another factor affecting the PEV charging. The charging system includes the charging station, interface, and the charging protocols. Siting and cost are two major barriers to the popularity of charging stations. The siting concerns include parking availability, safety, permits, and installation costs. Cost estimates for installing PEV chargers are shown in Figure 1.4, and the interface and hardware specifications are summarized in Table 1.2. More details can be found in the SAE J1772 [24] and IEC 62196 standards [25]. In this dissertation, it is assumed that all PEV owners will opt for the Level-1 charger at home as it is the cheapest option, which, however, imposes greater challenge in charging control because of the longer charging time. It is also assumed that all PEVs are demand response, meaning their power demand is controllable, and can be slowed or stopped if deemed necessary. However, the V2G (vehicle-to-grid) power flow is disallowed because frequent cycling reduces battery longevity.

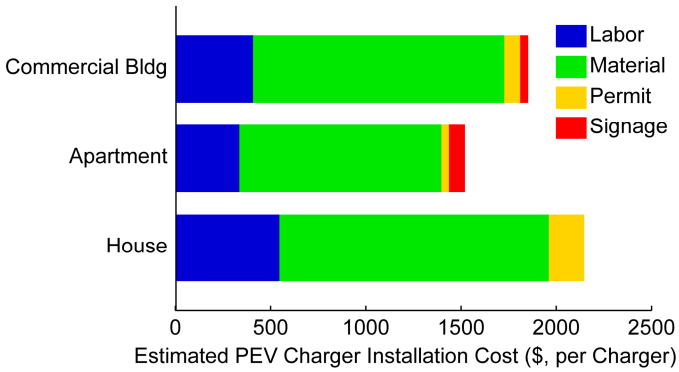

Figure 1.4 Estimated PEV Level-2 charger installation cost [26]

Table 1.2 PEV Charging Infrastructure [24-27]

	Level 1	**Level 2**	**DC Charging**
Voltage/Amperage	120 VAC/12A	240 VAC/40A	Under Development
Charging Power	1.44kW	3.3 kW (limited by vehicle)	
Charging Time for a 10kWh Battery	5-8 hours	1-2 hours	
Installation Cost Estimate (per Charger)	$878	House: $2,146 Apartment complex: $1,520 Commercial bldg.: $1,852	

PEVs will impact both the ground transportation sector and the electric grid because of the two-way power flow. In terms of the grid-to-vehicle (G2V) power flow, the fact that PEVs receive charging from the grid allows for a multiplicity of energy sources to be used in supplying power for PEVs—they can run on any type of energy as long as it is converted to electricity. This is a big leap toward petroleum displacement and energy sustainability. In terms of vehicle-to-grid (V2G) power flow, several studies have accessed the market potential of using PEV batteries to support grid operation [28-30]; however, as pointed out in above, due to concerns on battery longevity, V2G will not be considered in this dissertation. Last but not least, PEV owners benefit from the (equivalent) gas price of less than $1.00 per gallon [31]. Among the far-reaching impacts PEVs have, this dissertation focuses on PEVs' impacts to the electric grid.

1.2.2 Electricity Market

The electricity utility industry is less than one hundred years old, and the deregulated electricity market is an even more recent development [32]. Back in the time of the regulated electricity market before 1980, the electricity utility was owned and controlled by the government in a centralized fashion and there was no need for complicated coordination among power plants. The deregulation of electricity generation first happened in Chile in the early 1980's, and the U.S. gradually opened and privatized the electricity system in the mid 1990's. The motivation of deregulating the electricity market is the belief that the competition among privately-owned generation sellers and buyers can reduce the price and result in a more efficient operation. However, privatization fragments the electricity system, and coordination of generation scheduling and dispatch become a vital task in the grid operation.

The deregulated electricity market is run by an independent system operator (ISO), which is usually a governmental or non-profit agency that ensures security and reliability constraints are respected while maintaining least-cost operation. The ISO enforces different market rules for trading electricity generation and reserves.

The generation market is similar to the stock market: it is all about selling and buying. The ISO collects offers (bidding prices) from market participants (generation buyers and sellers) and clears the market price. The grid load (i.e. demand) prediction is of paramount importance because market participants rely on this information to adjust their bidding strategy and the ISO also clears the market price based on this information. The market clearing price is determined by solving a large-scale constrained optimization to minimize the total generation cost [33]; the various constraints include, but are not limited to, generation capacity, transmission line capacity, and ramping limits [34]. Bidding prices lower than the clearing price will be accepted and sellers, usually the power plant owners, receive payments if they fulfill the contract in their offers. Sellers are paid at the market clearing price rather than the bidding price, and, mathematically, the market clearing price is the marginal cost [35].

Reserves may also be called ancillary services, and they are often provided by fast-responding power plants, such as natural gas turbines or hydro generators, to make up for unexpected load fluctuations or generation shortage. The reserves market is

sometimes called the capacity market, which has more variations. Each ISO has different rules on how much reserve to procure to ensure reliability and how the reserve sellers are paid [36]. In general, an auction mechanism is still used but is more complicated. In some markets, market participants submit two offers, one for electricity generation and the other for the reserve capacity; thus, sellers must commit to a certain amount of electricity generation to be eligible to sell reserves. After the price for electricity generation is cleared, the ISO then sorts reserve capacities based on their reserve offering prices. If these capacities are dispatched, they receive the reserve payment. In other markets, there is auction on reserves, but not on electricity generation. It is not uncommon that reserve sellers get paid for standing by without actual generation (i.e. being scheduled but not dispatched). Strategic market participants might bid low on the reserve price to be scheduled but bid high on the energy price to avoid actual generation. Furthermore, reserves usually have several classifications, such as primary, secondary, and non-spinning reserves; each has its own response time for different incidences on the grid, and thus might have different markets and prices [37-40].

The complex design of the electricity market is meant to match the supply and demand, and together with bidding price caps, right limitations, and other mechanisms, the market design is also meant to induce market participants to bid truthfully and prevent arbitrage [41]. Inadequate market designs could lead to a market crash. One infamous example is the California electricity crisis in 2001 where several market participants exploited the market by forcing shortage in the capacity market, resulting in multiple large-scale artificial blackouts and brownouts in California [42-44].

In this dissertation, the deregulated electricity market is simplified to the merit order dispatch, meaning that the ISO sorts all power plants based on their generation costs and dispatches the cheaper power plants before the more expensive ones. This essentially means that all power plants submit the same offers all the time truthfully to only cover their generation cost, and constraints of transmission line capacity or power plant ramping limits are not violated.

1.2.3 Renewable Energy

Renewable energy has had impressive growth in the U.S. since 2005, according to the historical histogram shown in Figure 1.5. However, the shares of renewable energy in the U.S. energy system are still low. The 2011 statistics in Figure 1.6 show that renewable energy contributed only 9% of the energy supply in the U.S. The non-intermittent renewable sources, hydropower and biomass (biofuel and wood-derived fuel) accounted for most of the renewable generation. Among the intermittent renewable sources, wind power accounts for 13% of the renewable generation, and the share of solar power was even less.

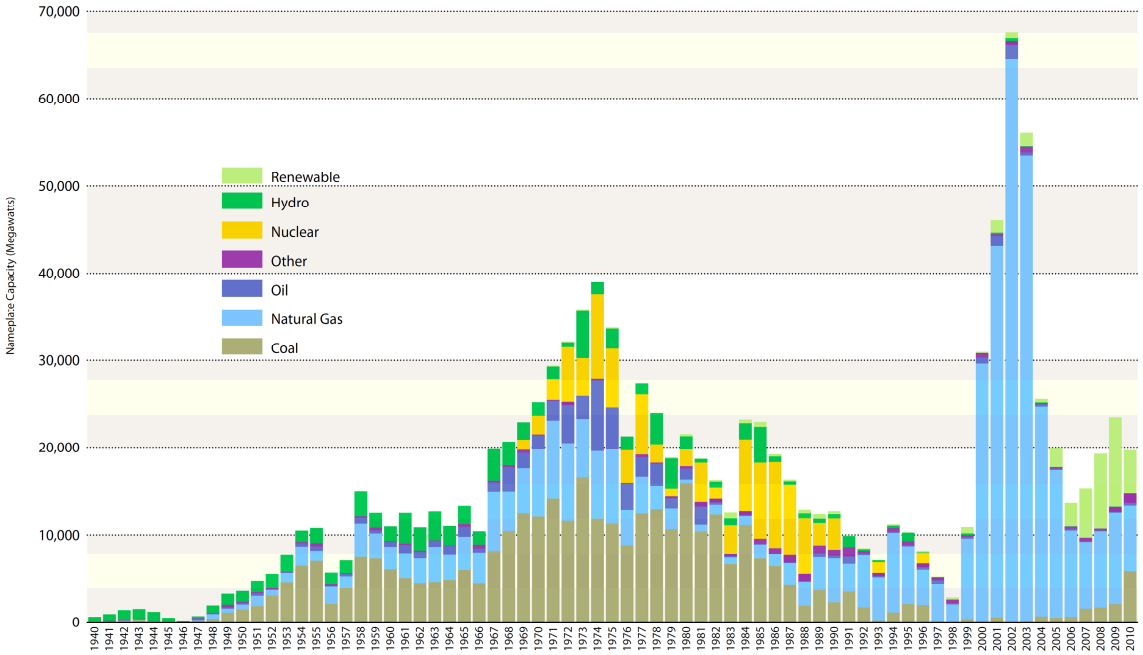

Figure 1.5 The U.S. electric generating capacity by in-service year [45]

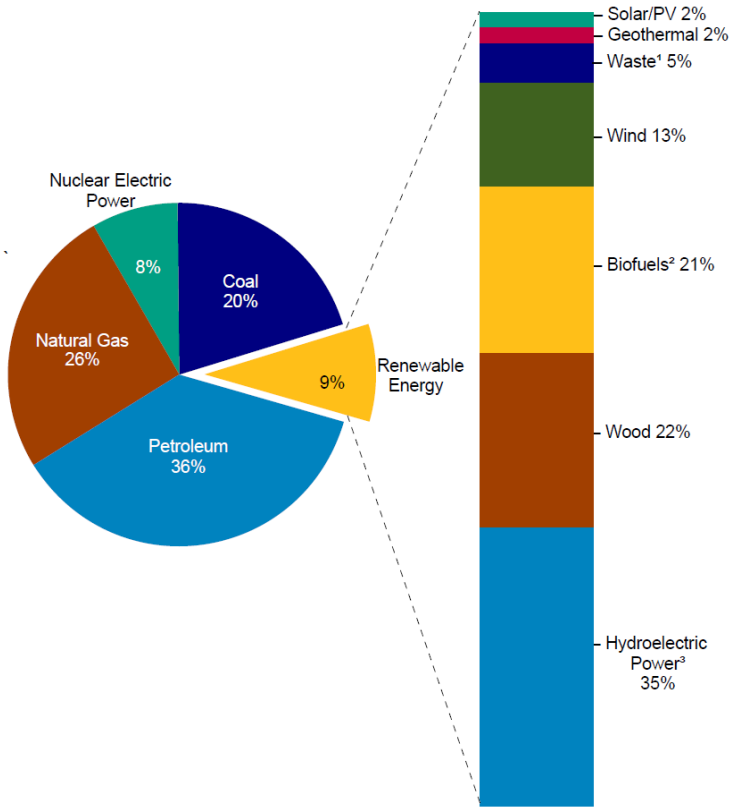

Figure 1.6 Shares of renewable generation in the U.S. energy supply in 2011 [46]

The non-intermittent renewable sources, hydropower and biomass, are beyond the scope of this dissertation, although they do play an important role in the energy supply around the world. Countries rich in hydropower, such as Brazil and New Zealand [47], even use it to support base loads on the electric grid; Nordic countries have been using hydroelectric power to mitigate wind power intermittency [48-52]. However, the availability of these two types of renewable energies has intrinsic limitations. A hydropower plant has to be near a large water body, and its operation largely depends on whether it is a dry or wet year. Biomass has the concerns of competing for agricultural land with crops and harvesting efficiency. If biomass is not acquired from environmentally sustainable sources, its overall emissions may be worse than using natural gas. Unfortunately, the scarcity of these two renewable energies cannot be addressed via demand-side controls, and thus this dissertation will not discuss them in-depth.

Wind and solar power both have contributed significantly to the new generating capacity of the U.S. electric grid in recent years (which is particularly true in 2012,

according to the FERC statistics shown in Table 1.3), and the innovations of technology continue to drive down the installation costs (see Figure 1.7 and Figure 1.8). The installation costs of wind farms averaged at $1,750/kW in 2012 [53], and solar farms cost $6,200/kW in 2010 [54]. In fact, wind farm installation costs are now almost comparable to coal-fired power plants [7, 8], but the price of solar power is still much more expensive than conventional generation and has a long way to achieve grid parity. Furthermore, the intermittent outputs from wind and solar power may cause issues to grid operation, especially when high volumes of wind and solar power are deployed onto the grid. For example, the capacity factor of a typical wind farm is only around 35%, meaning that the outputs of the wind farm are on average only one third of the nameplate capacity. Studies have shown that wind power may cost $5/MWh-$10/MWh to pay for reserves in order to accommodate for its intermittence [55]. Thus, the operation cost of wind and solar power may not be low, despite the fact that their generation does not require paying for fossil fuel, which is the major expense of operating non-renewable power plants.

Table 1.3 New Electricity Generating Capacity Installed in 2012 in the U.S. [5]

Primary Fuel Type	No. of Units	Installed Capacity (MW)
Coal	8	4,510
Natural Gas	94	8,746
Nuclear	1	125
Oil	19	49
Water	13	99
Wind	164	10,689
Biomass	100	543
Geothermal Steam	13	149
Solar	240	1,476
Waste Heat	1	3
Other	5	0
Total	658	26,387

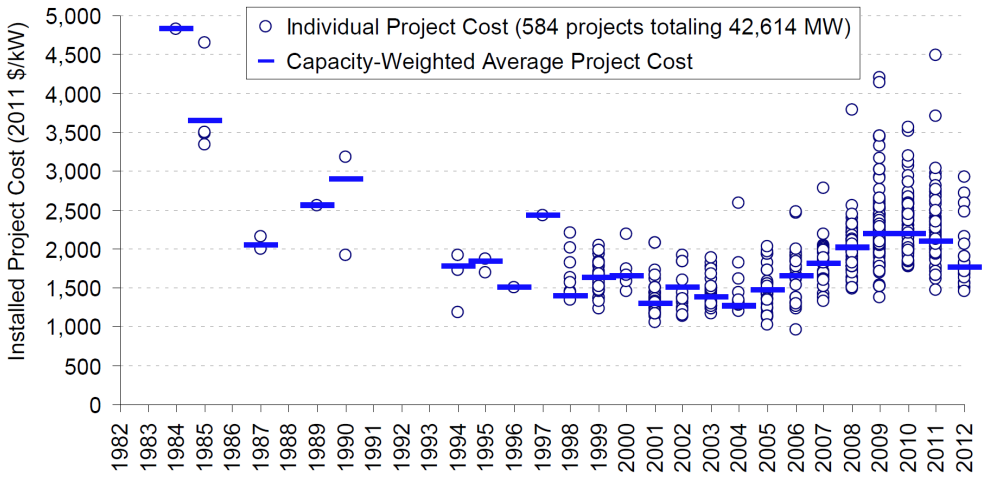

Figure 1.7 Installation cost of wind power in the U.S. [53]

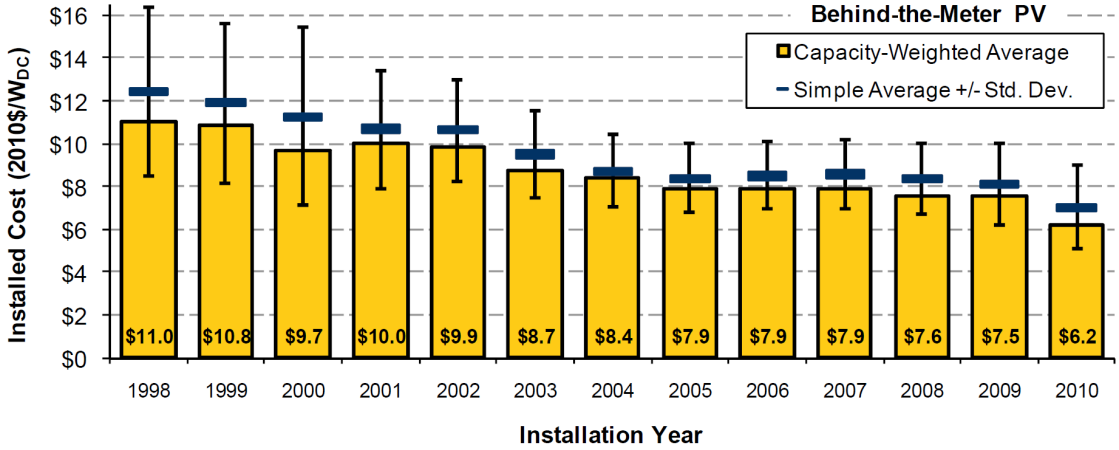

Figure 1.8 Installation cost of solar power in the U.S. [54]

The intermittent renewable energy brings various challenges to the grid operation, in addition to the increasing requirement of reserves to compensate for the fluctuating generation mentioned in the previous section. Transmission planning and construction, real-time grid operation and market redesign may all be needed to integrate renewable energy into the electric grid.

New transmission lines are needed to connect far-flung renewable generation to load centers or existing transmission corridors. Inadequate transmission will cause congestion, which may force the grid operator to curtail the renewable generation. Market efficiency will also suffer because the price will be forced to clear at a less preferable value due to transmission constraints. Furthermore, the planning and construction of transmission lines take much longer time than building wind or solar farms because they

usually involve approval from multiple states and governmental agencies. Therefore, the preparation of grid transmission has to start much earlier. In addition, the question of who should pay for it is also an issue. Existing market participants have no incentive to share this extra cost, so it very likely will be left to the renewable generation plant owners or the government. FERC is starting multiple initiatives to promote economic planning or BOT (build-operate-transfer) projects, which hopefully will create incentives for new transmission lines to be built [56].

Generation scheduling and dispatch need significant changes to accommodate the intermittent renewable generation. Real-time operation will be needed to deal with the sub-hour variations in renewable generation when scheduling and dispatching both conventional and renewable electricity generation. New analysis tools for reliability assessment, maintenance planning, and reserve procurement that include the probabilistic characteristic of renewable generation will also be needed.

Market redesign is desired to reduce obstacles for renewable energy to enter the electricity market. Several market rules originally designed to prevent arbitrage, such as the imbalance penalty in transmission tariffs [56], prevent renewable generation from entering the market. These rules need to be revised; otherwise, renewable generation will be at a disadvantage compared to conventional generation sources. FERC is proposing to eliminate the imbalance penalty payment for renewable energy [56]. Many market supporting mechanisms are in place in the U.S. and Europe to facilitate renewable generation. In particular, the guaranteed buy-in prices will ensure the intermittent renewable generation to be dispatched, so that owners of wind and solar farms can receive guaranteed payment [55, 56]. A summary of various market supporting mechanisms and financing options for renewable generation is provided in Table 1.4 [57].

Table 1.4 Market Supporting Mechanisms for Renewable Energy
(adopted from [57])

	Direct		Indirect
	Price-Driven	**Quantity-Driven**	
Regulatory			
Investment-Focused	• Investment incentives • Tax credits • Low interest loans	• Investment grant	• Environmental taxes • Simplification of authorization procedures
Generation-Based	• (Fixed) feed-in tariffs • Premium system	• Long-term contracts quota certificate system	• Transmission charges • Regulation costs
Voluntary			
Investment-Focused	• Shareholder programs • Contribution programs		• Voluntary agreements
Generation-Based	• Green tariffs		

Besides the external factors mentioned above, forecasting the renewable generation also draws a great amount of attention. For example, many research efforts have focused on estimating wind generation by integrating numerical weather forecasts and statistical techniques, several of which are already online in the U.S. and Europe to assist generation scheduling [55, 58-60]. However, in this dissertation, the forecasts of wind power generation are assumed to be known and available several hours prior to the operation, and improving the forecast accuracy is not within the scope of discussion.

1.2.4 Smart Grid

The Smart Grid is a concept to enhance the delivery of electricity from power plants to consumers. With advanced metering systems deployed to the grid to provide two-way communication, feedback, and control on customer appliances, the grid will be transformed from a passive operation system into a proactive control network system. The grid operator will have better knowledge about status of the supply, demand, and transmission, so the grid operator can better prevent and alleviate incidences. The Smart Grid is expected to save energy, improve operation efficiency, provide better quality of service, enhance reliability, and accommodate renewable generation. New services or markets might also emerge and create new types of energy commerce [61-63].

While the descriptions about the Smart Grid are often about the hardware deployment of the advanced metering systems, the studies in this dissertation focus on developing the intelligence (i.e. control algorithms and optimization schemes) to achieve many of the goals mentioned in the Smart Grid by integrating the PEV charging and wind power.

1.3 Research Scope and Objectives

It was mentioned earlier that the focus of this dissertation is about the impacts to and changes of the electric grid brought by PEVs and wind power, and this section provides more specific descriptions about the research scope and objectives.

Figure 1.9 depicts the various grid entities in four quadrants, where the bottom two quadrants show the existing entities (the traditional loads and conventional generating technologies), and the top two quadrants show the new entities (the plug-in electric vehicles (demand response) and renewable generation). In this dissertation, PEV is the designated demand response and wind power is the designated renewable generation. Another way to read Figure 1.9 is that the supply in the two quadrants on the right will produce electricity for the demands in the two quadrants on the left. In terms of the new grid entities, this dissertation tackles the challenges of incorporating large numbers of PEVs and wind power via various control and optimization techniques. Later, the developed control and optimization techniques are expanded to address issues of existing grid entities; more specifically, the dissertation discusses the CO_2 emissions of non-renewable generation and long-term generation planning. More detailed descriptions on the research problems for each grid entity are provided below.

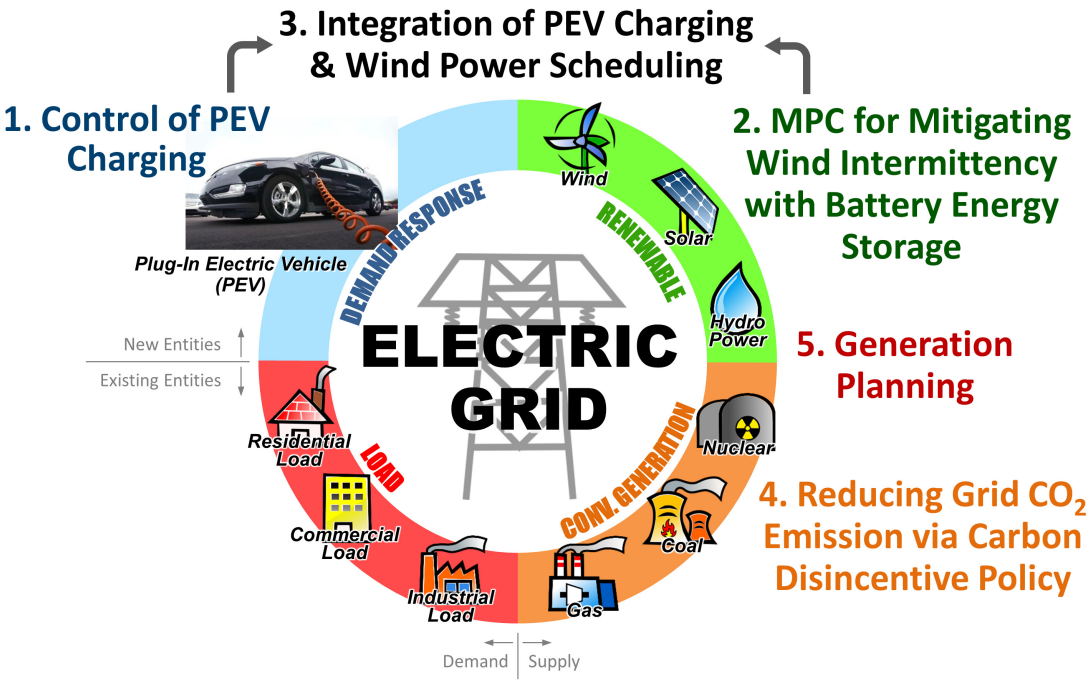

Figure 1.9 The vision of grid integration

First, a PEV charging control algorithm is developed. It is recognized that unmitigated PEV charging may cause grid congestion; therefore, the objective of the PEV charging control algorithm is to avoid congestion while fully charge all PEVs. Another objective is to make the PEV fleet an asset to facilitate the grid operation, such as providing reserves for grid frequency regulation, with one-way power flow, i.e., no V2G power.

Secondly, this dissertation explores means to mitigate wind intermittency, so that the wind farm owner can schedule and sell more wind generation and become more competitive with non-renewable generation. In addition to using conventional reserves, battery energy storage system (BESS) is considered, which can be dedicated batteries or PEVs. Model predictive control (MPC) is used because of its superior performance in solving horizon problems. Meteorologists now can provide forecasts of wind generation up to several hours in the future with reasonable accuracy, and such future predictions can be incorporated in the framework of MPC. The effect of BESS capacity sizing is also investigated.

Thirdly, to accommodate both PEVs and wind power on the grid, a hierarchical control algorithm is proposed to integrate PEV charging and wind power

scheduling/dispatch. The integration harnesses the synergy between PEV and wind power and creates a win-win situation for them. More specifically, the PEV fleet replaces BESS to provide reserves to mitigate wind intermittency, and wind generation provides cleaner electricity to charge PEVs. The features in the control algorithm previously developed for PEV charging and wind scheduling are included in this hierarchical controller.

Next, we consider methods to reduce grid CO_2 emissions. The need to understand the CO_2 emissions on the grid still exists after renewable generation is deployed to the grid because some conventional generating capacities will continue to operate. A carbon disincentive policy is proposed to promote the use of low-carbon power plants for electricity generation. The tradeoff between the generation costs and grid CO_2 emissions is investigated.

Lastly, the long-term generation planning is studied. Generation planning is the decision making prior to operation integration, as it determines when and what type of new power plants should be constructed to meet the demand increases. Today, it is a commonly-agreed objective to increase the share of renewable generation. Therefore, the renewable intermittency and costs of reserve scheduling and dispatch are included into the generation planning problem to provide a more accurate assessment of the cost of wind power. A systematic methodology is developed to evaluation the total costs of the new power plant construction, in which the new aspects related to renewable generation will be addressed.

All the control and optimization techniques developed are applicable to utility-scale power systems. In this dissertation, the Michigan grid is used as the targeting grid, which has a coal-dominant generation mix. In addition, although the current market shares of PEVs and wind power are quite low in Michigan, it is assumed that the market shares of both PEVs and the capacity of wind power are substantial. This represents the scenario when both green technologies are mature and have been widely adopted, so that the grid integration is needed.

Despite the attempt to include most aspects of PEVs and wind power related to the electric grid in this dissertation, several simplifications are adopted. In particular, this dissertation ignores the transmission line properties (line resistance and impedance) and limitations (power and current limits). Thus, no assessment can be made on the known

concerns on voltage raises if PEV chargers are tripped off simultaneously due to a grid fault or when wind generators absorb substantial reactive power from the grid.

1.4 Contributions

This dissertation aims to integrate two green technologies, PEV and wind power, onto the electric grid. The inclusion of these two technologies presents new challenges and opportunities for grid operation, and the synergy existing between them also has great potential to facilitate or improve the grid operation. This dissertation harnesses that synergy via various control and optimization techniques. Numerical simulations quantify gains of introducing these two green technologies properly, and illustrate the potential pitfalls if they are added to the grid without coordination. The main contributions of the dissertation include the following:

1. The modeling work in this dissertation covers key features of the grid entities in all of the four quadrants shown in Figure 1.9, including the temporal distributions of the PEV population, stochastic wind power generation, grid frequency dynamics, CO_2 emissions, and costs of electricity generation and power plant construction. The comprehensive modeling enables various studies to investigate the interactions between supply and demand on the electric grid. These studies provide invaluable information on the challenges and opportunities of the evolving electric grid. The modeling work is presented in several different sub-sections in Chapters 2-6.

2. A PEV charging control algorithm is developed to utilize the idle generating capacity in the late evening to charge a large number of PEVs, so that the aggregate load can achieve "valley filling." This is a desired feature seen in the literature to control demand-response appliances because it avoids creating congestion on the grid. However, unlike the several highly centralized schemes in the literature, the control algorithm adopts a partially-decentralized structure to address two important attributes of individual PEVs, the battery state of charge and the plug-off time. This allows the majority of PEVs to be fully charged before they unplug. The algorithm also includes a feedback mechanism for grid frequency regulation; therefore, the PEV fleet can replace conventional reserves in the valley hours. This PEV charging control algorithm utilizes

the leeway existing in the PEV fleet, and turns the PEV fleet into a positive asset to facilitate the grid operation while satisfying the charging demand of individual PEVs.

3. MPC is used to control the charging and discharging of BESS to compensate for wind intermittency. MPC has been used in the literature to mitigate wind intermittency; however, most studies focused on theoretical discussions with quadratic objective functions. The BESS control problem studied in this dissertation uses objective functions that capture the real operation costs to the wind farm owner; in particular, the reserve costs to cover wind surplus or deficit are included. This addresses the realistic scheduling problem a wind farm owner will fact in the future: to compete with non-renewable generation by selling wind generation in the open market. Furthermore, the BESS sizing analysis reveals the benefit to adopt the more sophisticated horizon-based MPC controller; MPC can secure the same revenue for the wind farm owner with a much smaller BESS.

4. A three-level hierarchical control algorithm is developed to harness the synergy between PEV and wind power. The top-level control algorithm solves a scheduling optimization problem to minimize the costs of electricity generation, which provides assessment to the full potential of manipulating both supply and demand on the grid. The middle- and bottom-level controllers are based on the control algorithms previously developed for PEV charging and wind power scheduling. The hierarchical structure allows the features in the different control algorithms to be preserved, including minimum generation costs, full vehicle battery charging, and grid frequency regulation. The results indicate that the PEV fleet and renewable power should grow together to realize their full potentials.

5. A carbon disincentive policy is proposed as a supply-side interference to alter the dispatch order of power plants, which allows the more expensive low-CO_2 generating capacities to be dispatched before the cheaper high-CO_2 generating capacities. The carbon disincentive policy is based on the concept of the Pigovian tax. However, the carbon disincentive policy is designed to be revenue neutral and no tax revenue is collected, which reduces the burden to consumers on the grid. In fact, the proposed carbon disincentive policy is better interpreted as a tuning knob to the grid operator to adjust the carbon content in the generation mix. The tradeoff between the generation

costs and grid CO_2 emissions is investigated using the optimal Pareto front. It is further found that a better tradeoff can be obtained by introducing both PEVs and wind power on the grid. Analyses indicate that introducing wind power can significantly reduce the generation costs, but not the CO_2 emissions; manipulating both the supply and demand is necessary to address both the generation costs and CO_2 emissions.

6. A systematic methodology of cost evaluation is proposed for generation planning. The methodology considers the evolutions in both the supply and demand on the electric grid, including annual increases in the grid load and changes in the merit order when new power plants are commissioned. Furthermore, to introduce renewable generation to the grid, the renewable intermittency and reserve-related costs are considered, which are new features not seen in the literature. The cost evaluation identifies the construction cost as the bottleneck preventing wind power entering the market.

7. This dissertation demonstrates that PEVs and wind power are complementary to each other. Furthermore, the proposed control and optimization schemes have implications in economics and the practices of grid operation, such as the economic gains and losses between coordinated and uncoordinated PEV charging, and the necessity of controlling supply and demand to reduce grid CO_2 emissions.

1.5 Outline of the Dissertation

Chapters 2-6 contain the technical results of this dissertation. Some chapters have been published in conferences or journals independently. Nevertheless, the results of these chapters combined together demonstrate the multi-faceted potentials of a well-integrated electric grid. Chapter 2 presents the PEV charging control algorithm; Chapter 3 presents the MPC algorithm for controlling BESS to mitigate wind intermittency; Chapter 4 presents the hierarchical control algorithm to integrate PEV charging and wind power scheduling into the grid operation; Chapter 5 presents the use of a carbon disincentive policy to reduce grid CO_2 emissions; Chapter 6 presents the methodology of evaluating long-term investment choices of upgrading generating capacities; and, a conclusion of this dissertation and suggested future work are presented in Chapter 7.

CHAPTER 2
PEV Charging Control

PEVs are usually equipped with sizable batteries, which allow more all-electric driving; therefore, PEVs are very capable of replacing the use of fossil fuel with electric energy in the ground transportation sector. However, PEVs are not problem-free. Charging PEV batteries burdens the electric grid with extra loads. If left unmitigated, PEV charging may cause negative impacts on the grid and jeopardize the grid operation. Fortunately, PEVs often stay parked for substantial amounts of time and the charging is interruptible, since the driving performance of PEVs is not critically dependent on when their batteries are charged by the grid. By controlling the timing and charging power, PEVs can be served by the idle generating capacity in valley (off-peak) hours, meaning that PEVs are charged by the existing grid without adding new power plants as long as the charging load is within the grid capacity. In this chapter, a PEV charging control algorithm is proposed. The algorithm controls the timing and charging power of individual PEVs based on their battery state of charge (SOC) and plug-off time and consolidates the charging in the valley hours, so that PEVs do not become an additional stress on the grid during peak hours and "valley filling" can be achieved.

This chapter is organized as follows: Section 2.1 reviews the relevant literature; Section 2.2 presents models for the grid and the PEV fleet; Section 2.3 shows the derivations of the PEV charging control algorithm; Section 2.4 presents numerical simulations; and, Section 2.5 gives concluding remarks.

2.1 Literature Review

PEVs impact the electric grid in various ways, and several early studies have adopted rule-based charging algorithms to manage the load and evaluate the impacts brought by high numbers of PEVs on the grid [64-66]. Some of these simple charging rules are quite arbitrary and do not represent the full potential of well-managed PEV

charging. However, most of them found that coordinated charging is needed, else the aggregate load in peak hours may increase and adversely affect grid reliability. Since the PEVs can be treated as controllable loads on the electric grid, various load-side management algorithms were investigated first, followed by a review of studies more specific to PEV charging control. A summary of relevant literature is listed in Figure 2.1.

The resource allocation methods [67] provide a centralized scheme to allocate the available assets to serve customers. To use the resource allocation methods to control PEV charging, one may take the sum of the battery SOC of individual PEVs as the optimization objective, and then the battery charging can be maximized. However, this approach is centralized as it requires collecting information from all PEVs. In addition, this approach is instantaneous, i.e., it does not consider the plug-in and plug-off times of PEVs, nor does it explore the valley in the load profile. For schemes that are horizon-conscientious, scheduling and queuing theories are used. The scheduling theory provides systematic guidelines to prioritize and sort tasks, and many heuristics have been developed with theoretically guaranteed performance, such as minimum wait time or lateness [68]. The queuing theory has been used in manufacturing factories and hospitals [69], and many empirical variations have been developed to accommodate specific applications [70-72]. However, most of these application-specific scheduling and queuing heuristics are highly centralized and do not extend to PEV charging easily.

For schemes directly related to PEV charging, several studies solve centralized optimization problems with various objectives, such as valley filling [73, 74], coordination with CHP (combined heat and power) [75], and using PEVs as grid reserves [76, 77]. Also, there are optimizations designated to solve the optimal PEV charging timing to mitigate wind intermittency, which will be discussed in detail in Chapter 4. However, to keep the problem numerically tractable, many of these optimization problems treat the whole PEV fleet as one large battery and do not take into account the plug-on/plug-off time and SOC of individual vehicles. Therefore, the solutions of these centralized optimizations do not provide implementable algorithms for PEV charging. Decentralized resource allocation methods for demand response [78] and PEV charging [79] have also been found in the literature, which usually involve auctions [80]. In addition, a revised allocation rule, the proportional sharing, is adopted [78] as a more

considerate alternative to low bidders in the auction. However, the practicality of these decentralized schemes is still in question as they require massive two-way communications and some even require iterations to reach a consensus. For real-time implementable schemes, dual tariffs are now available to PEV owners in several utility service regions [81, 82], in which distribution companies offer PEV owners a lower electricity price in late evenings as an incentive to delay their vehicle charging. However, dual tariffs are only suitable to the scenario when the market share of PEVs is low. Studies have shown that dual tariffs become inadequate when the PEV fleet is large, in that an undesired load increase will happen at the time when the low-price window starts [83, 84]. Another real-time implementable scheme is the on/off control for regulating thermostatic loads [85-87], one of which has been extended to PEV charging control [88].

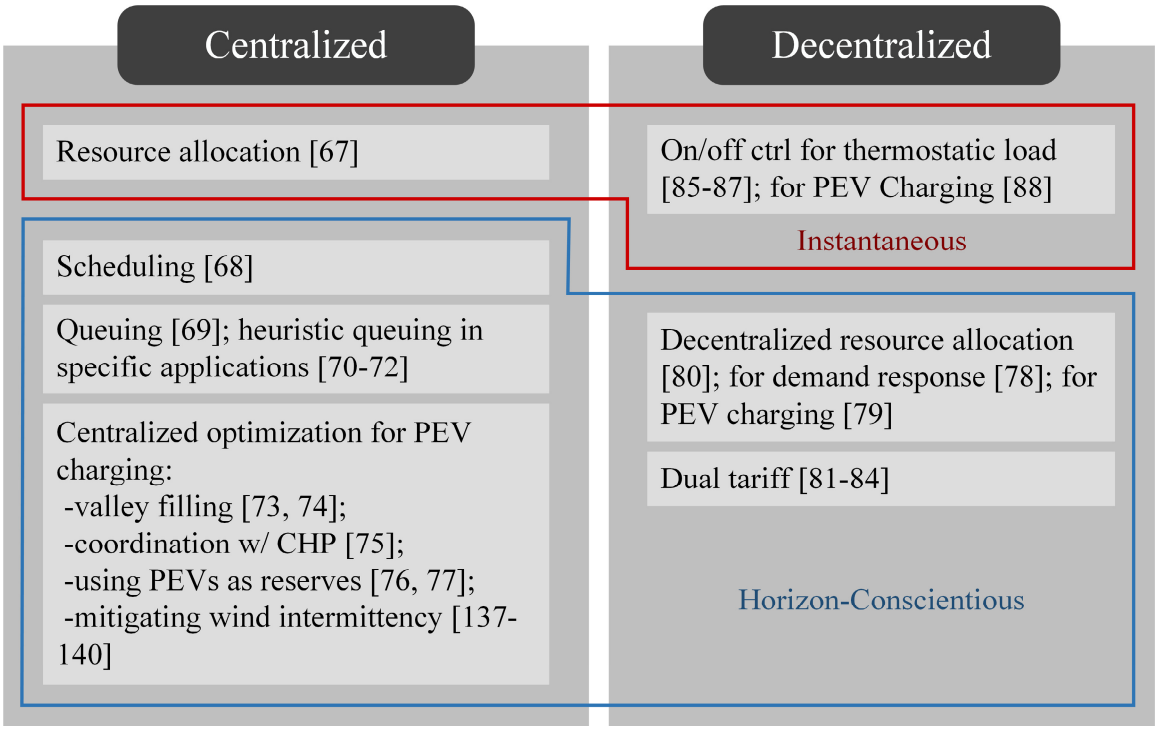

Figure 2.1 Summary of literature related to PEV charging control

In addition, it has been mentioned in the literature that hierarchical and partially-decentralized algorithms are more appropriate for PEV charging [88], as a hierarchical structure allows both system- and individual-level objectives to be considered and a decentralized control algorithm may reduce/eliminate the need to collect individual

vehicle states, such as battery SOC. In this chapter, a two-level control architecture for PEV charging is proposed. The control algorithm is designed to be horizon-conscientious and partially decentralized. The first level is inspired by the centralized optimization in [74], which addresses the system-level objective of valley filling over a long time horizon. The second level is decentralized, which resembles the proportional sharing scheme in [80] and addresses the individual-level objective of SOC servicing. This partially decentralized arrangement allows this scheme to be applied to an indefinite number of PEVs. Feedback is then added to this control architecture based on the scheme in [86] to regulate the grid frequency, so that the requirement of conventional reserves can be reduced or even eliminated. Notice that the control algorithm will only alter the timing and charging power (i.e. speed up or slow down the charging) but it will never discharge PEV batteries to support grid operation; this is because V2G power flow is assumed to be unavailable in this study to avoid extra energy cycling on the PEV batteries. The results have been published in [89].

2.2 Modeling

This section presents models of the electric grid and the PEV fleet. The grid model describes the background non-PEV grid load and the grid frequency dynamics, and the model of the PEV fleet describes the plug-on/plug-off time distributions and battery SOC.

2.2.1 Electric Grid

The electric grid model is developed to represent the situation in the state of Michigan, and the hourly load data from the area serviced by Detroit Edison [90] is used to represent the nominal non-PEV load on the grid, which ranges between 5,500-8,000 MW. Sub-hour fluctuations are generated by a random process to match the typical fluctuations on state-wide power systems [91]. The nominal load and modeled load with fluctuations are shown in Figure 2.2.

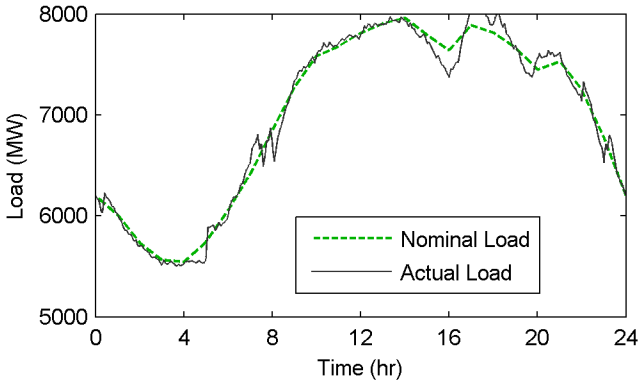

Figure 2.2 Nominal and actual load profiles

The frequency of the AC electric grid deviates from the nominal 60 Hz when mismatches happen between the load and generation. The electric grid is assumed to have two groups of generating units; the slow-generating units (nuclear or coal-firing power plants) are deployed to follow the hourly scheduling to fulfill the predicted load, whereas the fast-responding units (diesel or natural gas power plants) provide reserves when the actual load deviates from the prediction and the frequency deviates from nominal. However, exception happened in 2012 when natural gas had a substantial price drop and it was used to supply base loads in that period [92], even though gas turbines are fast-responding power plants. The grid frequency dynamics are approximated by the rotational dynamics shown in Eq. (2.1), in that electricity generation will increase the grid frequency (ω) and loads will reduce the grid frequency. The model structure for the electric grid is depicted in Figure 2.3.

$$\dot{\omega} = \frac{P_{\text{surplus}}}{I\omega_0} = \frac{-P_{\text{L}} + P_{\text{gen}} + P_{\text{reserve}} + P_{\text{R}}}{I\omega_0} \tag{2.1}$$

where I is the system inertia, and ω_0 is the nominal frequency. P_{L} is the actual grid load, and P_{gen} and P_{reserve} represent the electric power generated by the slow-generating units and the fast-responding units. The frequency-dependent term, P_{R}, captures the phenomenon that rotary loads, such as motors, slow down and consume less electricity when the grid frequency decreases, which is modeled as Eq. (2.2).

$$P_{\text{R}} = DP_{\text{L}}\left(\frac{\omega_0 - \omega}{\omega_0}\right) \tag{2.2}$$

where D is an empirical constant suggested in [93].

Equations (2.3) and (2.4) show that both P_{gen} and $P_{reserve}$ are assumed to be first-order dynamics, but with different time constants and implications. In Eq. (2.3), the hourly nominal grid load ($P_{L,nom}$) is used as the load prediction, which P_{gen} will try to follow. Eq. (2.4) shows that the fast generation, $P_{reserve}$, is assumed to be controlled by a PI-controller to regulate the grid frequency.

$$\dot{P}_{gen} = -\frac{1}{\tau_1}\left(P_{gen} - P_{L,nom}\right) \tag{2.3}$$

$$\dot{P}_{reserve} = -\frac{1}{\tau_2}\left\{P_{reserve} - [-k(\omega - \omega_0) - k_I \int (\omega - \omega_0)dt]\right\} \tag{2.4}$$

where τ_1 and τ_2 are time constants. τ_1 is chosen to be 5 minutes and τ_2 is chosen to be 3.33 seconds to resemble the ramp rate limits in each type of generation [93]. The controller gains, k and k_I, are chosen so that the frequency deviation matches the typical value around 1% reported in [86]. The model shown in Figure 2.3 using conventional reserves to regulate the grid frequency will be used as the baseline for comparison.

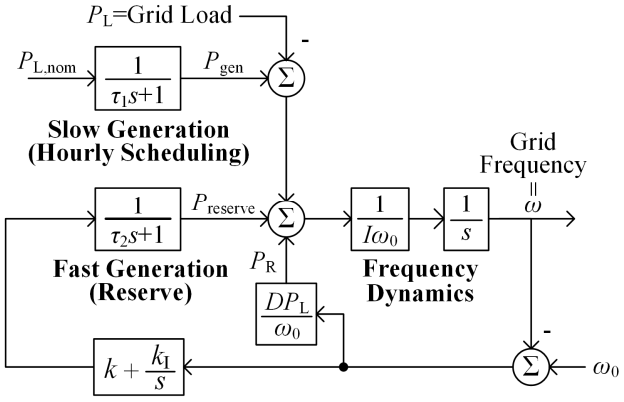

Figure 2.3 Electric grid model

2.2.2 PEV Fleet

The total number of PEVs is assumed to be two million, corresponding to a 25% penetration in the Michigan fleet. This is an aggressive projection of PEV penetration in the ground transportation in 2020 [94], representing the situation when PEVs have

captured a sizable market and their charging becomes a real issue. All PEVs are assumed to use smart chargers and thus controllable. The total number of PEVs does affect the performance in the SOC satisfaction of individual PEVs and grid frequency regulation; therefore, in addition to simulations and analyses with two million PEVs shown in Sections 2.4.1 and 2.4.2, cases with different numbers of PEVs and unexpected changes in the fleet population are presented in Sections 2.4.3 and 2.4.4.

The PEV fleet is characterized by the plug-in time, the plug-off time, and the battery SOC at plug-in. The SOC quantifies the energy requirement to fully charge all PEVs, so that the grid operator can schedule extra generation to accommodate the PEV charging demand, and the plug-in/plug-off time prioritizes the PEV fleet and determines which vehicle receives immediate or delayed charging service. These three variables are assumed to have normal distributions that are mutually uncorrelated. Figure 2.4 shows the three distributions. The mean and standard deviation (std) of plug-in and plug-off time are chosen to match temporal distributions of the data reported in [95]; the raw data can be found in Appendix A. The SOC distribution at plug-in is assumed to have a mean of 50% and std of 10%. The PEV fleet is created by sampling the three distributions two million times, and then the three sets of samples are shuffled randomly, so that PEVs with all possible combinations of plug-in time, plug-off time, and SOC are covered. In this random-sampling process, some rarely-existing cases may be inadvertently introduced. For example, a vehicle with a very late plug-in time and a very early plug-off time will have an extremely short dwell time for battery charging. Thus, this hypothetical PEV fleet is more challenging to charge fully than in reality. However, the above assumptions are adopted in the proof-of-concept simulations in this chapter. A more realistic PEV fleet based on real commute data is modeled in Chapter 4.

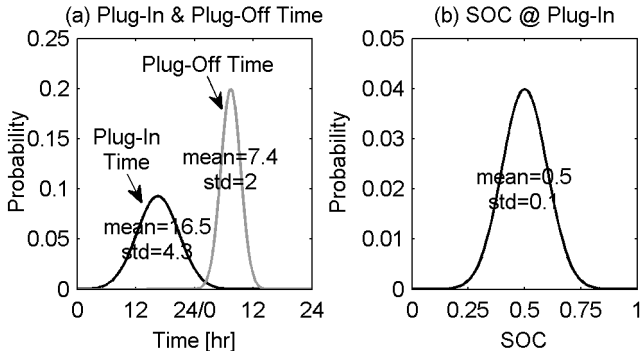

Figure 2.4 Distributions of plug-in time, plug-off time, and SOC at plug-in

The battery capacity of all PEVs are assumed to be 16kWh, which is the capacity seen on PEVs with a 40-mile electric driving range, and 80% SOC is defined as fully charged. With the battery capacity and the SOC distribution known, the total energy requirement to fully charge the PEV fleet can be calculated using Eq. (2.5); this information will be used in Section 2.3.1 when calculate the centralized broadcast for valley filling. The maximum charging power is 1,440W, assuming that all PEV owners opt for Level-1 charger at home [24]. Although the Level-1 has a lower power rating, it requires only the 120VAC power source, but not the 220VAC power source, which is readily available in most residential houses or apartments and requires minimum hardware upgrades. In addition, only night charging at home is allowed. Battery dynamics are ignored and the efficiencies of both charging and discharging are assumed to be perfect; therefore, the SOC dynamics are simplified to the governing equation in Eq. (2.6).

$$K = \sum_{i=1}^{N} (0.8 - SOC_{\text{ini}})_i \cdot Q \tag{2.5}$$

$$\dot{SOC} = -\frac{P_{\text{batt}}}{Q} \tag{2.6}$$

where Q is the battery capacity, SOC_{ini} is the battery SOC at the plug-in, and P_{batt} is the battery discharge power.

2.3 Two-Level PEV Charging Control

The proposed PEV charging controller consists of two levels. The first level is the *centralized broadcast* performed by the grid operator, which utilizes the predicted base load and adjusts the charging setpoint to achieve valley filling. The second level is the *charging power allocation rule* executed by individual PEVs, which regulates charging power for SOC satisfaction in a decentralized manner. The feedback is designed to mimic the PI-controller in Figure 2.3. With the PEV charging control algorithm in place, the conventional reserves can be replaced by the controlled PEV charging load, and the block diagram of the grid frequency dynamics changes from Figure 2.3 to Figure 2.5, where the centralized broadcast is denoted as C, the PEV charging rule is denoted as G, and the feedback gains are denoted as k_{soc} and $k_{I,soc}$.

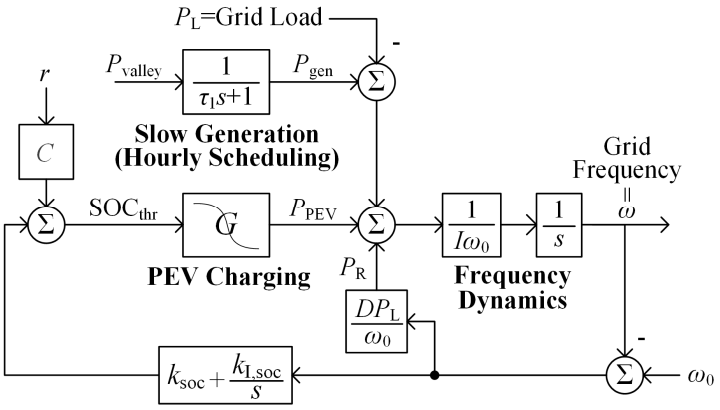

Figure 2.5 PEV charging control for frequency regulation

The centralized broadcast (C) and the feedback gains (k_{soc} and $k_{I,soc}$) will be derived by the grid operator off-line. During the derivation, the grid operator is assumed to know the total number of PEVs and distributions of the plug-in time, plug-off time, and SOC at plug in of the PEV fleet. The distributions may be acquired from transportation statistics or market sales reports from automakers. The exact data points of individual vehicles are not needed. The centralized broadcast can be interpreted as the feedforward component in the PEV charging control algorithm. The feedback gains are designed based on the sensitivity analysis. The feedforward and feedback terms then are given to individual PEVs, so that the local controller on the smart charger can carry on to

calculate the charging power for individual. The local controller is decentralized, which address the different SOC and plug-off time of individual PEVs. It is assumed that the smart charger can read the SOC from the PEV automatically, but not the plug-off time. PEV owners will have to input this information to the smart charger. Sections 2.3.1-2.3.4 present how C, G, and the feedback controller gains are derived.

2.3.1 Centralized Broadcast

First, the grid operator uses Eq. (2.5) to calculate the total energy needed to fully charge all PEVs. Note that this estimation of total energy for charging the whole PEV fleet is based only on the total number of PEVs and the SOC distribution; the plug-in and plug-off times of individual PEVs are not considered at this moment. Based on the SOC distribution in Figure 2.4-(b), it is found that 11.2GWh of energy is needed to fully charge two million PEVs. Then, the grid operator finds the extra generation required to accommodate the PEV load through iterations, assuming if a perfect valley filling can be achieved. As illustrated in Figure 2.6, the generation needs to support the nominal (non-PEV) load and the extra PEV load will fill the load profile up to 7,214MW, which is denoted as P_{valley} in the figure. In addition, Figure 2.6 shows that the PEV charging will between 10:04PM-8:52AM if the grid operator wishes to realize the perfect valley filling.

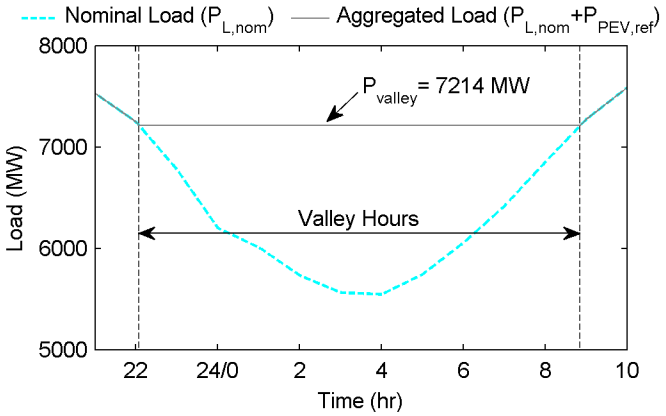

Figure 2.6 Perfect valley filling

P_{valley} is then used to derive the feedforward component for PEV charging, in which an SOC threshold, SOC_{thr}, is derived by Eqs.(2.7)-(2.8), and the grid operator broadcasts it to smart chargers to coordinate the charging of the whole PEV fleet. Equation (2.7) is nothing but an algebraic calculation to find the reference, r, which is the

idle generating capacity that will be used to charge PEVs. Equation (2.8) then converts r to SOC_{thr} by inverting the downstream system, i.e., the charging power allocation rule, G (detailed in the next section).

$$r = P_{\text{valley}} - P_{\text{L,nom}} \tag{2.7}$$

$$C = \{G^{-1} : r \rightarrow SOC_{\text{thr}}\} \tag{2.8}$$

2.3.2 Charging Power Allocation Rule

The aforementioned calculations done by the grid operator do not consider the SOC or plug-off time of individual PEVs; therefore, it is yet uncertain if all PEVs can be fully charging in the valley hours. To complete as much charging as possible, it is intuitive that PEVs with low SOC and early plug-off time should have a higher priority to receive the charging. Therefore, two strategies are developed; the charging power allocation rule will address the battery SOC, and the scaling factor will address the plug-off time of individual PEVs. These two strategies are the local control algorithms that are assumed to be programmed on the smart charger and executed by individual PEVs in a decentralized manner.

The idea of the charging power allocation rule is to allocate more power to low-SOC vehicles; this is inspired by the proportional sharing scheme in [80] and supported by the optimal PEV charging in [74]. More specifically, the charging power allocation rule is defined by the hyperbolic tangent curve shown in Figure 2.7, which maps low SOC to high charging power and vice versa. The centralized command SOC_{thr} is relevant, in that this curve is symmetric to SOC_{thr} and will shift to the right if SOC_{thr} rises. Therefore, SOC_{thr} serves as the tuning knob to the grid operator for commanding the charging of all PEVs. Furthermore, although all PEVs are assumed to have the same battery capacity in this study, it is believed that the hyperbolic tangent curve can handle the scenario of PEVs with different battery capacities because the curve maps the charging power based on the SOC, which is a normalized measure, rather than actual energy content in the battery.

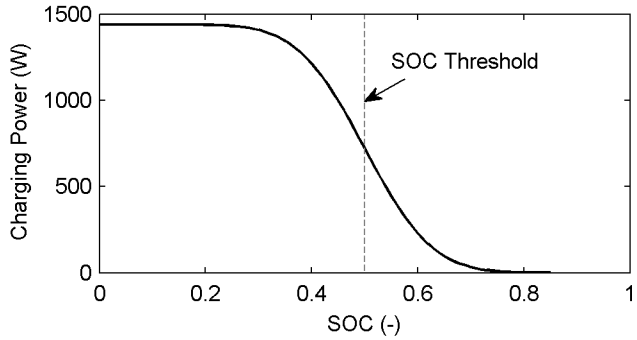

Figure 2.7 Charging power allocation rule

The plug-off time will be the information provided by the vehicle owner, and another strategy is developed to address PEVs with early plug-off times. The scaling factor, f, defined in Eq. (2.9), allows PEVs that unplug earlier than 8:52AM to charge at a higher power. For example, a vehicle with the plug-off time at 7:04AM will have the scaling factor equal to 1.2, i.e., its charging power will be scaled up by 20%. Since it is assumed that the grid operator is given information about the PEV fleet (i.e. the three distributions in Figure 2.4), the amount of additional PEV load due to early plug-off can also be incorporated into the derivation for SOC_{thr}.

$$f = \max\left\{1,\ \frac{T_{\text{end}} - T_{\text{start}}}{(\text{Plug-Off Time}) - T_{\text{start}}}\right\} \tag{2.9}$$

where T_{start} and T_{end} are the starting and ending time of the valley hours.

To further elaborate the power allocation rule, the curve in Figure 2.7 does not possess optimality under any criterion. In fact, any decreasing curve may do the job, although a smooth curve is preferable for designing the feedback gains in the next section. Similarly, the scaling factor to handle the early plug-off PEVs can have other forms. For example, a squared term can further favor vehicles with early plug-off times. Nevertheless, the current choice in Eq. (2.9) was found sufficient as the simulation with the nominal load profile shows that the majority of PEVs can be fully charged. Furthermore, the fact that most PEVs receive full battery charge indicates that the temporal distributions of the PEV plug-in time and plug-off time have enough leeway, meaning that there are sufficient vehicles staying plugged-in for prolonged hours, so that the charging can be interrupted or delayed.

2.3.3 Feedback Gains

The challenge in designing the feedback controls for the PEV charging lies in the fact that the chosen curve in Figure 2.7 makes the input/output relation of G nonlinear, and the feedback gains k_{soc} and $k_{\text{I,soc}}$ must be designed for robust stability and performance under varying plant sensitivity, which is defined in Eq. (2.11) below. Indeed, k_{soc} and $k_{\text{I,soc}}$ are designed based on the sensitivity analysis, assuming that the controller gains, k and k_{I}, in Figure 2.3 can be found.

The controller gains, k and k_{I}, in Figure 2.3 can be designed by several existing approaches, such as the pole placement or root locus technique. Furthermore, the proportional gain, k, has the physical meaning as the inverse sensitivity of frequency (the state) to the regulation power (the control input), which is shown in Eq.(2.10).

$$k = \frac{\partial P_{\text{reserve}}}{\partial \omega} \tag{2.10}$$

In the proposed scheme of controlling PEV charging to regulate the grid frequency, the proportional gain k_{soc} needs to embody a similar physical meaning as the inverse sensitivity of the state to the new control input, SOC_{thr}, which can be calculated using Eqs. (2.11) and (2.12). Eq. (2.11) first defines $\boldsymbol{S}$, which is the sensitivity of P_{PEV} (the aggregate PEV load) to SOC_{thr} and can be numerically calculated (illustrated in the next section). Then, Eq. (2.12) calculates k_{soc} by dividing k with $\boldsymbol{S}$. The integral gain, $k_{\text{I,soc}}$, can be found in the same way, as shown in Eq. (2.13).

$$\boldsymbol{S} = \frac{\partial P_{\text{PEV}}}{\partial SOC_{\text{thr}}} \tag{2.11}$$

$$k_{\text{soc}} = \frac{\partial SOC_{\text{thr}}}{\partial \omega} = k \frac{\partial SOC_{\text{thr}}}{\partial P_{\text{PEV}}} = \frac{k}{\boldsymbol{S}} \tag{2.12}$$

$$k_{\text{I,soc}} = \frac{k_{\text{I}}}{\boldsymbol{S}} \tag{2.13}$$

In fact, $\boldsymbol{S}$ is the linearization of G, and Eqs. (2.11) and (2.12) ensure that the two systems shown in Figure 2.3 and Figure 2.5 have the same closed-loop poles. Furthermore, due to the much faster response of PEV charging than conventional

reserves because the former is controlled by electronics, it is possible to achieve better performance in frequency regulation. This is achieved by choosing the closed-loop poles for the system in Figure 2.5 faster than those of the system in Figure 2.3.

2.3.4 Sensitivity of the PEV Load

Figure 2.8 and Figure 2.9 illustrate how to compute $\boldsymbol{S}$ numerically. Figure 2.8 is obtained by the off-line computation, which uses the distributions of the plug-in time, plug-off time, and SOC in Figure 2.4 to find all possible P_{PEV} values by searching through every possible control input (SOC_{thr}) in the valley hours. Figure 2.9 is an example of extracting the sensitivity information from Figure 2.8 at a specific time (4 AM), and the slope of the extracted curve is $\boldsymbol{S}$ to be used in Eqs. (2.12) and (2.13).

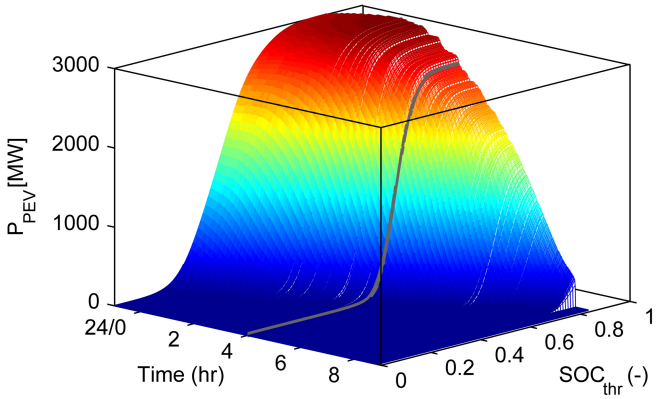

Figure 2.8 All possible values of P_{PEV} in valley hours

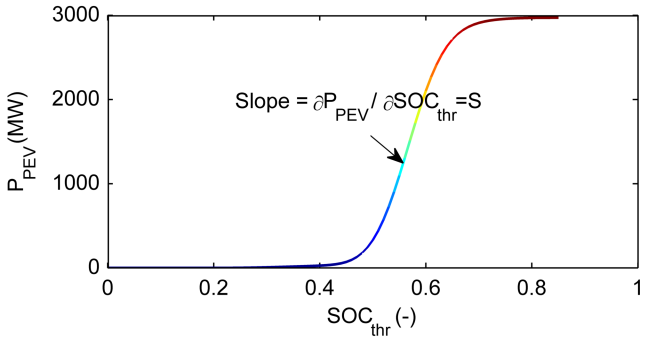

Figure 2.9 Extracted values of P_{PEV} at 4AM

Due to the fact that $\boldsymbol{S}$ changes over time, the feedback gains k_{soc} and $k_{\text{I,soc}}$ are not constant. A simplified constant gain controller is further derived by using the median value of $\boldsymbol{S}$ in Eqs. (2.11) and (2.12), which is easier to implement and possesses some

interesting stability properties. It also serves as a benchmark for the gain-scheduled algorithm illustrated in Eqs. (2.10)-(2.13). The stability will be discussed in the next section.

2.4 Simulations

The following simulations compare the PEV charging control algorithm (shown in Figure 2.5) with the baseline scenario (shown in Figure 2.3) on the performance of SOC satisfaction, frequency regulation, and valley filling.

Assumptions used in the simulations are as follows. Both simulations have two million PEVs, and the hourly scheduling (i.e. the slow-generating unit) is set up to follow the new load valley, P_{valley}, instead of the hourly nominal grid load, $P_{\text{L,nom}}$, during the valley hours to produce extra electricity for PEV charging. In terms of the non-PEV grid load, the actual load profile with sub-hour fluctuations shown in Figure 2.2 are used. Furthermore, in the case with the PEV charging control algorithm, it is assumed that the conventional reserves are turned off during the valley hours unless the frequency deviations are larger than 1 Hz. The threshold to re-activate conventional reserves is set to be larger than the typical range of the grid frequency deviation (which is around 1%), so that there will be a clear indication when the PEV fleet starts to lose control authority as an actuator for grid frequency regulation if this ever happens. The simulation horizon is confined between 10:04PM-8:52AM, which covers all valley hours, since it is assumed that only the home charging in the evening is available. Stability analysis on the PEV charging controller and simulations of other perturbed cases with different numbers of PEVs and unexpected changes in the fleet population are also reported to validate the robustness.

2.4.1 Performance Comparison

In terms of SOC charging satisfaction, both simulations have 98.5% of PEVs fully charged, which is attributed to the fact that the control algorithm takes the SOC and plug-off time of individual PEVs into consideration, and, therefore, the delays or interruptions in the PEV charging are appropriate.

However, these two simulations have different performances in frequency regulation and valley filling. Figure 2.11 shows the grid frequency trajectories and Figure 2.10 shows the aggregate load profiles. As stated in Section 2.3.3, faster closed-loop poles are chosen when designing the feedback gains for the PEV charging control algorithm. The real parts of the closed-loop poles for the PEV charging are about 2.85 times faster than those of using conventional reserves, and this is reflected in both figures. The PEV charging controller outperforms conventional reserves in that the grid frequency has much smaller deviations and the aggregate load is flat except for the very beginning and the very end of the valley hours. The former is because G is almost singular (the input/output relation is close to zero); the latter has the grid deviating to 62.3 Hz due to the fact that most PEVs are fully charged and, as a result, the PEVs start to lose control authority to regulate grid frequency.

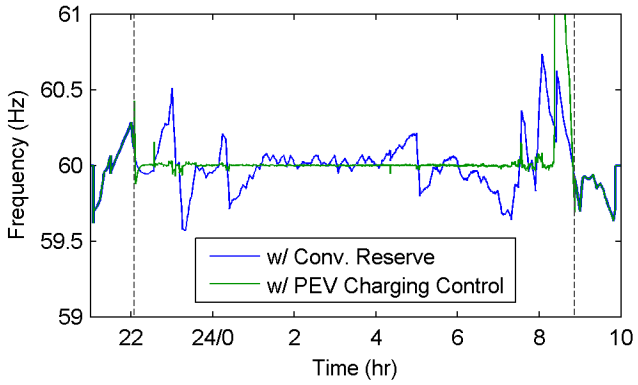

Figure 2.10 Grid frequency trajectories

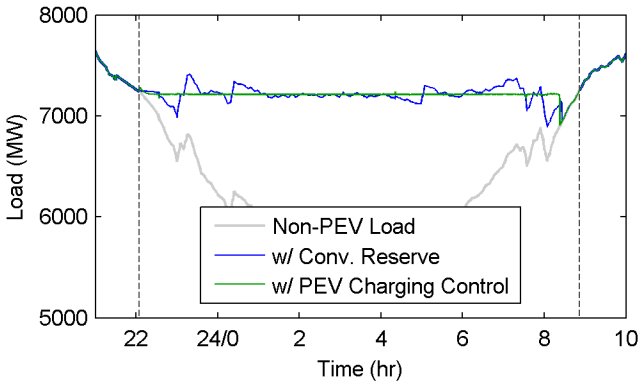

Figure 2.11 Aggregate load profiles

2.4.2 Stability of the PEV Charging Controller

Stability analysis is performed on the system shown in Figure 2.5, which has two time-varying elements, I (the system inertia) and G (the PEV charging allocation rule depicted in Figure 2.7). The system inertia varies with the magnitude of the grid load, and G is singular at the beginning of the valley hours but non-singular otherwise.

To conduct the stability analysis using the Nyquist plot, the block diagram in Figure 2.5 is rearranged and shown in Figure 2.12, so that the open-loop transfer function can be clearly recognized. In Figure 2.12, the mismatch between the grid load and the hourly generation from slow power plants are denoted as disturbances to cause grid frequency deviations, and the PEV charging control algorithm is represented by the PI-controller and the actuator dynamics, the latter of which is denoted as a time-varying constant gain. The time-varying gain, denoted as G, is essentially the sensitivity of the PEV charging load shown in Eq. (2.11), and is found to range between 0.0043 and 3.7231 with the unit of MW (megawatts). The fact that the actuator dynamics are represented as a gain reflects the assumption that the response of the PEV charging is instantaneously fast. Since the rearranged block diagram has a unity feedback path, its open-loop transfer function will be that shown Eq. (2.14).

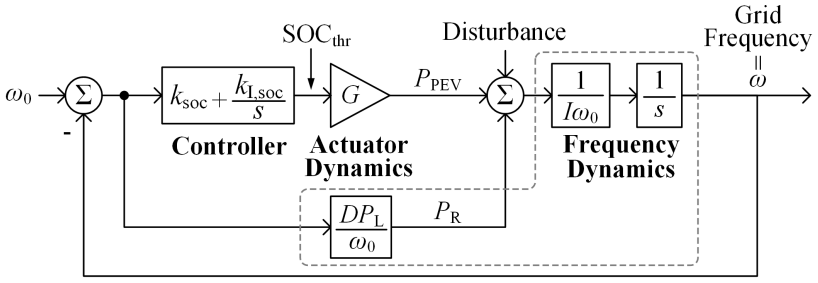

Figure 2.12 Block diagram of grid frequency dynamics with PEV charging control

$$L_{\mathrm{PEV}}(s)=\left[\left(k_{\mathrm{soc}}+\frac{k_{\mathrm{I,soc}}}{s}\right)G+\frac{DP_{\mathrm{L}}}{\omega_0}\right]\left(\frac{1}{I\omega_0 s}\right) \tag{2.14}$$

A similar rearrangement was made on the block diagram in Figure 2.3 for the case of conventional reserves, and the rearranged block diagram is shown in Figure 2.13, in which the actuator represents the first-order dynamics of the conventional reserves shown in Eq. (2.4). The open-loop transfer function is shown Eq. (2.15).

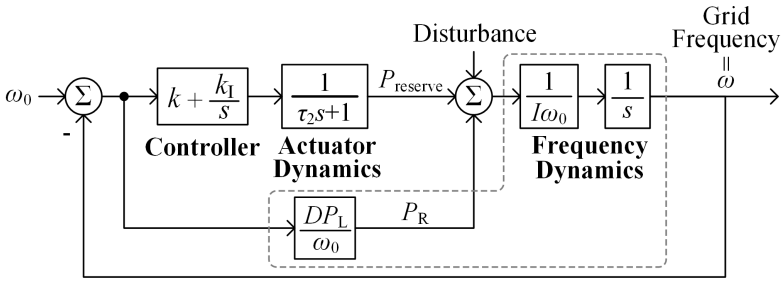

Figure 2.13 Block diagram of grid frequency dynamics with conventional reserves

$$L_{conv}(s)=\left[\left(k+\frac{k_I}{s}\right)\left(\frac{1}{\tau_2 s+1}\right)+\frac{DP_L}{\omega_0}\right]\left(\frac{1}{I\omega_0 s}\right) \tag{2.15}$$

In fact, the open loop dynamics of the grid frequency are always stable, including the moment when G is singular, although the frequency deviation may not stay within 1% if large mismatches between the load and generation happen. Furthermore, the PEV charging controller is found to have a good stability margin in the Nyquist plot with all possible combinations of I and G. Figure 2.14 shows the Nyquist plot of the two cases when the system inertia is at its minimum and G at its largest value, which happens in the middle of the valley hours (around 4AM). This is the moment when the smallest stability margin occurs. In fact, using the PEV charging control algorithm has a better (larger) stability margin (phase margin = 78.5 degrees) than using conventional reserves (phase margin = 33.0 degrees). This is because the PEV charging is assumed to have immediate response to the grid command whereas the response of the conventional reserves is limited by the actuator dynamics shown in Eq. (2.4).

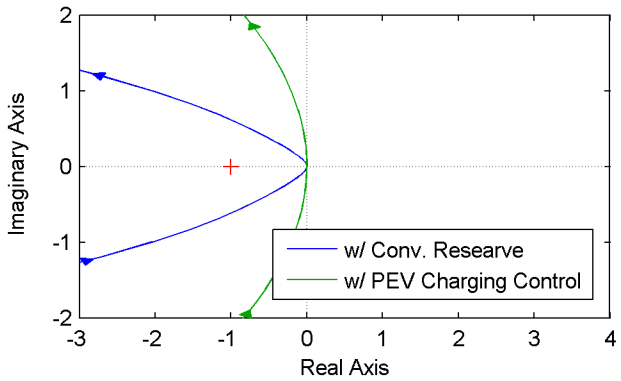

Figure 2.14 Nyquist Plot when the smallest stability margin happens

Table 2.1 summarizes the performance comparison between the PEV charging controller and the baseline scenario with conventional reserves. The maximum frequency deviation was measured only up to the moment before the PEV charging controller lost the control authority (around 8 AM), and the stability radius is defined as the shortest distance between the trajectory of the open-loop transfer function and the point at (-1,0) in the Nyquist plot. The fact that the PEV charging controller outperforms the conventional reserves is based on the assumption that the response of the PEV charging is instantaneous, which is idealized. However, the larger stability margin (compared with conventional reserves) shown in Figure 2.14 indicates that, as long as the communication delay of this control scheme is shorter than today's practice, the grid stability should be no worse than the current grid. This is most certainly the case, considering the fact that some of the conventional reserves are dispatched using phone calls made by human operators. In other words, even though communication delays are not considered in our simulation study and it is recognized that they will deteriorate the performance in grid frequency regulation, it is believed that they will not pose stability issues.

Table 2.1 Performance between Conventional Reserve and PEV Charging Control

	Max Freq. Deviation	**Max Load Deviation**	**PEV Charging Completion**	**Stability Radius**
w/ Conv. Reserve	1.24%	2.58%	98.45%	0.56
w/ PEV Charging Control	0.05%	0.13%	98.50%	1.00

2.4.3 Simulations of Fleets with More PEVs

The PEV charging controller is further applied to fleets with more PEVs. As shown in Table 2.2, the performance remains intact when the PEV number increases to 3 million. The SOC satisfaction, however, starts to decline when the vehicle number goes above 3.35 million. This limitation is because the charging algorithm determines the valley hours based only on the PEV SOC distribution (see Section 2.3.1) and not on the plug-off time distribution. To achieve the perfect valley filling, the valley hours will be longer when the fleet size is large; for example, a fleet of 3.35 million of PEVs will have

the charging happen between 3:11PM-11:39AM. The fact that most PEVs unplug before 10:30AM makes it impossible to fully charge every vehicle if the grid operator wishes to keep the aggregate load profile *perfectly* flat. A compromised solution will be to relax the cap on the aggregate load (i.e., to allow the parameter, P_{valley}, to bump up for several hours in the middle of the valley hours) and dispatch more power plants to accommodate the very large PEV fleet. Essentially, this means that, when the PEV fleet size is significantly large, there will be a compromise between the grid-level objective to achieve the valley filling and the vehicle-level objective to fully charge every PEV. However, the compromise will only happen when the PEV fleet size is very large.

Table 2.2 Charging Performance with Different PEV Fleet Sizes

PEV Fleet Size	Max. Load Deviation	Max Freq. Deviation	PEV Charging Completion
2 Million	0.13%	0.05%	98.50%
2.5 Million	0.24%	0.06%	98.60%
3 Million	0.11%	0.02%	97.85%
3.35 Million	0.09%	0.02%	91.8%

2.4.4 Early Plug-Off and Late Plug-In

Cases with unexpected PEV population changes, such as early plug-off and late plug-in, are also simulated. These two cases are essentially variations of changes in the PEV fleet size; however, here the fleet size is deliberately changed in the middle of valley hours. The early plug-off scenario has the PEV fleet size reduced at 6 AM and the late plug-in scenario has the fleet size increased at 12AM. Simulations show that the PEV charging controller can still regulate the grid frequency for most of the time in the valley hours when the PEV fleet size has ±20% variations, but the performance deteriorates. In the early plug-off case, the PEV fleet loses the control authority over grid frequency sooner because those PEVs that remain plugged-in got fully charged earlier and the controller had fewer vehicles available for manipulation. The late plug-in case suffers from the SOC satisfaction because the slow-generating units were not adjusted accordingly when more PEVs plug onto the grid. The case with substantial unexpected

late plug-in PEVs will be a difficult situation in the current grid practices because the scheduling slow-generating units is determined one day ahead and often will not change until the next day.

These simulations of unexpected PEV population changes offer another data point supporting the belief that the proposed PEV charging control algorithm can robustly regulate the grid frequency as long as adequate numbers of PEVs are connected to the grid. However, large changes in the PEV population may still impact the performance of SOC satisfaction because the current grid operation does not include intra-day adjustment in the hourly scheduling for slow-generating units.

2.5 Conclusion

The chapter presents a control algorithm for charging a large number of PEVs on the Michigan grid. The controller consists of two levels. The first level is the *centralized broadcast* done by the grid operator, and the second level is the *charging power allocation rule* executed by individual PEVs. The first level provides a means for the grid operator to command the charging to meet the grid-level objective, i.e., valley filling. The second level is a local controller, which addresses two important attributes of individual PEVs, the battery state of charge and the plug-off time, in a decentralized fashion. The local controller ensures the vehicle-level objective is satisfied, i.e., fully charging up PEV batteries. The algorithm also includes a feedback mechanism for grid frequency regulation; therefore, the PEV fleet can replace conventional reserves in the valley hours.

Simulations show that the local controller can satisfy the individual charging demand; in the nominal scenario with two million PEVs on the Michigan grid, 98.50% of PEVs can receive full battery charge. In addition, the proposed PEV charging algorithm achieves good frequency regulation during the valley hours, except at the very beginning and the very end. Conventional reserves will still be needed in those times. The good performance in the grid frequency regulation is attributed to the fact that the PEV charging is assumed to be able to respond to the grid command instantaneously fast, although the practicality, such as communication delays in the real implementation, is yet to be studied. Furthermore, valley filling and grid frequency regulation do not contradict

each other because these two dynamics are at very different time scales. Grid frequency has dynamics at the millisecond scale and requires very little energy to be regulated; hence, it will not affect the performance of valley filing, which has a time horizon about half-day long.

In terms of stability and robustness, the algorithm has a good stability margin in the Nyquist plot and has been validated in simulations with different sizes of PEV fleets. However, the control algorithm is still limited by the leeway granted by the PEV plug-in time and plug-off time distributions. When the PEV fleet size is extremely large and exceeds the grid capacity, the percentage of PEVs got fully charged will start to decrease. Simulations have also shown that this control algorithm is robust even when the size of the PEV population changes unexpectedly in the middle of the valley hours. It is also worth mentioning that this PEV charging control algorithm may slow down the PEV charging but will not discharge the batteries, and thus there is no extra energy cycling on PEV batteries to decrease the battery life.

CHAPTER 3

Control of Battery Energy Storage to Mitigate Wind Power Intermittency

Intermittency is a major challenge for the integration of wind power to the electric grid. Studies have shown that more reserves will be needed to cover the wind intermittency [96, 97]. In the current practice, reserves are provided by fast-acting dispatchable sources, such as natural gas turbines or hydro generators. However, there is a new interest in using energy storage devices to mitigate the wind intermittency due to the emerging plug-in electric vehicles, and it has been shown in the previous chapter that they can be a useful asset to facilitate grid operation by controlling the battery charging. Therefore, although various technologies are being considered as the energy storage system for utility-scale operations [98-101], the following discussion focuses on the battery energy storage system (BESS).

Figure 3.1 depicts how BESS can be used to mitigate wind power intermittency as opposed to using conventional reserves. The assumption is that the wind farm owner will choose the amount of wind power to sell to the grid to isolate the power grid from fluctuations in the actual fluctuating wind generation, instead of treating wind power as a negative load on the grid. Treating wind power as a negative load may work when the wind power is a small fraction of load, but not so when the wind penetration is high. This decision making done by the wind farm owner will be called *wind power scheduling* in the following discussion. In Figure 3.1-(a), with conventional reserves, a conservative control action, i.e., scheduling wind power lower than the forecast, will likely lead to wind curtailment and revenue loses. On the other hand, an aggressive control action will likely require dispatching conventional reserves in order to cover wind deficit, which incurs costs. In Figure 3.1-(b), with BESS, a conservative (aggressive) control action implies charging (discharging) the battery, and, as long as the battery SOC can be

controlled within an appropriate window, there is no need to curtail wind power or dispatch conventional reserves.

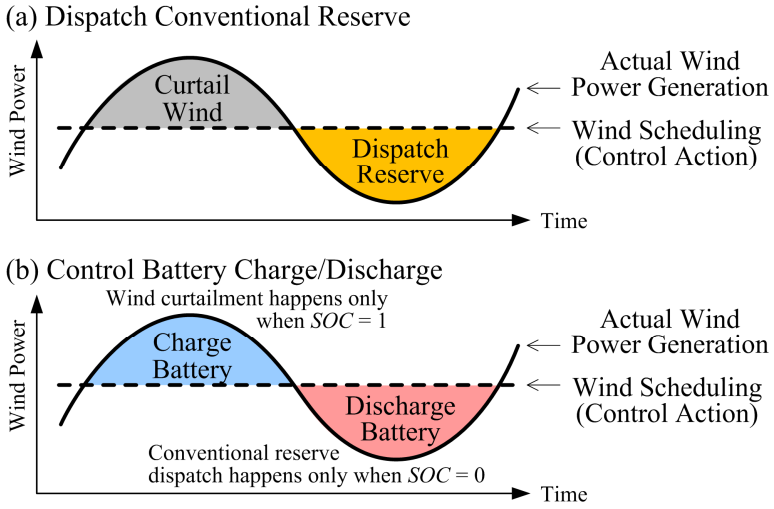

Figure 3.1 Two different ways to mitigate wind power intermittency

From the concept depicted in Figure 3.1, there is no doubt that BESS will be more effective than conventional reserves in absorbing wind power fluctuations. However, a more interesting question is what is the appropriate capacity of BESS to secure revenues for the wind farm owner. The answer will depend on the control algorithm for BESS charging and discharging. Therefore, this chapter will discuss the control and sizing of BESS for mitigating wind intermittency. In particular, the model predictive control (MPC) technique is used to control the charging and discharging of BESS to compensate for wind power forecast errors and minimize operation costs to the wind farm owner. The ultimate goal is to make wind power dispatchable on an hourly basis like fossil fuel power plants so that renewable generation can compete with non-renewable generation in the wholesale market in the future.

The rest of the chapter is organized as follows: Section 3.1 reviews the relevant literature; Section 3.2 presents models to describe the stochastic wind power outputs and the battery SOC dynamics; Sections 3.3 shows the performance of baseline scenarios with conventional reserves and a heuristic algorithm for BESS; Sections 3.4 presents the development of the MPC controller; Section 3.5 discusses the sizing of BESS; and, Section 3.6 gives concluding remarks.

3.1 Literature Review

Depending on the time scales in the grid operation, BESS can be designed and controlled to defer upgrades, achieve price arbitrage, or support reserves [101, 102]. Arbitrage refers to the strategic practice in which arbitrageurs take advantage of price differences in the market by buying the product when the price is low and selling it when the price is high. Consequently, methodologies for sizing the BESS capacity and associated control algorithms for energy management differ. A summary on related literature is shown in Figure 3.2, and the various methodologies are highlighted blow.

Many different studies for sizing BESS to accommodate intermittent renewable energy exist in the literature, including: minimizing costs of battery system installation and reserve dispatch by stochastic linear programming [103] or by mixed-integer programming [104], maximizing the annual revenue to the wind farm owner by dynamic programming [105], using the artificial neural network as control strategies to schedule wind power [106], using Discrete Fourier transform to decompose forecast errors and quantify imbalances to be compensated by the energy storage system [107], conducting Monte-Carlo simulations to access the minimum storage requirement based on the degree of risk that the power producer choses to be exposed to [108], and conducting detailed dc-bus voltage simulations to find the minimum storage capacity to meet voltage regulation requirement [109]. A common theme can be identified from the diverse BESS sizing strategies: methodologies focusing on shorter time scale dynamics (such as voltage and frequency regulation) generally lead to BESS with smaller capacities, whereas methodologies focusing on longer time scale objectives (such as price arbitrage) result in BESS with larger capacities.

Other studies concerning only control algorithms for BESS and not sizing include: adopting droop control or PI-control algorithms to regulate voltage and/or frequency [110-112], using MPC to track battery SOC and to smooth wind power outputs [113-117], and solving optimizations for price arbitrage by linear programming [118]. There are also studies solving price arbitrage optimizations with hydro power [51, 119] or hydrogen storage [120] instead of BESS.

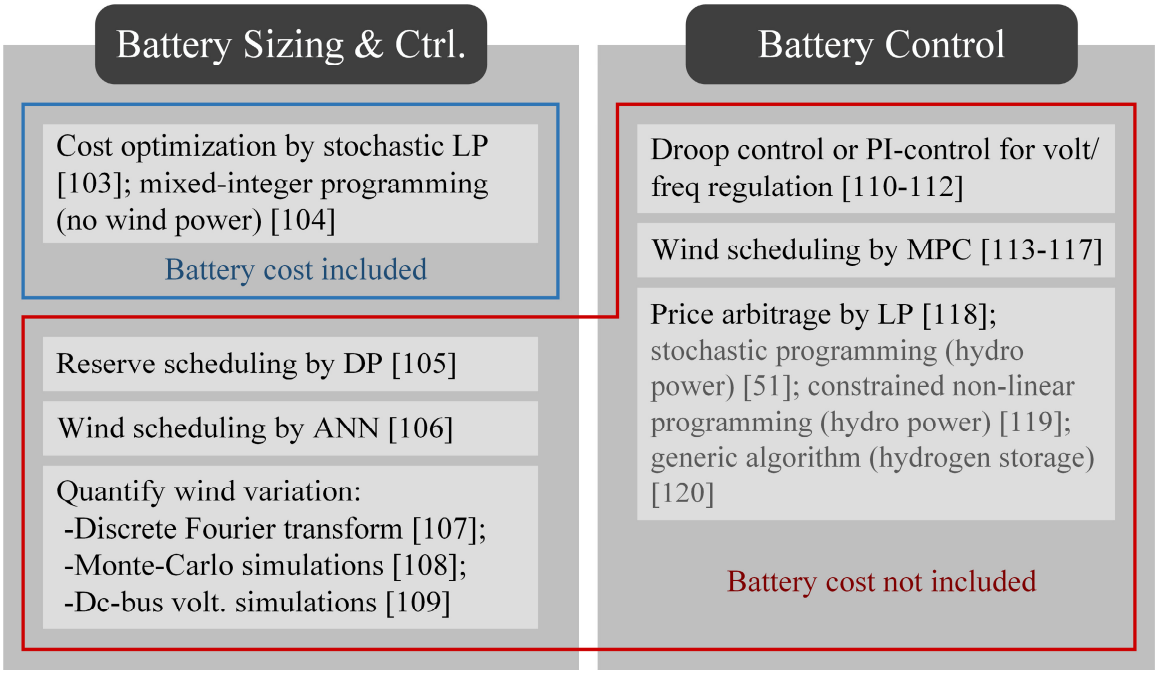

Figure 3.2 Summary of literature related to BESS sizing and control for wind power

The literature has shown many possibilities of introducing BESS to facilitate different grid operations. In this chapter, the focus is to make wind power dispatchable on an hourly basis, and thus the role of BESS is to supply hourly-long reserves. The wind power scheduling/dispatch will be formulated as a cost optimization problem to maximize revenues to the wind farm owner. MPC is used because of its superior performance in solving horizon problems. Meteorologists now can provide forecasts of wind power outputs up to several hours to the future with reasonable accuracy [121, 122] and such future predictions can be incorporated in the framework of MPC. However, unlike the quadratic objectives used in most existing MPC studies for state tracking or output regulation, the realistic operation costs to the wind farm owner, in particular, the reserve costs to cover wind intermittency, will be used in this Chapter as the objective function to find the optimal control actions for BESS. In addition, MPC can help to enforce constraints on battery SOC in future time steps, so MPC may help to downsize BESS. This work has been published in [123].

3.2 Modeling

This section presents models for the stochastic wind power output and the battery. The wind generation will be described by probability distributions, and the battery model includes the SOC dynamics and power limits for charging and discharging.

3.2.1 Wind Power

The intermittency of wind power can be described by the probability distribution. A wind farm with an 800 MW nameplate capacity in the eastern area of Michigan is chosen from the Eastern Wind Dataset of the National Renewable Energy Laboratory (NREL) [124]. The raw data includes two data strings; one is the 4-hour-ahead wind forecast, and the other is the actual wind power generation. Therefore, in this study, it is assumed that the 4-hour-ahead wind forecast is known information to the wind farm owner, although the actual wind power generation remains unknown. Also, the forecast horizon of the wind power output dictates the receding horizon of the MPC controller to be no longer than 4 hours (see more details in Section 3.4.1). Furthermore, it is possible to improve the forecast accuracy by fusing the forecasted and actual wind power outputs with a Kalman filter or other sensor fusion techniques, but this is not considered in this study. Figure 3.3 shows a one-week long snapshot of the forecast and actual wind power outputs of this wind farm. The whole year-long data in [124] are used to extract the conditional probability distribution, denoted as $\mathbf{P}(w_a|w_f)$, which represents the (stochastic) actual wind generation (w_a) under a given forecast (w_f), shown in Figure 3.4. The temporal correlation of wind power outputs is not considered. The peak value of each distribution is close to the forecast value, w_f, implying that the forecast is generally good.

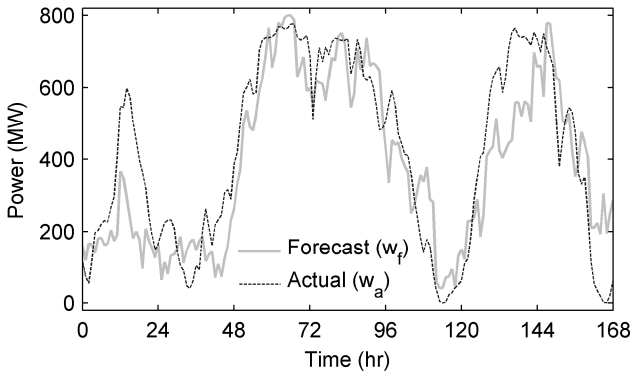

Figure 3.3 One-week long power outputs of an 800MW wind farm

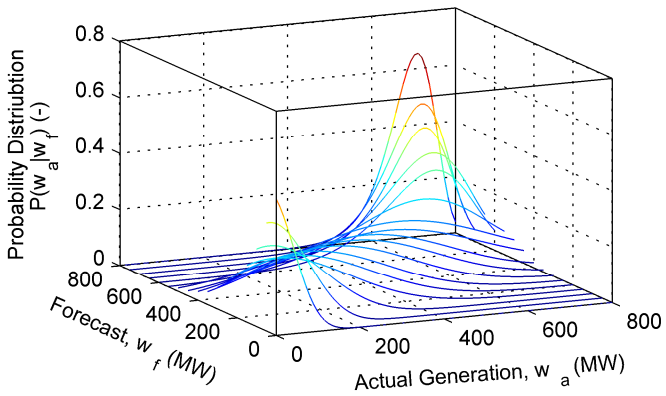

Figure 3.4 The conditional probability distributions, $\mathbf{P}(w_a|w_f)$

The probability distribution is then used to derive the reserve requirement ($R_{w,rqd}$) and *expected* wind power deficit (w_d) by Eqs. (3.1) and (3.2). The assumptions behind Eqs. (3.1) and (3.2) are that wind over-production can always be curtailed and reserves need to be scheduled to cover 95% of under-production. Curtailing surplus wind outputs has been seen in real-world practices for stability-related reasons [125], and it is likely to become a norm for the wind farm owner or grid operator to avoid risks in the market when the wind penetration level is high in the future.

$$R_{w,rqd}(w_f, w_s) = [w_s - \mathbf{F}^{-1}(0.05)]^+ \tag{3.1}$$

$$w_d(w_f, w_s) = \mathbf{E}\{[w_s - w_a]^+\} \tag{3.2}$$

where both $R_{w,rqd}$ and w_d are functions of w_f and w_s. w_s is the scheduling of wind power, which is a control variable to be detailed in Section 3.3 and 3.4. **F** is the cumulative

probability distribution function of $\mathbf{P}(w_a|w_f)$, and $\mathbf{F}^{-1}$ is the inverse of $\mathbf{F}$. Then, $\mathbf{F}^{-1}(0.05)$ is the guaranteed wind power generation for 95% of time. Figure 3.5 shows the example of $\mathbf{F}$ at w_f = 400MW, and its inverse is found to be 58MW. This can be interpreted as follows: when the forecast is at 50% of the nameplate capacity, the actual wind output will be at least 7.25% of the nameplate capacity for 95% of time. Then, Eq. (3.1) quantifies how much reserves need to be *scheduled* when the wind farm owner decides to schedule wind power higher than 7.25% of the nameplate capacity, and Eq. (3.2) quantifies the amount of reserves that are expected to be *dispatched*. Both the reserve scheduling and reserve dispatch matter because they induce costs to the wind farm owner. The plus sign (+) in both Eqs. (3.1) and (3.2) indicates the truncation of negative values, and the expectation (the operation imposed by **E**) in Eq. (3.2) is taken with respect to w_a.

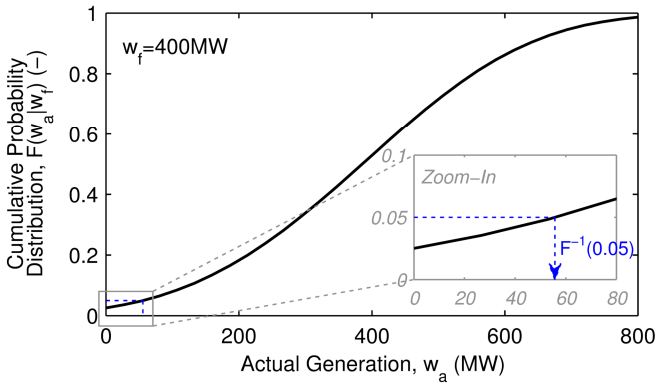

Figure 3.5 The cumulative probability distributions, $\mathbf{F}(w_a|w_f)$, at w_f = 400MW

3.2.2 Battery

The dynamics of the battery SOC is governed by Eq. (3.3), with the assumptions that efficiencies of both charging and discharging are perfect and responses of both charge and discharge are instantaneously fast.

$$SOC(t+1) = SOC(t) - \frac{P_{batt} \cdot \Delta t}{Q} \tag{3.3}$$

where P_{batt} is the battery discharge power, the time step, Δt, is one hour, and Q is the battery capacity. This battery model is essentially identical to that in Eq. (2.6) for the PEV battery.

Since the focus here is to make wind power dispatchable on an hourly basis, the role of BESS is to supply hour-long reserves. Assuming that the remaining energy content in the battery can be discharged in one hour, the power limits for charging and discharging then can be derived based on the level of SOC. Thus, it can be understood that BESS with a larger capacity will have larger discharge and charge power limits. For example, an 800 MWh BESS will have the discharging limit as 800MW at full SOC, whereas a 200MWh BESS will have the discharging limit only as 200MW at full SOC. Figure 3.6 shows the power limits of various BESS capacities as functions of SOC. The power limits saturate at ±800MW because the wind surplus and deficit will never exceed the nameplate capacity. Note that these limits are imposed to guarantee that BESS can cover wind power surplus or deficit for at least one hour before the next scheduling update happens, and these limits are not based on physical limitations of battery chemistry and power electronics. It is further assumed that the wind power deficit exceeding the battery discharging limit must be backed up by conventional reserves, and the wind surplus exceeding the battery charge limit will be curtailed. The former induces additional costs on the wind farm owner and the latter reduces revenues. Thus, it is crucial to control the battery SOC, so that the BESS can compensate for wind forecast errors as much as possible.

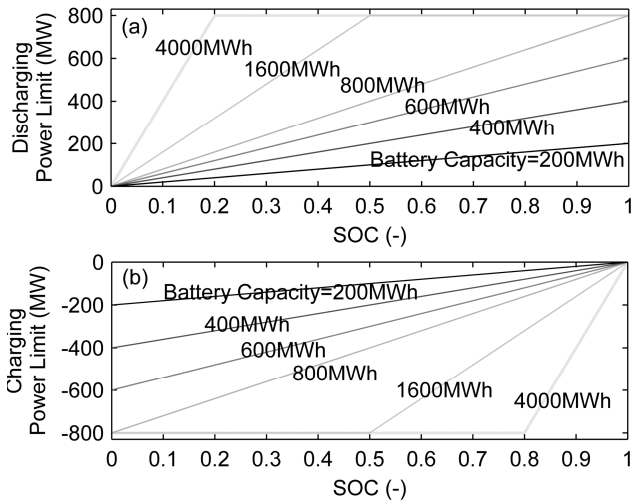

Figure 3.6 Power limits of battery. Subplot (a): discharge; (b): charge

3.3 Mitigating Wind Power Intermittency

In this section, two scenarios are investigated to quantify the effectiveness of BESS over conventional reserves for mitigating wind intermittency. The scenario with conventional reserves involves solving an instantaneous cost optimization problem, and the scenario with BESS adopts a heuristic algorithm to control BESS to absorb wind fluctuations. In both scenarios, the wind forecast of the *current* operation hour is assumed to be known to the wind farm owner, who has to determine the wind power scheduling, i.e. the amount of wind generation to sell to the grid. This is contrast to the MPC controller that will be presented in the next section, which is assumed to know the wind forecasts over several hours long. The comparison will reveal the value of factoring the future information in the wind power scheduling.

3.3.1 Conventional Reserve

When using conventional reserves to mitigate wind intermittency, the wind farm owner solves the instantaneous optimization problem shown in Eq. (3.4) every hour to find the optimal wind power scheduling to minimize J, which is the total hourly cost to the wind farm owner. The objective function J consists of three terms: 1) the revenue of selling wind power to the grid, 2) the expense of scheduling conventional reserves, and 3) the expense of dispatching conventional reserves when wind under-production occurs. Notice that wind over-production is assumed to be curtailed and reserves need to cover only under-production. Since the grid is assumed to have no energy storage or demand response, the wind farm owner has to schedule conventional reserves up to the quantity defined in Eq. (3.1) and is *expected* to dispatch conventional reserves at the quantity defined in Eq. (3.2). The problem formulation is similar to the wind scheduling study in [126], and reflects that fact that, if the reserve-related costs to compensate for wind intermittency are considered, scheduling wind power will not be entirely free.

$$\min_{u} : J = -C_1 \cdot u + C_2 \cdot R_{\mathrm{w,rqd}} + C_3 \cdot w_{\mathrm{d}} \tag{3.4}$$

where the control, u, is the wind scheduling (w_{s}). The coefficients C_1, C_2, and C_3 are the unit price of electricity generation, and unit cost of reserve scheduling and reserve

dispatch; their values are defined in Eq. (3.5). The assumptions for reserve costs are: 1) the reserve scheduling cost is 3% more expensive than the price of electricity generation, based on the statistics in [127]; and, 2) the reserve dispatch cost is the same as the generation price and only occurs if the reserve is dispatched. Furthermore, these three price/cost coefficients are normalized, and thus they only demonstrate that reserves are relatively more expensive than the electricity generation but not represent the face value the wind farm owner may earn or pay for. The optimization is solved with the assumption that the wind forecast (w_f) at the current time step is known.

$$C_1 = 1; \quad C_2 = 1.03; \quad C_3 = 1 \tag{3.5}$$

Figure 3.7 shows the optimal wind power scheduling in a one-week long time window with a 4,000MWh BESS (the black trajectory), in which the wind power scheduling is conservative (i.e., much lower than the forecast) for most of the time because the optimization directs the wind farm owner to avoid paying for conventional reserves. A one-year long simulation shows that more than 60% of wind power outputs are curtailed. This motivates us to use BESS to mitigate wind power intermittency because, according to the illustration in Figure 3.1-(b), BESS can, not only make up wind defect by discharging the battery, but also absorb wind surplus by charging the battery.

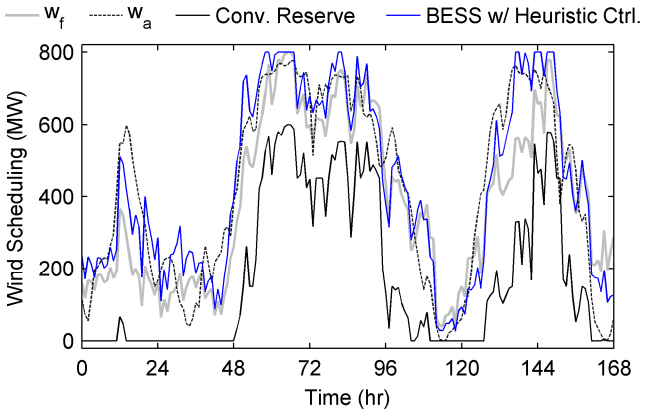

Figure 3.7 Wind scheduling with conventional reserves and BESS (Q = 4,000 MWh)

3.3.2 Heuristic Control Algorithm

To use BESS to compensate for wind intermittency, a control algorithm is needed to regulate the battery SOC. A heuristic rule based on the current wind forecast and battery SOC is designed to schedule the wind power, as shown in Eq. (3.6).

$$u = w_s = w_f \cdot g \tag{3.6}$$

where g is a scaling factor varying with respect to battery SOC. Figure 3.8 shows two sets of scaling factors: the blue line means that the wind farm owner adopts a simple-minded strategy which uses the wind forecast directly as the control without manipulation, whereas the red line means that the wind farm owner is concerned about the battery SOC and will schedule wind power at half of the forecast when SOC is at zero and at twice of the forecast when SOC is at one. Once the wind scheduling is known, the battery discharge power can be computed using Eq. (3.7) to update the battery SOC.

$$P_{batt} = u - w_a = w_s - w_a \tag{3.7}$$

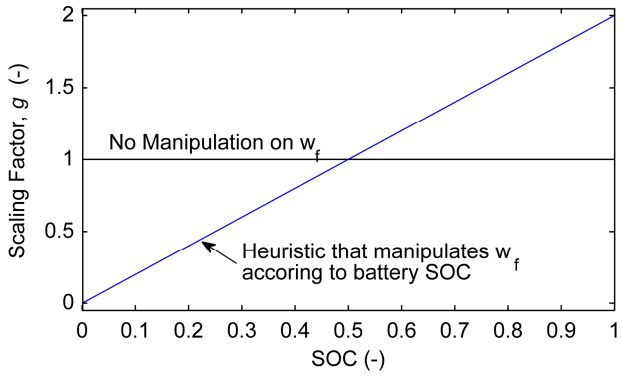

Figure 3.8 Scaling factor for the heuristic control

Simulation results using a 4,000MWh BESS with the heuristic control algorithm to mitigate wind power intermittency are shown Figure 3.7 (the blue trajectory). Compared to the optimal scheduling with conventional reserves (the black trajectory), the heuristic control algorithm is less conservative, which increases the revenue (the converse of the cost) to the wind farm owner by five times (see Figure 3.16) and reduces the wind curtailment down to 0.6% (see Figure 3.18). However, to achieve zero wind curtailment,

the battery capacity needs to be significantly larger (16,000MWh), which was found by the exhaustive search over a wide range of BESS capacity.

The heuristic control, which uses only the current wind forecast to control BESS, shows promising results in reducing wind curtailment. Therefore, there is hope that if MPC is used to factor in the future wind forecasts, more sophisticated control algorithms can be obtained to improve performances or downsize the BESS. The MPC control algorithm is presented in the next section.

3.4 Model Predictive Control (MPC) for BESS

MPC is a control design framework whose control action is determined based on the solution of an on-line optimal control problem rather than a pre-defined relation to observed state [128]. A cost function is formulated over a future interval, a model that represents the underlying system is incorporated to predict future system response as a function of the control input, and both the current and future constraints and/or predictions are taken into account in deriving the optimal control sequence. As a receding horizon approach, only the first element in the optimal control sequence will be implemented, and the optimization procedure is repeated in the next time step using a new updated state.

MPC is suitable for controlling BESS to mitigate wind power intermittency because, in general, the wind farm owner will have information on wind forecasts several hours prior to the operating time. This information can be well incorporated in the framework of MPC to better utilize the storage function granted by the BESS to maximize revenues (minimize costs) of the wind farm owner. However, unlike the quadratic objectives commonly used in MPC studies for state tracking or output regulation [113-115], the realistic operation costs to the wind farm owner will be used here as the objective function to find the optimal control actions for BESS. This allows the MPC results to be compared with those reported in the previous section.

3.4.1 MPC Design

The MPC controller uses the objective function in Eq. (3.8) to find the optimal wind power scheduling. The objective function J_k is designed to be comparable (although

not identical) to that in Eq. (3.4), in that the revenue of selling wind power to the grid, the expense of scheduling conventional reserves, and the expense of dispatching conventional reserves are included. In addition, a penalty on the terminal state is included for stability consideration and the coefficient C_N weighs the importance of the state stability relative to the total costs over the optimization horizon. The time resolution of this optimization problem is one hour.

$$\min_{u} : J_k = \sum_{t=k}^{k+N-1} \left[-C_1 \cdot u_1(t) + C_2 \cdot R_{\mathrm{s}}(t) + C_3 \cdot R_{\mathrm{d}}(t) \right] + C_N \cdot (x(k+N) - x_{\mathrm{ref}})^2 \tag{3.8}$$

where the control, u, is again the wind scheduling (w_{s}), the state, x, is the battery SOC, and x_{ref} is the desired SOC. R_{s} is the scheduling of conventional reserves, and R_{d} is the expected dispatch of conventional reserve, both of which are functions of u, x, and w_{f}, as defined in Eqs. (3.9) and (3.10). The optimization horizon is denoted as N.

$$R_{\mathrm{s}} = [R_{\mathrm{w,rqd}} - P_{\mathrm{dis,lmt}}]^+ \tag{3.9}$$

$$R_{\mathrm{d}} = [w_{\mathrm{d}} - P_{\mathrm{dis,lmt}}]^+ \tag{3.10}$$

The implication of Eqs. (3.9) and (3.10) is that using the BESS is preferred over dispatching conventional reserve as the latter induces costs. Since conventional reserves are still kept as an option for mitigating wind intermittency in addition to BESS in Eq. (3.8), at least one feasible solution is guaranteed to exist. This means that the optimization will just reduce to that defined in Eq. (3.4) in the worst case scenario when the battery is fully charged ($P_{\mathrm{chg,lmt}} = 0$) or completely depleted ($P_{\mathrm{dis,lmt}} = 0$).

Several constraints on the state and control are imposed, including Eqs. (3.3) and (3.7) on the state dynamics, and Eqs. (3.11)-(3.13) for lower and upper bounds on the state and control.

$$0 \le x \le 1 \tag{3.11}$$

$$0 \le u \le U \tag{3.12}$$

$$P_{\mathrm{chg,lmt}} \le P_{\mathrm{batt}} \le P_{\mathrm{dis,lmt}} \tag{3.13}$$

where U is the upper bound for the control and takes the value of the nameplate capacity of the wind farm (800MW), $P_{\text{chg,lmt}}$ and $P_{\text{dis,lmt}}$ are the power limits of battery charge and discharge (as shown in Figure 3.6). The time horizon of the optimization is chosen to be 4 hours long because the 4-hour-ahead wind forecast is readily available in the NREL wind dataset [124]. The Dynamic Programming technique is used to solve the optimization problem defined by Eqs. (3.8)-(3.13). A review of Dynamic Programming can be found in Appendix B.

Before diving into the implementation of the MPC controller, a hypothetical scenario with $w_f = w_a = 400$MW throughout the receding horizon is examined. This hypothetical scenario allows us to analyze and decipher the solutions to the optimization problem in Eq. (3.8). The battery capacity (Q) is assumed to be 1,600MWh in this hypothetical scenario, and the desired SOC (x_{ref}) is chosen to be 0.5. The initial condition has the state starting at 50% SOC.

Impact of C_N on the optimal solution: There is no surprise that C_N will affect the optimal control, which will steer the state trajectory to avoid the penalty on the terminal state (x^*_{k+N}). Figure 3.9 and Figure 3.10 show the optimal control and state trajectories with four different values of C_N. The $C_N = 0$ case [see Figure 3.9-(a) and Figure 3.10-(a)] has the highest revenue because a part of the revenue comes from selling the energy residing in the battery. As C_N increases, u^* will take less aggressive values in the middle of the receding horizon to avoid discharging the battery and to avoid the penalty on x^*_{k+N}.

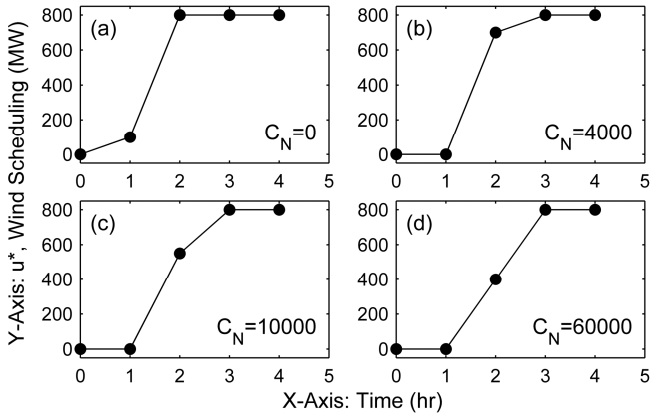

Figure 3.9 Evolution of the optimal control trajectories when C_N increases ($w_f = w_a = 400$MW at all times; $Q = 1{,}600$MWh; $x_{\text{ref}} = 0.5$)

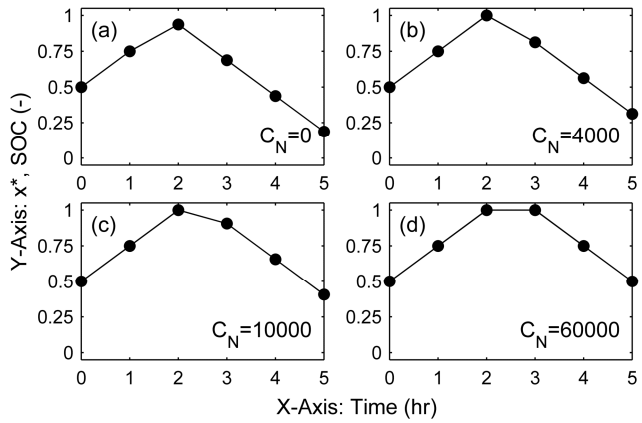

Figure 3.10 Evolution of the optimal state trajectories when C_N increases ($w_f = w_a$ = 400MW at all times; Q = 1,600MWh; x_{ref} = 0.5)

However, although the value of C_N impacts the optimal solution to Eq. (3.8), Figure 3.9 shows that the four cases with different C_N all have the same u_1^*. Since MPC only implements the first element of the optimal control sequence, the impact of C_N, surprisingly, may not be as pronounced as expected in the MPC realization for this specific choice of the objective function and prediction horizon. If one wishes to have better state regulation, the objective function needs to include penalties on the state at each and every time step, rather than only on the terminal state. On another note, for downsizing BESS, it is found to be more preferable not to impose constraints on the battery SOC, so that the BESS capacity can be better utilized. In fact, the sizing study in Section 3.5 is done with $C_N = 0$.

Non-unique optimal solutions: Eq. (3.8) has non-unique optimal solutions due to the truncation operation in Eqs. (3.1)-(3.2) and Eqs. (3.9)-(3.10). More specifically, the truncation operation makes the objective function indifferentiable to different control actions if the reserve requirements stay below the discharging limit of BESS. Figure 3.11 and Figure 3.12 show six sets of representative optimal solutions (among the infinite sets of optimal solutions) with C_N fixed at 60,000 in the hypothetical scenario. The value of C_N is chosen to be substantially large for the analysis purpose, although it was set to zero when implementing the MPC controller. Having C_N larger than 60,000 will force the terminal state to land right at 50%, which is the same as the initial state, meaning that the BESS will have no SOC changes at the end of this hypothetical scenario. This allows a fair comparison. Figure 3.11 and Figure 3.12 use consistent color codes, meaning that the

red control trajectory in Figure 3.11 produces the red state trajectory in Figure 3.12 and vice versa. Under the premise that all the six sets of solutions have the same terminal state x^*_{k+N} and the same optimal cost (J_k^* = -2000), the optimal control trajectories are very different. In particular, u_1^* can take a value from zero to 800 (i.e. the rated power the wind farm), which implies completely different wind scheduling strategies for MPC implementations. Adopting an aggressive u_1^* is likely to result in low battery SOC, which helps to reduce wind curtailment, whereas adopting a conservative u_1^* is likely to result in high battery SOC, which helps to avoid using conventional reserves. The fact that the chosen objective function in Eq. (3.8) processes non-unique solutions makes it numerically more difficult to solve the optimization problem. Two other objective functions based on Eq. (3.8) are proposed in the next section to assure uniqueness of the solution to the optimization problem, although having multiple optimal solutions may not be a bad thing in reality, in that the wind farm owner has the flexibility to choose among multiple options to better serve a specific preference or to accommodate other secondary objectives.

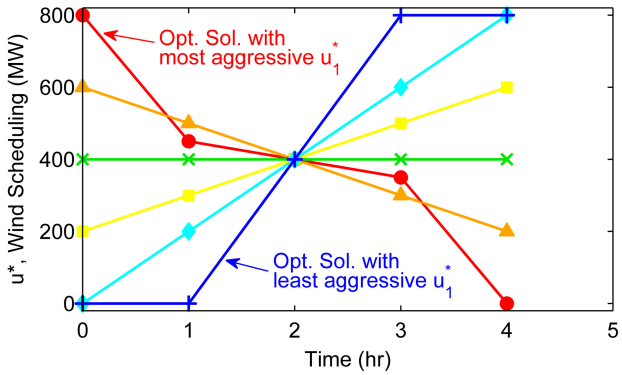

Figure 3.11 Non-unique optimal control trajectories
($w_f = w_a = 400$MW; $Q = 1{,}600$MWh; $x_{ref} = 0.5$; $C_N = 60{,}000$)

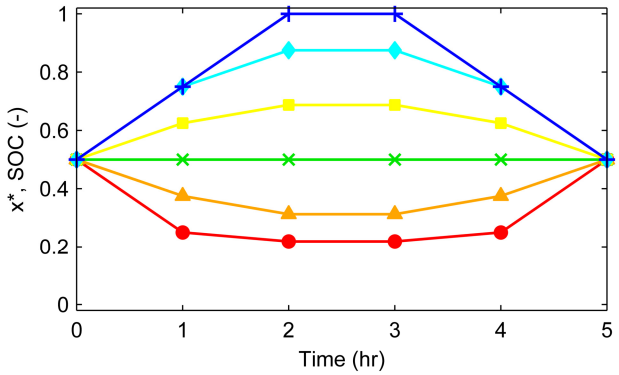

Figure 3.12 Non-unique optimal state trajectories
($w_f = w_a = 400$MW at all times; $Q = 1{,}600$MWh; $x_{ref} = 0.5$; $C_N = 60{,}000$)

3.4.2 Revised Optimization Formulation for MPC

Two more optimization formulations are proposed based on Eq. (3.8) to eliminate the non-unique solutions; the first was to impose a forgetting factor on the objective function, as shown in Eq. (3.14), and the second was to impose a penalty on the *change* in wind power scheduling, as shown in Eq. (3.15).

$$\min_{u} : J_{1,k} = \sum_{t=k}^{k+N-1} \left[-C_1 \cdot u_1(t) + C_2 \cdot R_s(t) + C_3 \cdot R_d(t) \right] \cdot \gamma^{t-k} \tag{3.14}$$

$$\min_{u} : J_{2,k} = \sum_{t=k}^{k+N-1} \left[-C_1 \cdot u_1(t) + C_2 \cdot R_s(t) + C_3 \cdot R_d(t) + C_4 \cdot \left| u(t) - u(t-1) \right| \right] \tag{3.15}$$

where is γ the forgetting factor, which is a positive number slightly less than one, and C_4 is the ramp rate cost and takes the value defined in Eq. (3.16), which is derived by normalizing the pricing data in [129].

$$C_4 = 30/55 \tag{3.16}$$

The idea of imposing a forgetting factor on the objective function originates from the fact that MPC will only implement the first element in the optimal control sequence; therefore, the cost at the first step deserves a higher weight. Moreover, it is also generally true that the prediction for the immediate future is more accurate than those further down the road. This treatment takes advantage of knowing the particular way in which MPC executes and guarantees a unique solution. In fact, the red trajectory in Figure 3.11 will

be the optimal solution for $J_{1,k}$ because it has the most aggressive u_1^*. Note that, due to the forgetting factor imposed on the objective function, a control sequence with aggressive controls in earlier time steps will result in a better (lower) cost. Figure 3.13 shows the wind scheduling when a forgetting factor of 0.999 is used in the MPC implementation. The result is qualitatively similar to the heuristic algorithm shown in Figure 3.7, in that the wind farm owner is more daring in scheduling wind power than the scenario with conventional reserves; however, with MPC, the wind farm owner is able to do so with a much smaller BESS.

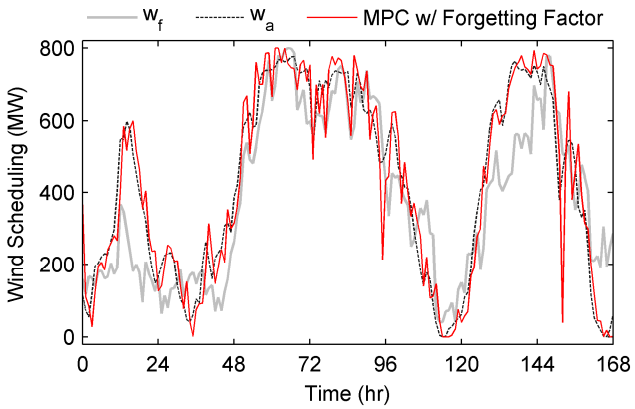

Figure 3.13 MPC implementation with forgetting factor (Q = 800MWh; C_N = 0)

The second idea of imposing a penalty on the change in wind power scheduling is based on the practical consideration that smooth wind power outputs are more preferable. In fact, minimizing wind output fluctuations has been used as the optimization objective in most MPC-related studies [113-117]. Although rigorous mathematical proof is not available, extensive numerical simulations show that this treatment also produces unique optimal solution. Furthermore, the optimal solution for $J_{2,k}$ turns out to be the green trajectory in Figure 3.11 because it has the least fluctuations. Figure 3.14 shows the wind scheduling when the penalty on wind scheduling changes is imposed in MPC, and it can be seen that the wind scheduling is indeed smoother than that in Figure 3.13.

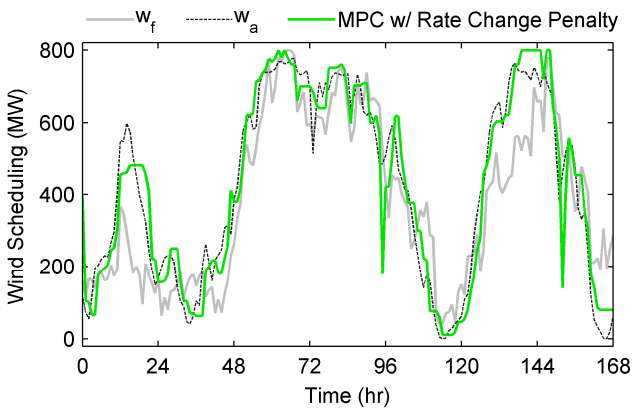

Figure 3.14 MCP implementation with penalty on wind scheduling changes (Q = 800MWh; C_N = 0)

Another difference that can be observed between these two revised optimization formulations is the SOC trajectory. Figure 3.15 shows that the formulation with the penalty on the wind scheduling change ($J_{2,k}$) will result in more oscillatory SOC as BESS has to absorb more wind power fluctuations.

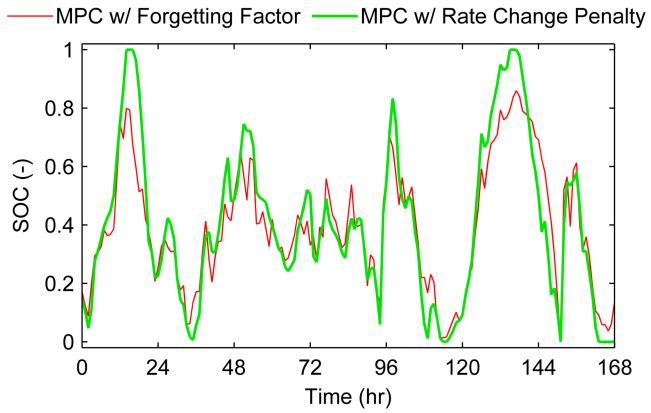

Figure 3.15 Optimal state trajectories (Q = 800MWh; C_N = 0)

3.5 Sizing of BESS

The analysis on BESS sizing is done by evaluating the annual revenue (the converse of the operation cost) to the wind farm owner. Note that battery cost is not considered as a criterion for sizing BESS because it is an expense that should be paid off throughout the lifespan of BESS, rather than in one single operation year. Therefore, subtracting battery cost from the annual revenue is not meaningful. An appropriate way

to incorporate the battery cost in the grid operation has to consider the discount rate and asset depreciation, which will be discussed in detail in Chapter 6. In this section, a more straightforward goal for BESS sizing is used: to reduce the BESS capacity as much as possible while maintaining reasonable revenues to the wind farm owner.

Two comparisons on the annual revenues are presented: Figure 3.16 summarizes the MPC results based on the optimization formulation in Eq. (3.14), whereas Figure 3.17 summarizes results based on Eq. (3.15). The revenue difference in these two figures ranges between 10-40%, which provides the ballpark value of the cost to smooth wind power outputs. The revenues of using conventional reserves and BESS with the heuristic algorithm are also included, and all revenues are normalized to the best value in Figure 3.16 when BESS capacity is five times of the wind farm nameplate capacity. As expected, both cases support the argument that BESS is more effective than conventional reserves even with relatively small battery size. Furthermore, it is found that the MPC controller is, in general, better than the heuristic algorithm, especially when the BESS capacity is small. Simulations show that the MPC controller only requires a 600MWh BESS (75% of the wind farm nameplate capacity) to cover most of the wind intermittency and can secure revenues similar to those when much larger BESSs are used, whereas the heuristic algorithm requires a 1,600MWh BESS to secure similar revenues. This is true whether the changes in wind scheduling are penalized or not. On another note, the performance gap between MPC and the heuristic algorithm reduces when the BESS capacity gets bigger, which is consistent with the intuition that a bigger battery will be more tolerant in wind forecast errors, and, therefore, an instantaneous control algorithm may be suffice.

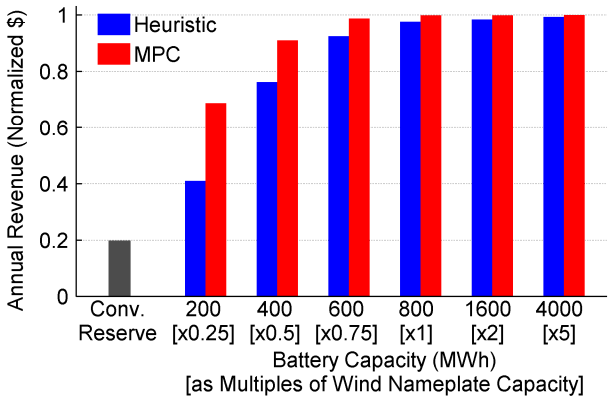

Figure 3.16 Annual revenue with the forgetting factor in the MPC formulation

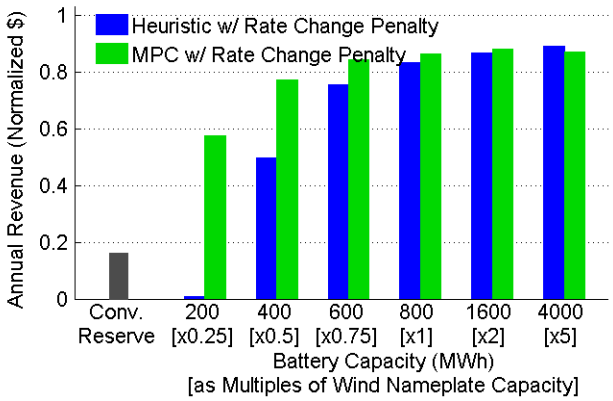

Figure 3.17 Annual revenue with penalty imposed on rate changes in wind scheduling

The annual wind power curtailment is another measure to evaluate how well the wind intermittency is mitigated, although wind curtailment is not explicitly penalized in the problem formulations in this study. Figure 3.18 summarizes the annual wind power curtailment, and, indeed, using BESS can achieve lower wind curtailment than using conventional reserves. In fact, BESS with a capacity merely one-quarter of the wind farm nameplate capacity can outperform conventional reserves by more than 50% (the former has the curtailment below 30%, whereas the latter above 60%) for all three different strategies evaluated. Surprisingly, the heuristic control algorithm has lower wind power curtailment than MPC when the BESS capacity is very small (the 200MWh case), although this does not result in better revenue to the wind farm owner. The optimization formulations in Eqs. (3.14) and (3.15) suggest that it is more profitable to play it safe and be conservative in scheduling wind power when the BESS capacity is really small. Furthermore, MPC becomes more effective than the heuristic algorithm to reduce wind curtailment as the BESS capacity increases, particularly the one with the forgetting factor. MPC only need an 800MWh BESS to reach zero wind curtailment, whereas the heuristic algorithm requires a BESS larger than 16,000MWh to do so.

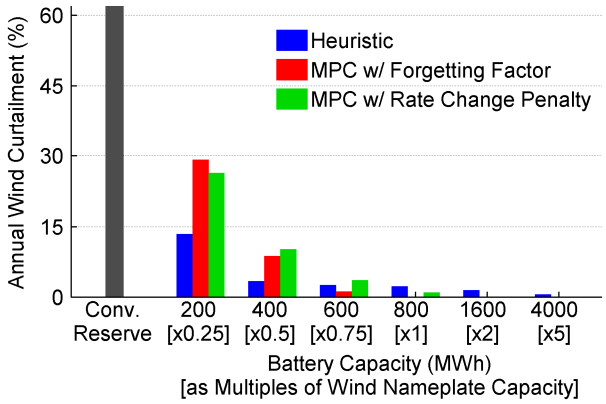

Figure 3.18 Annual wind curtailment

3.6 Conclusion

This chapter proposes using MPC to control the charging and discharging of battery energy storage system (BESS) for mitigating wind intermittency, so that wind power can be dispatchable on an hourly basis like fossil fuel power plants. The MPC controller is designed based on the optimization that minimizes operation costs for the wind farm owner where multiple-step wind forecasts (predictions) are included. The optimization is formulated in a way that the MPC results can be compared to conventional reserves and the heuristic algorithm that uses only the current wind forecast. All the three approaches are compared based on the resulting revenues to the wind farm owner after the control algorithms are implemented. The MPC controller is further revised to include a forgetting factor or an additional penalty on the rate changes in the wind power scheduling to assure a unique optimal solution. The second treatment is also effective to suppress the variations in the wind power scheduling, but has the consequence that the revenue to the wind farm owner will drop. The revenue drop ranges between 10-40% depending on the different BESS capacities.

Simulation results confirm that BESS is more effective than conventional reserves to absorb wind power fluctuations. BESS can help the wind farm owner to generate revenues 3 to 5 times higher than conventional reserves and lower wind curtailment by at least 50%. In addition, the BESS sizing analysis shows that, with the MPC controller, the BESS capacity only needs to be 75% of the wind farm nameplate capacity to cover most of the wind intermittency and to secure the wind farm owner's revenue. The heuristic

algorithm, in general, needs larger BESS to secure the same revenue, but the performance gap between MPC and the heuristic algorithm reduces when the BESS capacity gets bigger, owing to the fact that bigger batteries have more leeway to tolerate wind forecast errors and thus the requirements on the control algorithms can be relaxed. However, the fact that the MPC controller has consistently outperformed the instantaneous heuristic algorithm supports the argument that factoring in future wind information is important, which is especially true when downsizing BESS.

Several aspects demanding further investigation to better incorporate BESS to a wind power system include: 1) incorporating a more sophisticated battery model to better represent power limitations, efficiencies of charge and discharge events, and state of health, and 2) conducting more comprehensive analyses on costs, including not only operation but also installation, to provide more insight into the feasibility of deploying BESS on the electric grid. Chapter 6 will have some discussion on the second aspect.

CHAPTER 4

Synergistic Control for PEV Charging and Wind Power Scheduling

The previous two chapters have addressed the emerging challenges brought by high volumes of PEVs and wind power on the electric grid separately. This chapter intends to take advantage of the synergy between PEVs and wind power and proposes a hierarchical control algorithm to integrate PEV charging and wind power scheduling. The intention is to use wind power to charge PEVs and to control the PEV charging to cancel the wind intermittency, which will be a win-win situation for both PEVs and wind power.

The rest of the chapter is organized as follows: Section 4.1 reviews related literature; Section 4.2 presents modeling work for the PEV fleet, wind power, and the electric grid; Section 4.3 shows the derivations of the hierarchical control algorithm; Section 4.4 presents simulation results; and Section 4.5 provides concluding remarks.

4.1 Literature Review

In addition to the literature reviewed in Chapters 2 and 3 that addresses PEV charging and mitigating wind power intermittency separately, there are studies discussing the integration of these two new entities on the electric grid. In particular, it is worth mentioning that there are many different ways, other than BESS, to incorporate wind power into the grid operation, some of which provide inspiration for the development of the hierarchical controller in this chapter. Also, several scheduling optimizations that integrate PEV charging and renewable energy on the grid are also reviewed.

Besides bringing energy storage systems to the grid, researchers tackle the wind intermittency in various ways. It is recognized that aggregating outputs of multiple turbines or wind farms can help to smooth the fluctuations [130], and many research efforts have focused on reducing the prediction errors of wind power to assist grid operations [121, 122]. Another research direction is to develop strategies for scheduling wind generation. Some studies included wind power statistics in the optimization

formulations for generation scheduling [131, 132]. Fuzzy logic also has been used as to schedule wind power [133]. Besides the grid-wide scheduling optimizations, wind farm-centric optimizations that find bidding strategies for wind power producers (rather than the whole grid) to maximize individual profits have also been seen in the literature [126, 134-136].

In terms of integrating PEV charging and renewable energy to the grid, different methodologies have been proposed in the literature to determine the timing of PEV charging and/or scheduling of wind power. Some studies treat wind generation as a negative load and solve an optimization to determine the optimal PEV charging timing to accommodate as much wind power as possible [137, 138]; some work allows the V2G power flow to further reduce wind curtailment [139]. Another study solves an optimization for both PEVs and wind power producers with the assumption that the former is a reserve producer and the latter is an energy producer in the market [140]. However, as mentioned in the literature review in Chapter 2, many of these optimization problems treat the PEV fleet as one large battery and do not consider the fact the PEVs have different plug-in/plug-off times and battery SOC levels, and thus may not be suitable for real implementation.

In this chapter, the goal is to combine the control algorithms developed in Chapters 2 and Chapter 3 to realize the synergy between PEVs and wind power. To achieve this goal, a three-level hierarchical control algorithm is proposed to merge features of the two previously developed control algorithms. Some modifications are made so that the two control schemes can be pieced together seamlessly.

The hierarchical control algorithm starts with the top-level controller solving a grid-wide scheduling optimization problem for the conventional generation and wind power. The scheduling optimization inherits several features from the wind scheduling optimization presented in Chapter 3, such as penalizing use of conventional reserves to cover wind power intermittency. However, the scope changes from the wind-farm-centric profit optimization to the grid-wide cost minimization. Solving a grid-wide optimization implies that the grid operator is given the full authority to manipulate both supply and demand on the grid, including the conventional non-renewable power plants, wind

generation, and PEV charging. The optimal solution will reveal the full potential of harnessing the synergy between PEVs and wind power.

The middle- and bottom-level controllers are based on the PEV charging control algorithm presented in Chapter 2. The middle-level controller uses the optimal solution from the top-level controller as the reference signal to allocate charging power to individual PEVs. The bottom-level controller regulates the PEV charging based on grid frequency deviations; therefore, the PEV charging also serve as reserves to regulate grid frequency. The results have been published in [141] and [142].

4.2 Modeling

Several models are needed to describe the system-level dynamics of the PEV fleet, wind power, and electric grid. The PEV fleet model in Section 2.2.2 is updated with the real temporal distributions of daily commute in the southern Michigan to better represent the PEV population. The wind power model developed in Section 3.2.1 will continue to be used. The grid model describing the load and frequency in Section 2.2.1 will also continue to be used, and an additional element is added to describe the cost of electricity generation.

4.2.1 PEV Fleet

Similar to the fleet modeled in Chapter 2, the total number of PEVs is assumed to be two million, which corresponds to 25% of the vehicle fleet in Michigan, and all PEVs are assumed to use smart chargers and their charging is controllable. To better represent the PEV population in the State of Michigan, the data in [143] is used to extract the distributions of the plug-in time, plug-off time, and the SOC at plug-in. The raw data can be found in Appendix A, and the extracted probability distributions are shown in Figure 4.1 and Figure 4.2. These three distributions are different than those in Figure 2.4 in several ways. The peak of the plug-in time distribution in Figure 4.1 is three hours later than that in Figure 2.4, and the plug-off time distribution in Figure 4.1 is skewed, instead of normal. In addition, although not reflected by the histograms in Figure 4.1, there is a mild correlation between the distributions of the plug-in time and plug-off time, because people who go to work early often go home early. Furthermore, the trip length data also

has a skewed distribution because the short-range commutes outnumber the long-range commutes. This new PEV fleet model is more realistic because it is based on the data of real vehicle field tests, which include more information about the temporal distributions of real-world commute than the transportation statistics used to model the PEV fleet in Chapter 2 [95].

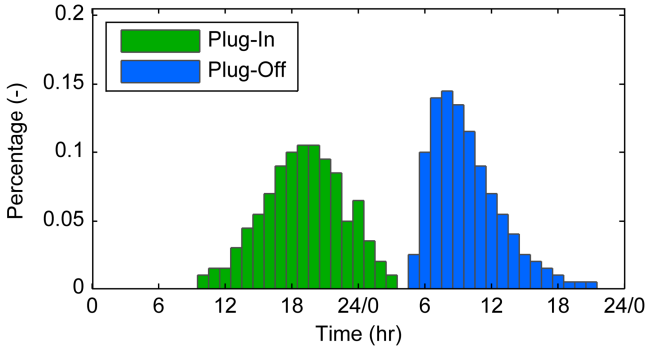

Figure 4.1 Distributions of the plug-in time and plug-off time [143]

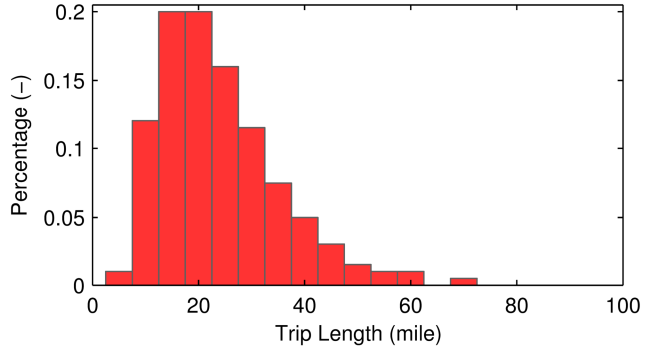

Figure 4.2 Distributions of the trip length [143]

Assuming that charging only happens at home, the time a vehicle arrives at home is treated as the plug-in time, and the time a vehicle leaves home the next morning is treated as the plug-off time. The trip length is used to derive the SOC at plug-in by Eq. (4.1), which then is used in Eq. (4.2) to find the total energy requirement to charge the whole PEV fleet. Equation (4.2) is, in fact, identical to Eq. (2.5).

$$SOC_{\text{ini}} = \begin{cases} 0.8 - (0.8 - 0.3) \cdot \dfrac{L}{\text{AER}}, & \text{if } L < \text{AER} \\ 0.3, & \text{otherwise} \end{cases} \tag{4.1}$$

$$K = \sum_{i=1}^{N} (0.8 - SOC_{\text{ini}})_i \cdot Q \tag{4.2}$$

where L is the trip length and AER is the all-electric range of the PEV. Eq. (4.1) limits the initial SOC to reside in the window of 30-80%, which is determined based on the information given in [144]. Q is the battery capacity and is assumed to be 16kWh (the same size as the 2013 Chevrolet Volt, which is a PEV with the AER close to 40 miles). Assumptions on the charger limits and battery dynamics are identical to those in Chapter 2: the maximum charging power is 1,440W, limited by the Level-I electric vehicle charger [24], and the SOC dynamics are described by the governing equation in Eq. (4.4), which is identical to Eq. (2.6). The efficiencies of both charging and discharging are assumed to be perfect. Using these vehicle and battery parameters, one can find that 7.38GWh of energy is required to fully charge the two million PEVs. The total energy requirement here is less than that used in Chapter 2 because, according to the data in [143], many vehicles have short trip lengths and require less charging. The total energy requirement will be a parameter to the optimization problem in Section 4.3.1.

$$\dot{SOC} = -\frac{P_{\text{batt}}}{Q} \tag{4.3}$$

where Q is the battery capacity and P_{batt} is the battery discharge power.

4.2.2 Wind Power

An 800 MW wind farm is assumed to be connected to the electric grid, which can support about 10% of the peak load in Michigan when running at the rated power. The wind power model in Section 3.2.1 is adopted to describe the stochastic wind power outputs. In particular, the conditional probability distributions in Figure 3.4 and Eqs. (3.1) and (3.2) are used to calculate the reserve requirement ($R_{\text{w,rqd}}$) and expected wind power deficit (w_{d}). However, it is assumed that there is no BESS on the electric grid. PEVs will take the place of BESS to provide reserves for mitigating wind intermittency.

4.2.3 The Electric grid

The grid models derived in Section 2.2.1 are used to describe the non-PEV load and the grid frequency dynamics. The model approximates the grid frequency dynamics

as lumped first-order rotational dynamics. In addition, a new piece of model is developed to describe the cost of electricity generation using the data from the Oak Ridge Competitive Electricity Dispatch Model [145]. The cost model consolidates all expenses of electricity generation into a cost curve. Figure 4.3 shows the cost curve of power plants in Michigan, in which power plants are sorted in ascending order according to their generation costs. The grid operator is assumed to dispatch generating capacities based on the merit order, meaning that cheaper power plants will be dispatched before expensive ones. Note that the price curve rises in a staircase fashion because the price jumps when an additional (more expensive) power plant is dispatched.

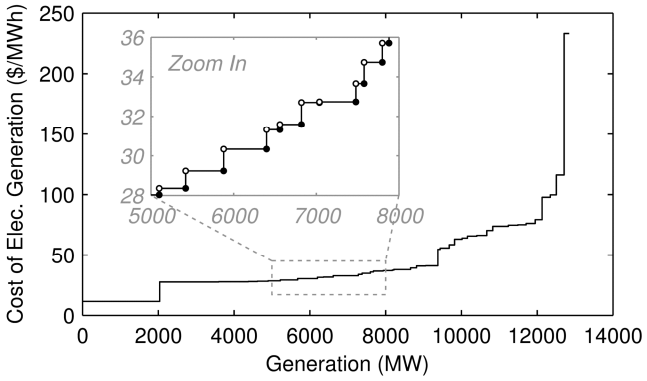

Figure 4.3 Cost of electricity generation in Michigan [145]

The assumptions on the reserve costs are similar to those in Chapter 3, in that there are two costs associated with reserves: 1) the reserve scheduling cost is 3% more expensive than the price of electricity generation, based on the statistics in [127]; and, 2) the reserve dispatch cost is the same as the generation cost and only occurs if the reserve is dispatched. However, in this chapter, instead of counting costs in the normalized units, the actual per unit cost in Figure 4.3 is used.

4.3 Hierarchical Controller

As mentioned at the beginning of this chapter, a hierarchical controller is designed to incorporate both the PEV charging and wind power into the electric grid. Figure 4.4 depicts the structure of the controller, which consists of three levels: the top-level controller (marked as the red light bulb in the upper left corner) optimizes the

hourly scheduling for wind power and conventional power plants; the middle-level controller (C and G) plans PEV charging based on the battery SOC and plug-off time of each vehicle to follow the generation scheduling; and the bottom-level controller (k_{soc} and $k_{I,soc}$) uses grid frequency as the feedback cue to regulate the PEV charging. The objectives and time step resolutions of each controller are summarized in Figure 4.5. The details of each controller are presented in the following sub-sections.

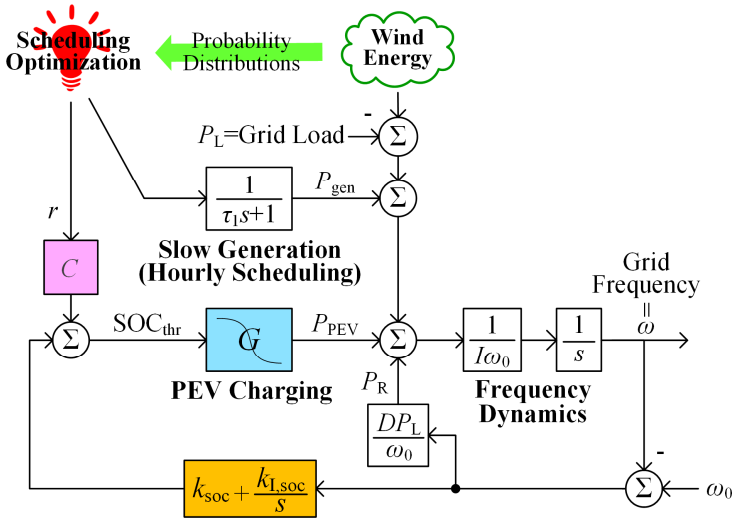

Figure 4.4 the structure of the hierarchical controller

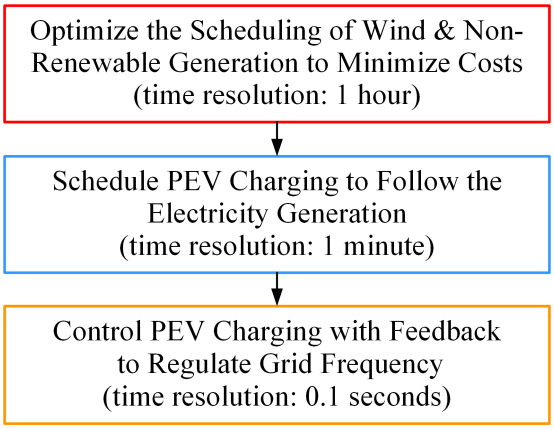

Figure 4.5 Objectives and time resolutions of the hierarchical controller

4.3.1 Top-Level Controller: Scheduling Optimization

An optimization problem is formulated to find the optimal hourly scheduling of the non-renewable electricity generation and wind power to satisfy the grid load and PEV charging demand at minimum cost. The optimization problem is stated in Eqs. (4.4)-

(4.14). Note that this optimization problem is different from the one defined in Eqs. (3.8)-(3.11) in several ways. The objective function, Eq. (4.4), is different from the one in Eq. (3.8), because the scope of the optimization changes from maximizing the profit for the wind farm owner to minimizing the total costs of electricity generation for the grid. To elaborate further, the objective function, Eq. (4.4), includes three terms: costs of electricity generation (C_g), reserve scheduling (C_{Rs}), and expected reserve dispatch (C_{Rd}). Due to the different problem scope, the first term takes a different sign than that in Eq. (3.8). In addition, here the PEV load takes over the BESS to provide reserves for mitigating wind intermittency. Furthermore, to avoid additional energy cycling on the PEV batteries, additional constraints are imposed on the PEV load to prohibit the V2G power. This means that, if wind deficit occurs, the control algorithm will only slow down the PEV charging but never discharge PEVs. The rewards to PEVs for supporting reserves, if considered, can also be included in the objective function, although such remuneration is not considered here. The time resolution is one hour, and the time horizon is chosen to cover all valley hours (in Eq. (4.4), the beginning of valley hour has t=1, and T represents the last valley hour). The two controlling variables, u_1 and u_2, are the non-renewable electricity generation (P_{gen}) and the scheduling of wind power (w_s). The state, x, is the *remaining* PEV charging demand, which can be interpreted as the converse of the SOC if one imagines the whole PEV fleet as one large battery. The nominal non-PEV load ($P_{L,nom}$), total PEV demand (K) and the wind forecasts (w_f) are known information in this optimization. $P_{L,nom}$ is shown in Figure 2.2; K is found in Eq. (4.2); and, w_f is acquired from the NREL wind dataset [124], and some of which is shown in Figure 3.3. The state dynamics and constraints on the state and control variables are listed in Eqs. (4.5)-(4.14).

$$\min_{u_1,u_2} : J = \sum_{t=1}^{T} \left[C_g(u_1(t)) + C_{Rs}(R_s(t)) + C_{Rd}(R_d(t)) \right] \tag{4.4}$$

subject to

$$u_1(t) + u_2(t) - P_{L,nom}(t) = P_{PEV}(t), \ \forall t \tag{4.5}$$

$$\sum_{t=1}^{T} P_{\text{PEV}}(t) \cdot \Delta t = K \tag{4.6}$$

$$0 \le P_{\text{PEV}}(t) \le \min\{x(t),\ U_{\text{PEV}}\},\ \forall t \tag{4.7}$$

$$x(t+1) = x(t) - P_{\text{PEV}}(t) \cdot \Delta t,\ \forall t \tag{4.8}$$

$$x(0) = K \tag{4.9}$$

$$R_{\text{L,rqd}}(t) = 0.05 \cdot P_{\text{L,nom}}(t),\ \forall t \tag{4.10}$$

$$R_{\text{w,rqd}}(t) = [u_2(t) - \mathbf{F}^{-1}(0.05)]^+,\ \forall t \tag{4.11}$$

$$R_{\text{s}}(t) + P_{\text{PEV}}(t) \ge R_{\text{L,rqd}}(t) + R_{\text{w,rqd}}(t),\ \forall t \tag{4.12}$$

$$w_{\text{d}}(t) = \mathbf{E}\{[u_2(t) - w_{\text{a}}(t)]^+\},\ \forall t \tag{4.13}$$

$$R_{\text{d}}(t) = [w_{\text{d}}(t) - P_{\text{PEV}}(t)]^+,\ \forall t \tag{4.14}$$

where,

$P_{\text{L,nom}}$: nominal non-PEV load (MW)

P_{PEV} : aggregate PEV charging load (MW)

U_{PEV} : charging limit (MW)

K : total PEV energy demand (MWh)

$R_{\text{L,rqd}}$: reserve requirement for grid load (MW)

$R_{\text{w,rqd}}$: reserve requirement for wind power (MW)

R_{s} : scheduling of conventional reserve (MW)

w_{d} : expected deficit of wind power (MW)

R_{d} : expected dispatch of conventional reserve (MW)

Equations (4.5)-(4.9) are constraints related to electricity generation: Eq. (4.5) states the balance between supply and demand (i.e. scheduled generation and loads); Eq. (4.6) ensures that the total PEV charging demand is satisfied; Eq. (4.7) states that the PEV load is bounded from below by zero to prevent the V2G power and bounded from above by the Level-I charger limit (the upper bound, U_{PEV}, is calculated by multiplying the power limit of a single charger with the total number of PEV); Eq. (4.8) describes the

state dynamics, which is consistent with the SOC governing equation in Eq. (4.3); and, Eq. (4.9) is the constraint on the initial state.

Equations (4.10)-(4.14) are related to the reserve scheduling and dispatch: Eq. (4.10) states the reserve requirement for the grid load, which is 5% of the nominal load magnitude according to [96]; Eq. (4.11) states the reserve requirement for wind power as derived in Eq. (3.1); Eq. (4.12) states that the total reserve requirement must be met by either the controllable PEV load or the scheduling of conventional reserves; Eq. (4.13) states the expected deficit of wind power as derived in Eq. (3.2); and Eq. (4.14) states the expected dispatch of conventional reserves if wind deficit exceeds the magnitude of the controllable PEV load. Notice that Eq. (4.12) counts the PEV load as reserves because it can be throttled back by the bottom-level controller if wind power drops unexpectedly. Finally, Eq. (4.14) implies that throttling back PEV load is preferred to dispatching the conventional reserves because the former is free.

In addition, several implicit influences of u_2 in the optimization problem are worth mentioning. Increasing u_2 can reduce the non-renewable electricity generation [u_1 in Eq. (4.5)], but it also increases the reserves required for wind power [$R_{\text{w,rqd}}$ in Eq. (4.11)] and the expected wind deficit [w_{d} in Eq. (4.13)]. Consequently, the scheduling and expected dispatch of conventional reserves may rise [R in Eq. (4.12) and r in Eq. (4.14)] if they exceed the range that the controllable PEV load can cover. These coupling constraints are the main reasons why this optimization problem is non- trivial.

The scheduling optimization is solved assuming that the following information is known: the generation costs (Figure 4.3), the nominal non-PEV grid load (the dash line in Figure 2.2), and wind forecasts (the grey line in Figure 3.3). However, the actual grid load and actual wind output are not known. The time horizon of the optimization problem is 11 PM to 8 AM, which is found based on the estimate of the time window to achieve perfect valley filling (See the details in Section 2.3.1). The time horizon turns out to be shorter than the valley hours in Chapter 2, since this more realistic PEV fleet requires less charging. The optimization problem is solved using the Dynamic Programming (DP) technique. More specifically, Eqs. (4.15)-(4.16) are the functional equations of DP that are used recursively to solve the designated scheduling optimization problem. More details about the DP technique can be found in Appendix B.

$$J_T^* = \phi_T(x(T)) \tag{4.15}$$

$$J_t^*(x(t)) = \min_{u(t)} \left[\psi_t(x(t), u(t)) + J_{t+1}^*(x(t+1)) \right], \forall t < T \tag{4.16}$$

where ϕ_T is the cost at final step T, and ψ_t is the instantaneous transitional cost at each step in the optimization horizon. For the specific scheduling optimization of interest, ϕ_T will be that shown in Eq. (4.17) and ψ_t shown in Eq. (4.18). In particular, Eq. (4.17) ensures that all PEV load is satisfied when the valley hours end.

$$\phi_T(x(T)) = \begin{cases} 0, \text{ if } x(T) = 0 \\ \infty, \text{ otherwise} \end{cases} \tag{4.17}$$

$$\psi_t(x(t), u(t)) = C_{\mathrm{g}}(u_1(t)) + C_{\mathrm{Rs}}(R_{\mathrm{s}}(t)) + C_{\mathrm{Rd}}(R_{\mathrm{d}}(t)), \forall t < T \tag{4.18}$$

Figure 4.6 shows the optimal controls generated by DP under the nominal condition. The four arrows marked at 2 AM illustrate that the constraint for the balance between supply and demand, Eq. (4.5), has been satisfied, and several properties in the optimal solution are observed:

1) A noticeable amount of PEV charging is scheduled to happen in the last hour, so that the control algorithm can still manipulate the PEV charging to cover the wind uncertainty, which helps to avoid the costs associated with conventional reserve scheduling and dispatch.

2) The scheduling of the non-renewable generation, u_1, is no longer targeting to achieve valley filling; instead, it takes advantage of the staircase kinks in the cost curve by using as much low-price generation as possible. This feature can be seen in Figure 4.6 where the generating capacities cheaper than \$30.3/MWh were fully utilized all the time. This is true except for the last hour, due to the need for wind power reserve stated above.

3) The optimization problem defined by Eqs. (4.4)-(4.14) has non-unique optimal solutions because there is no penalty on early or late PEV charging as long as it happens during the designated horizon. However, unlike the infinite solutions to the BESS control optimization in Chapter 3, the scheduling optimization with PEVs here has only finite

sets of optimal solutions (due to the constraint in Eq. (4.6) on PEV charging completion), and Figure 4.6 is one of the several possibilities.

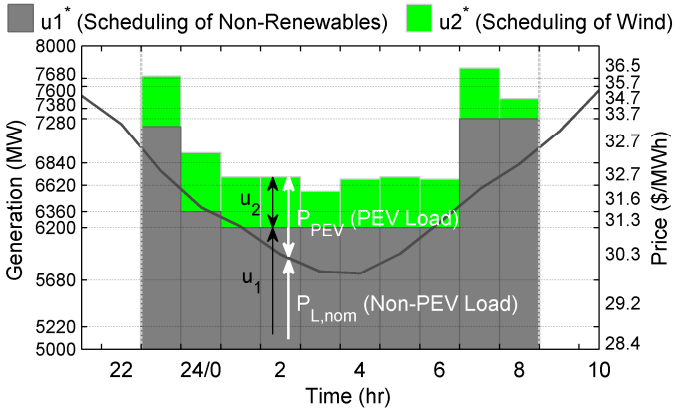

Figure 4.6 The optimal scheduling in the valley hours with the nominal grid load

The optimal solution will be carried into the middle-level controller; in particular, the scheduling of non-renewable generation, u_1^*, will replace the hourly nominal grid load, $P_{\text{L,nom}}$, in Eq. (2.3) as the reference for slow generation. Also, u_1^* and u_2^* together will affect the feed forward component in the middle-level controller for PEV charging.

4.3.2 Middle-Level Controller: Load Following

The middle-level controller adopts the PEV charging control algorithm developed in Section 2.3, which consists of the *centralized broadcast* and the *charging power allocation rule*. However, a modification is made to replace Eq. (2.7) with Eq. (4.19), because the reference for the centralized broadcast is no longer calculated based on the valley filling power but on the optimal scheduling from the top-level controller. Eq. (4.19) is essentially an updated version of Eq. (4.5). The hyperbolic tangent curve shown in Figure 2.7 is again used as the charging power allocation rule, and thus Eq. (2.8) will still be valid for calculating the feedforward component for controlling PEV charging.

$$r = u_1^* + u_2^* - P_{\text{L,nom}} \tag{4.19}$$

4.3.3 Bottom-Level Controller: Grid Frequency Regulation

The bottom-level controller, denoted as k_{soc} and $k_{I,soc}$ in Figure 4.4, is identical to that developed in Section 2.3.3, which was designed to mimic the feedback PI-controller used by conventional reserves. The only update needed here is to repeat the sensitivity analysis presented in Section 2.3.4 to tailor the controller gains, k_{soc} and $k_{I,soc}$, for this PEV fleet.

4.4 Simulations

Three simulations are conducted to demonstrate the effectiveness of the three-level controller. Table 4.1 lists the simulation setups, which have PEVs, wind power and the hierarchical control algorithm progressively included onto the electric grid. This allows the effects of PEVs, wind power, and the control algorithm to be isolated. Case *A* serves as the reference with unmitigated PEV charging. Cases *B* and *C* both have 25% PEVs in the transportation sector and 10% wind power in the electricity generation mix; however, Case *B* has only the top- and middle-level controller implemented but not the bottom-level controller, and the conventional reserve is still used for frequency regulation, whereas Case *C* has all three levels of controllers, and no conventional reverses are used except if the frequency deviation is larger than 1 Hz, which may happen if the PEV fleet loses control authority as an actuator for grid frequency. This may happen when most PEVs are fully charged or unplugged from the grid at the end of the valley hours. The time horizon of the simulations is 11PM-8AM.

Table 4.1 Simulations Setups with Different Control Algorithms

Case	PEV Penetration	Wind Power Penetration	Control Implementation
A (Ref.)	25%	None	No control integration
B	25%	10%	Only first two levels of control
C	25%	10%	All three levels of control

All three cases have 99.5% of PEVs fully charged, but their performances in the dispatch of the non-renewable generation, frequency regulation, and costs are different.

Figure 4.7 shows the actual dispatch, including both the electricity generation and reserves from conventional sources. Case *A* has a substantial generation increase before 11 PM because PEVs start charging in early evenings, while Cases *B* and *C* have the PEV load properly confined within 11PM-8AM. However, Case *B* does not achieve the maximum benefit because fluctuations in the grid load and wind power call for more conventional reserves to be dispatched. Case *C* has feedback to control the PEV charging and thus has the non-renewable electricity generation closely following the optimal scheduling (u_1^*), except beginning at 12AM, 1AM, and 7AM when u_1^* has large changes and the slow time constant τ_1 limits the ramping of the electricity generation (see dynamics of the slow generation in Eq. (2.3)).

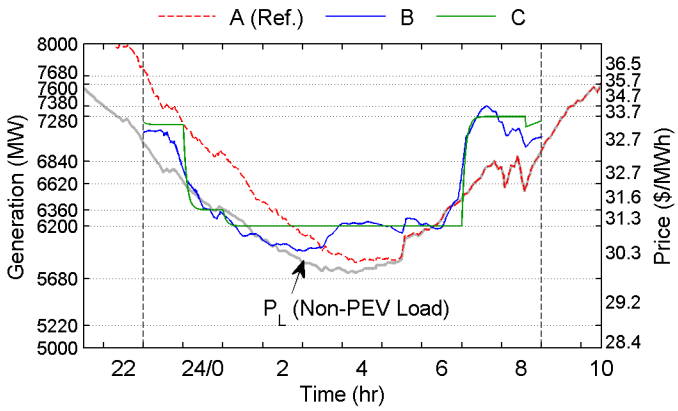

Figure 4.7 The dispatch of non-renewable generation sources

Figure 4.8 highlights the frequency regulation results. Cases *A* and *B* both use conventional reserves and have similar frequency deviations, whereas the grid frequency in Case C is regulated by controlling the PEV charging and has much smaller deviation most of the time. However, the performance in Case *C* deteriorates at the very beginning and very end of the valley hours due to the same reason pointed out in Section 2.4.1: the middle-level controller is singular at the very beginning in the valley hours, and most PEVs are fully charged at the end of valley hours. These conditions lead to poor performance in grid frequency regulation at the beginning and end of the valley hours.

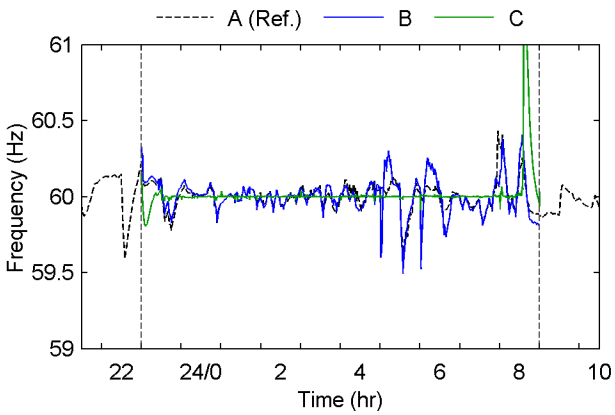

Figure 4.8 Grid frequency trajectories

Figure 4.9 shows the total costs of electricity generation and reserve procurement. Note that the wind generation itself is assumed to be free, although there maybe reserve costs associated with wind intermittency if the reserves are provided by non-renewable sources. However, reserves provided by controlling PEV charging is assumed to be free and PEV owners receive no rewards for providing reserves to facilitate the grid operation. In Figure 4.9, Case *A* represents the baseline costs for providing electricity generation for the loads and for procuring reserves to cover fluctuations in the loads. Case *B* has a smaller electricity generation cost but a larger reserve cost due to wind intermittency. In fact, the reduction in the generation cost is almost cancelled by the increase in the reserve cost. This implies that, if wind farm owners procure reserves from conventional (fossil fuel) sources, it will be very difficult for wind power to generate any revenue. Case *C* has an electricity generation cost similar to Case *B*, as both take advantage of the free wind generation, and Case *C* has a very low reserve cost due to the PEV charging control. However, the cost reduction shown here exclude the rewards to PEV owners for providing reserves and the costs related to wind generation, such as maintenance or mortgage payments. Hence, Case *C* can be interpreted as the best case scenario for the system operation costs with PEVs. In particular, if compensation is paid to PEV owners for providing reserves, the compensation should not be more than the cost difference between Case *B* and *C*, else it will be more economical to use conventional generators as reserves.

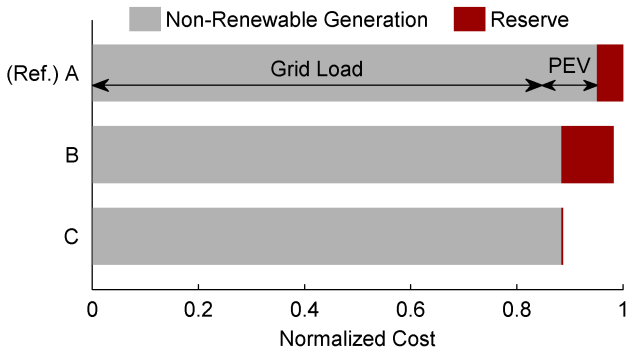

Figure 4.9 Total costs of electricity generation and reserve procurement

To further illustrate the value of the synergy between PEV and wind power, Figure 4.10 shows the cost difference between Cases *B* and *C* at various penetration levels of PEV and wind power. In other words, this contour plot highlights the difference between the uncoordinated and well-coordinated grid operations when the two green technologies are deployed to the grid. The cost difference is normalized to the cost of Case *B*, and also several markers of PEV and renewable energy targets [6, 146, 147] are included in the figure. It is found that the cost reduction barely exists if only one of the two green technologies is present on the grid, but the cost saving can reach a remarkable 20% when both technologies are deployed *and* the synergy is fully utilized. Again, the cost saving shown here represent the best case scenario when the two green technologies are well-coordinated. The saving will not be as good if PEV owners are given rewards to provide reserves are considered.

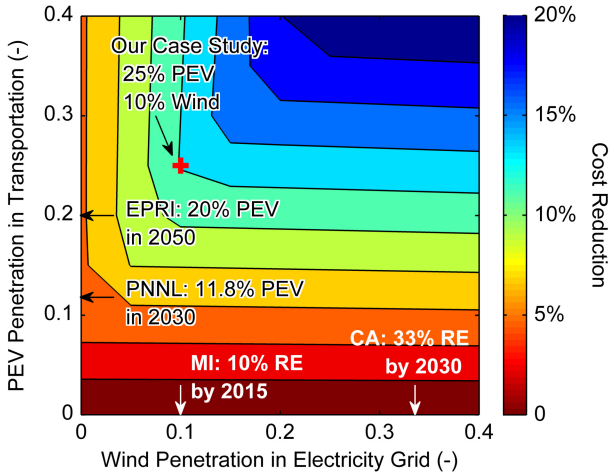

Figure 4.10 Cost reduction between uncoordinated and coordinated grid operations with PEVs and wind power

Furthermore, the above figure indicates the trend that the best cost reduction happens when the PEV penetrations are higher the wind power penetrations. However, one should not interpret this trend as a general principle because it is specific to Michigan. It is yet to be verified if the penetration of PEVs has to be higher than wind power to achieve the best cost reduction in other states or countries. The answer will probably depend on the number of vehicles per capita and the energy usage per capita of the specific location of interest; information of the former can be found in [148] and the later in [46, 149].

4.5 Conclusion

This chapter proposes a three-level hierarchical controller to capitalize the synergy between the controllable PEV charging and the intermittent renewable wind power: the top-level controller minimizes the grid-wide electricity generation costs and schedules both non-renewable generation and wind power; the middle-level controller allots charging power to individual PEVs based on their battery SOC and plug-off time to achieve load following; the bottom-level controller uses feedback to control PEV charging to regulate the grid frequency. The proposed hierarchical controller preserves the features of the control algorithms developed for the PEV charging and wind power operation in the earlier chapters.

The effectiveness of this controller is validated by simulations on a state-wide grid mode based on realistic data in Michigan. The algorithm can handle different PEV populations and large uncertainties in wind generation while still fully charging most PEVs and regulating the grid frequency. Extensive simulations with various PEV fleet sizes and wind power shares in the generation mix show that substantial cost saving can be achieved if these two green technologies are well-coordinated. The implication of the cost saving is that, not only should PEVs and wind power be deployed simultaneously, but also their operation needs to be properly coordinated. No economic gains can be achieved if these two green technologies are introduced blindly without integration.

The results in this chapter demonstrate the value of fully exploring the synergy between PEV and wind power. The concept is not limited to wind power and can be extended to other intermittent renewable sources. However, some open questions remain to be answered. In particular, the scheme of controlling PEV charging to mitigate wind intermittency is available only in the valley hours, but not all day long. This is limited by the assumption that PEVs are only charged in the evenings at home. An extension work to investigate the daytime PEV charging is worth considering, which can potentially improve the utilization of wind generation in peak hours and can add more values the integration of PEVs and wind power. Integrating PEVs and BESS together to mitigate wind intermittency is also an option to consider; the integration may allow BESS to be downsized further or more PEVs to be fully charged.

CHAPTER 5

Reducing Grid Emissions through a Carbon Disincentive Policy

The previous chapter uses the grid-wide costs of electricity generation to measure the benefits of exploiting the synergy between the PEV charging and wind power on the grid. In addition to economic gains, PEVs and wind power also has great potential to reduce CO_2 emissions from the electric grid and the ground vehicles. This chapter extends the discussions from the previous chapter and investigates effects of these two new grid entities on the grid CO_2 emissions. The discussion is only confined to the electricity generation, and excludes emissions in PEV driving and power plant construction/decommissioning. The cost optimization scheme developed in the previous chapter is revised to include the grid emissions; this allows us to study the tradeoff between the electricity generation costs and grid CO_2 emissions. In addition to coordinating the two new grid entities (PEVs and wind power), a carbon disincentive policy is introduced as a means to alter the operations of the existing non-renewable generation assets on the grid. Implications of imposing such a carbon disincentive policy are also discussed in detail in this chapter.

The remainder of this chapter is organized as follows: Section 5.1 reviews related literature; Section 5.2 presents the modeling work on the electric grid, renewable wind power, and the PEV fleet; Section 5.3 presents the optimization formulation and the carbon disincentive policy for minimizing the electricity generation costs and CO_2 emissions; Section 5.4 discusses the optimal solutions and the tradeoff between the two objectives; and, Section 5.5 provides concluding remarks.

5.1 Literature Review

A complete greenhouse gases (GHG) emission analysis on a particular energy technology should cover all stages of the technology and its fuel life-cycle. To date, a great variety of life-cycle emission assessments of electricity generation have been

conducted, and a comprehensive summary can be found in [150]. As shown in Figure 5.1, once the CO_2 emissions in the upstream (construction), operation, and downstream (decommissioning) stages of a power plant are all properly considered, nuclear and renewable generation are no longer zero-emission technologies, although they still outperform fossil fuel based generation. The CO_2 rates of nuclear and renewable generation are roughly an order of magnitude lower than non-renewable generation. Another fact reflected in Figure 5.1 is that CO_2 emissions of some energy technologies vary widely because the carbon content of the fuel is site-specific and the thermal efficiency of the technology can differ due to technology advancement and maintenance.

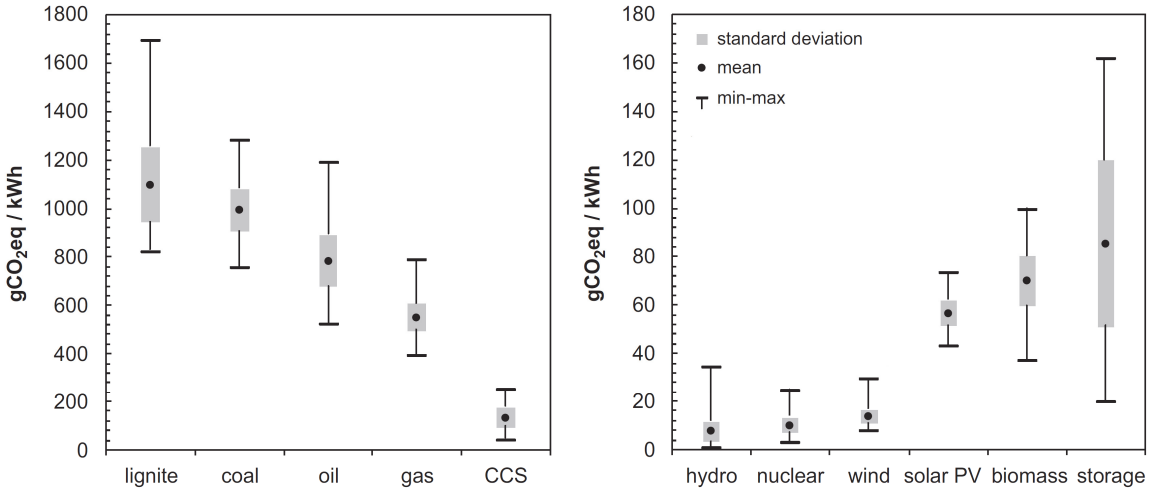

Figure 5.1 Summary of life-cycle GHG emissions for selected power plants [150] (CCS: carbon capture and storage; storage: energy storage systems)

Furthermore, the CO_2 emissions created by electricity generation are crucial in assessing the life-cycle emissions for PEVs. Figure 5.2 shows the major factors that impact PEV CO_2 emissions at different stages throughout the product life cycle. Since PEVs will have relatively lower tank-to-wheel emissions due to the better fuel economy granted by powertrain hybridization, the well-to-tank emissions will play a dominant role to determine the lifecycle emissions of PEVs. The literature has several studies focusing on CO_2 emissions on the well-to-tank stage for PEVs [146, 151-156]. Furthermore, CO_2 emissions on the well-to-tank stage can be reduced by integrating renewable generation to the grid [157], and this will be the focus of discussion in this chapter.

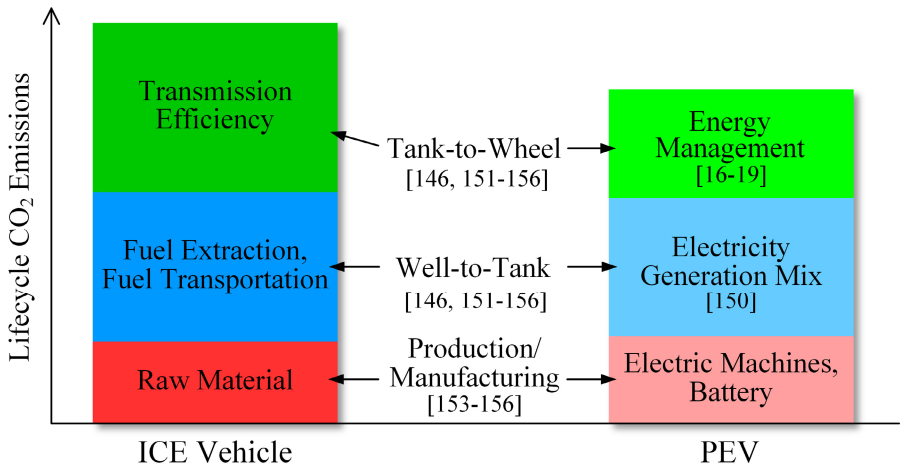

Figure 5.2 Life-cycle CO_2 emissions of vehicles
(This is only an illustration. Magnitudes of emissions on each stage are not to scale)

Reducing CO_2 emissions and electricity generation costs are often conflicting goals because low-cost power plants, such as coal power plants, often produce higher CO_2 than high-cost power plants, such as natural gas plants. However, as mentioned in Section 2.2.1, there was an exception in 2010-2012: the natural gas reached record-low prices and more natural gas was used for electricity production as it was more cost competitive than coal in that period [92]. The price dips in natural gas therefore helped to reduce the grid CO_2 emissions, but the price dips are usually temporary. The U.S. Energy Information Administration predicts that the natural gas price will gradually rise and reach the level before 2010 in the next few years [158].

Because the low-CO_2 generating technologies often are not favored in the open market due to their higher prices, non-market-driven means are needed to reduce the CO_2 emissions. Carbon taxation has been proposed in a number of EU countries since the 1990s [159, 160]. Many studies have discussed the effectiveness of carbon tax on reducing CO_2 emissions and its impact on economic activities [161-163]. Also, different designs of tax policies have been proposed; for example, the mechanisms to return or distribute the tax revenues [164, 165]. It was found that the macroeconomic costs (e.g., losses in GDP) can be reduced if tax revenues are effectively returned [166]. However, because it is difficult to quantify the societal cost of pollutants [164], the literature does not provide a consensus view on how high the tax rate should be [167-169]. The tax rate

varies between \$4 - \$185/ton of CO_2, although \$15-30/ton CO_2 are more commonly seen [161, 164, 166, 170, 171].

In this chapter, instead of suggesting an arbitrary carbon tax rate to suppress the use of high-carbon power plants, the optimal Pareto front will be used to show the trade-off between CO_2 emissions and electricity generation costs. Two approaches are adopted to include the grid CO_2 emissions into the cost optimization scheme developed in the previous chapter. The first approach directly penalizes the CO_2 emissions in the objective function, and the second approach uses a carbon disincentive to alter the dispatch order of power plants so that some expensive, low-CO_2 plants can replace cheap, high-CO_2 plants. In addition, substantial amount of PEVs and wind power sources are assumed to be present on the grid. The PEV charging is controlled to eliminate the intermittency of wind power, and the wind power provides low-carbon electricity to charge PEV. The implications of these two approaches are different and are discussed in detailed in this chapter. The results have been accepted for publication [172].

5.2 Modeling

The models developed in the previous chapters to describe the system-level dynamics of the PEV fleet, wind power, and electric grid will continue to be used, and an additional element is added to describe the CO_2 emissions of electricity generation.

5.2.1 Plug-In Vehicle Fleet

The total number of PEVs is assumed to be two million, which corresponds to 25% of the vehicle fleet in Michigan, and all PEVs are assumed to use smart chargers and are thus controllable. The PEV population is again represented by the three distributions of the plug-in time, plug-off time, and the SOC at plug-in shown in Figure 4.1 and Figure 4.2.

5.2.2 Wind Power

Wind power is assumed to have the nameplate capacity totaled at 800 MW, which can cover about 10% of the peak load in Michigan. The stochastic wind generation is again described by the conditional probability distributions shown in Figure 3.4, which

will be used in Eqs. (3.1) and (3.2) to calculate the reserve requirements to cover the wind uncertainties.

5.2.3 The Electric Grid

The models describing the non-PEV grid load and costs of electricity generation remain the same as those in the previous chapter. However, additional information is extracted from [173] to describe the CO_2 emissions. Figure 5.3 and Figure 5.4 show the costs and the corresponding CO_2 emission rates of power plants in the state of Michigan. Figure 5.3 is, in fact, a repetition of Figure 4.3, but with different color codes to represent different types of generation technologies. Note that Figure 5.3 includes only the costs during the power plant operation and leaves out the costs of constructing and decommissioning power plants. This assumption has been seen in the literature [65] and is appropriate because the dispatch decisions made by the grid operator will not change the costs on the upstream and downstream stages. Similarly, the data shown in Figure 5.4 include only the CO_2 emissions during the operation phase of a power plant but not emissions during fuel mining/transportation and plant decommissioning. Therefore, nuclear is assumed to have zero emissions. The general trend in Figure 5.3 and Figure 5.4 indicates that nuclear power has the lowest price and CO_2 emissions. Coal-fired generation, in general, is cheaper than natural gas, but has higher CO_2 emissions. Thus, it can be expected that, without the carbon disincentive, the grid operator will have to dispatch all coal plants before natural gas plants according to the merit order dispatch. Wind power, however, is not shown in Figure 5.3 and Figure 5.4 because it does not have a fixed sorting position in the merit order. This is due to the assumptions on the costs of wind power, which are the same as those in the previous chapter: the wind power generation is assumed to be free, but there will be reserve costs associated with wind intermittency if the reserves are provided by non-renewable sources; therefore, the cost of wind power is not constant. Furthermore, wind power is assumed to have zero emissions.

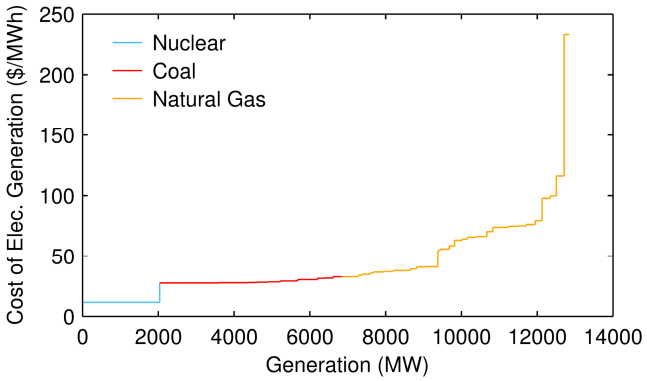

Figure 5.3 Cost of electricity generation in Michigan (extracted from [145])

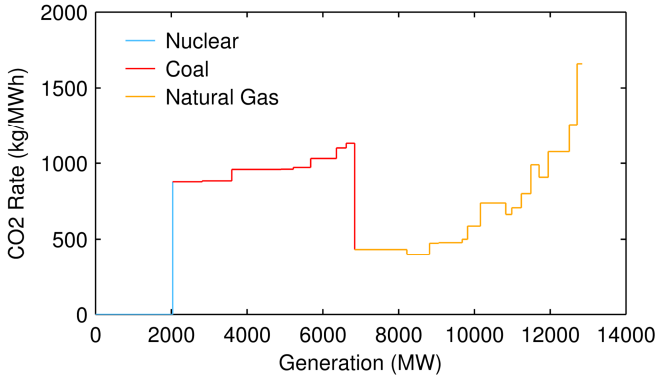

Figure 5.4 CO_2 emission rate of electricity generation (extracted from [173])

5.3 Scheduling Optimization for CO_2 Emission and Electricity Generation Cost

Two approaches are applied to the scheduling optimization framework developed in the previous chapter to investigate the tradeoff between the electricity generation cost and CO_2 emissions on the grid. The first approach penalizes CO_2 emissions directly in the objective function, and the second uses a carbon disincentive to alter the dispatch order of power plants. In the following sub-sections, the solution of the original optimization problem is first reviewed, and then the optimal solutions of the two approaches to include CO_2 emissions are discussed.

5.3.1 Original Scheduling Optimization: Minimize Electricity Generation Cost

The original scheduling optimization problem formulated in the previous chapter aims to minimize the grid-wide total costs of electricity generation. Its objective function is repeated in Eq. (5.1) for the readers' convenience, which includes costs of non-

renewable electricity generation (C_g), reserve scheduling (C_{Rs}), and expected reserve dispatch (C_{Rd}). The objective function is minimized by two control variables, u_1 and u_2; the former is the scheduling of the non-renewable generation and the latter is the scheduling of wind power. Constraints defined in Eqs. (4.5)-(4.14) are still applied to ensure that both non-PEV and PEV loads are satisfied and wind intermittency is covered by reserves or the controlled PEV load. This optimization formulation resembles the typical practice in the US market: power plants submit their bidding prices to the wholesale market, which presumably will cover their costs, and the grid operator sorts these bids and creates the merit order. Then, in each operating hour, the grid operator tries to minimize the overall electricity price for consumers by deploying power plants according to the merit order.

$$\min_{u_1,u_2} : J = \sum_{t=1}^{T} \left[C_g(u_1(t)) + C_{Rs}(R_s(t)) + C_{Rd}(R_d(t)) \right] \tag{5.1}$$

With the non-PEV grid load, total PEV demand, and wind forecast given, the scheduling optimization is solved using the Dynamic technique. The time horizon of the optimization problem is 11 PM to 8 AM. Figure 5.5 shows the optimal scheduling of the baseline case in the valley hours. The baseline case has the grid load at the nominal as shown in Figure 2.2, 800 MW of wind power in the generation mix, and two million PEVs plugging onto the grid. In fact, the optimal solution in Figure 5.5 is identical to that in Figure 4.6, but Figure 5.5 includes additional information about the types of power plants that are dispatched. They are marked with different colors using the same color scheme in Figure 5.3 and Figure 5.4. Furthermore, the right hand side axis shows not only the generation costs, but also CO_2 rate of different power plants. As explained in Section 4.3.1, dynamic programming plans the PEV load in a strategic way to cover wind intermittency, and both non-PEV and PEV loads are served by wind power and cheap generating capacities whenever possible. In terms of CO_2 emissions, the optimal solution shows that most loads are served by coal (and nuclear) power plants; only few natural gas power plants are dispatched at the beginning and the end of valley hours.

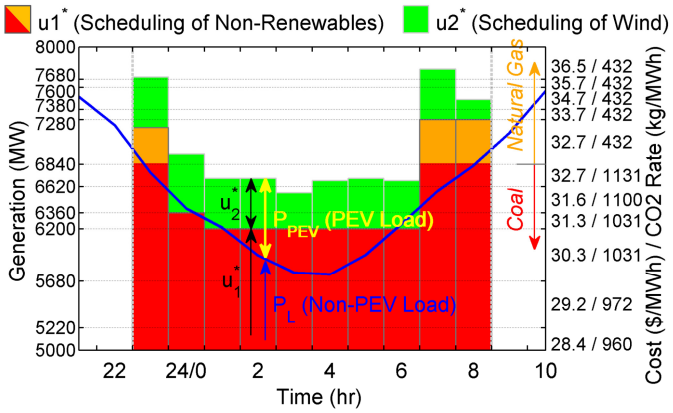

Figure 5.5 Optimal generation scheduling of the baseline case

5.3.2 Scheduling Optimization with Direct Penalty on CO_2

To reflect the importance of CO_2 emissions, a penalty on CO_2 is included in the objective function, as shown in Eq. (5.2).

$$\min_{u_1,u_2} : J_\alpha = \sum_{t=1}^{T} \left[C_g(u_1(t)) + C_{Rs}(R_s(t)) + C_{Rd}(R_d(t)) + \alpha \cdot CO_2(u_1(t)) \right] \tag{5.2}$$

where α is a weighting coefficient.

The new scheduling optimization posed in Eq. (5.2) is a multi-objective optimization problem with two control variables. Figure 5.6 shows the optimal solution with α = 10, which is the smallest weight that produces control signals different from the baseline case. The change is subtle, in that a small amount of non-renewable generation was shifted from Hour 24 to Hour 23. The non-renewable generation in Hour 23 increases from 7,200MW to 7,280MW, whereas the non-renewable generation in Hour 24 decreases from 6,360MW to 6,280MW. The shift allows more electricity to be generated by the natural gas power plant with a CO_2 rate of 432 kg/MWh rather than by the coal power plant with a CO_2 rate of 1,131kg/MWh. The shift of the non-renewable generation means that some of the controllable PEV load will be served at different times.

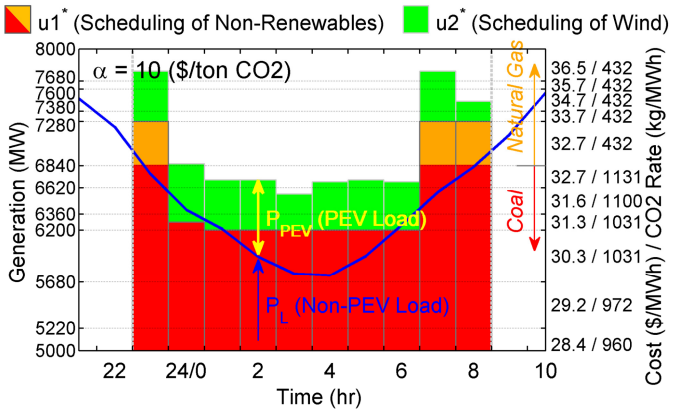

Figure 5.6 Optimal scheduling with a direct penalty on CO_2 emissions

Figure 5.7 shows the optimal solution with $\alpha = 55$, which is much larger than the previous value. As expected, more non-renewable generation is relocated to times when the low-CO_2 natural gas capacities are available, which creates undesired peaks at the beginning and the end of valley hours. Although this solution behavior is mathematically correct, the undesired peaks make this approach impractical. Thus, a different means, more than relocating the PEV load, needs to be developed to reduce the carbon emissions.

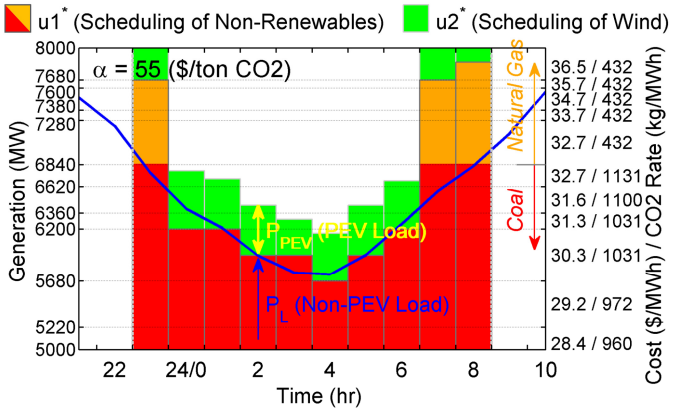

Figure 5.7 Optimal scheduling with a large direct penalty on CO_2 emissions

5.3.3 Scheduling Optimization with CO_2 Disincentive

The solutions in the previous section show that controlling the demand on the grid (by controlling the PEV charging) can only achieve limited reduction in the grid CO_2 emissions. Therefore, in addition to the demand-side control, a new approach to control the supply is proposed. The idea is to alter the dispatch order of power plants so that expensive low-CO_2 plants can be dispatched before cheap high-CO_2 plants. A carbon

disincentive, denoted as β, is introduced for this purpose. The generation price of each power plant is modified by adding a carbon disincentive based on plant emission levels, as shown in Eq. (5.3), and a new dispatch order is determined based on this modified prices.

$$p_\beta = p + \beta \cdot (\mathrm{CO_2\ rate}) \tag{5.3}$$

where p is the original price of electricity generation. Since coal-fired power plants generally have much higher CO_2 rates than natural gas power plants, it does not require a large β to swap the dispatch order of the most expensive coal-fired plant with the least-expensive natural gas plant. Figure 5.8 shows the new dispatch order with β = \$0.05/ton CO_2, the smallest disincentive rate to change the dispatch order. Therefore, by changing β, the grid operator has a means to alter the generation mix and to dispatch low-CO_2 power plants.

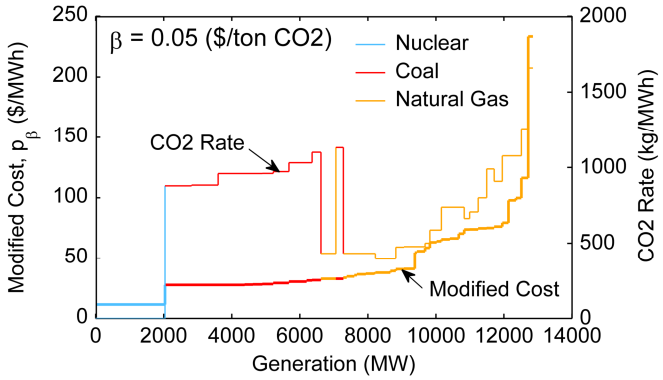

Figure 5.8 The modified cost curve and CO_2 rate with β = \$0.05/ton CO_2

The modified price curve and new dispatch order, such as the one shown in Figure 5.8, are then used in the optimization, and the objective function is revised from Eq. (5.1) to Eq. (5.4). Note that the new objective function does not contain explicit penalties on CO_2 emissions. However, due to the new dispatch order, more low-CO_2 generation capacities will be dispatched and the grid CO_2 emissions will be reduced.

$$\min_{u_1,u_2} : J_\beta = \sum_{t=1}^{T} \left[C_{\mathrm{g},\beta}(u_1(t)) + C_{\mathrm{Rs},\beta}(R_\mathrm{s}(t)) + C_{\mathrm{Rd},\beta}(R_\mathrm{d}(t)) \right] \tag{5.4}$$

The consequence of imposing the carbon disincentive is that the objective function, J_β, will increase substantially, because the optimization is based on the higher modified price defined in Eq. (5.3). Therefore, J_β includes the carbon tax revenue based on the CO_2 produced by dispatched power plants. More specifically, the carbon revenue will be the quantity shown in Eq. (5.5). However, if this extra revenue due to the carbon disincentive is not collected (or collected and later returned to consumers), consumers will need to pay only the modified costs shown in Eq. (5.6).

$$\rho = \sum_{t=1}^{T} \beta \cdot \mathrm{CO}_2(u_1^*(t)) \tag{5.5}$$

$$J'_\beta = \sum_{t=1}^{T} \left[C_{\mathrm{g},\beta}(u_1^*(t)) + C_{\mathrm{Rs},\beta}(R_\mathrm{s}(t)) + C_{\mathrm{Rd},\beta}(R_\mathrm{d}(t)) \right] - \rho \tag{5.6}$$

With the "revenue return mechanism", this carbon disincentive policy is revenue-neutral to the grid operator and is less burdensome to consumers. The assumption that the carbon disincentive policy collects no revenue is possible because, in general, the grid operator is a profit-neutral entity or a governmental agency. Again, it should be emphasized that the proposed carbon disincentive policy is not taxation, but a mechanism used by the grid operator to alter the dispatch order of power plants for CO_2 reduction.

Figure 5.9 shows the optimal solution when β = \$0.05/ton CO_2. The optimal controls turn out to be identical to those in the baseline case in Figure 5.5, but the CO_2 emissions are reduced by 0.13% at the costs of electricity generation increased by 0.04% after the carbon revenue is returned to consumers.

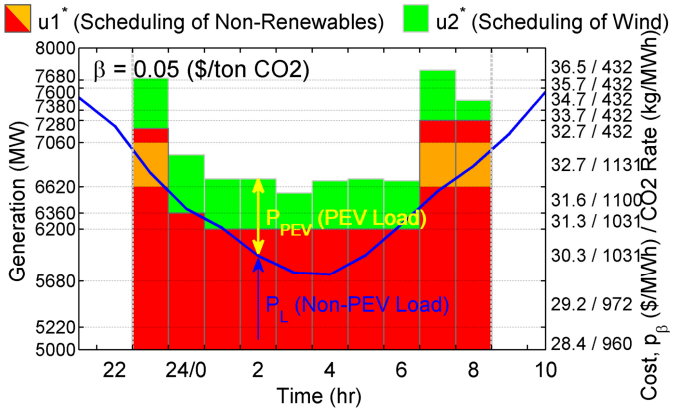

Figure 5.9 The optimal scheduling with β = \$0.05/ton CO_2

Figure 5.10 shows the modified price curve and dispatch order when the carbon disincentive is more aggressive (β = \$20/ton CO_2), in which about 25% of the coal-fired plants in the generation mix are replaced by natural gas plants. The optimal solution is shown in Figure 5.11. Notice that no spikes were created at the beginning or end of valley hours. Compared to the baseline case, the CO_2 emissions are reduced by 24.5% and the cost increased by 19.5%.

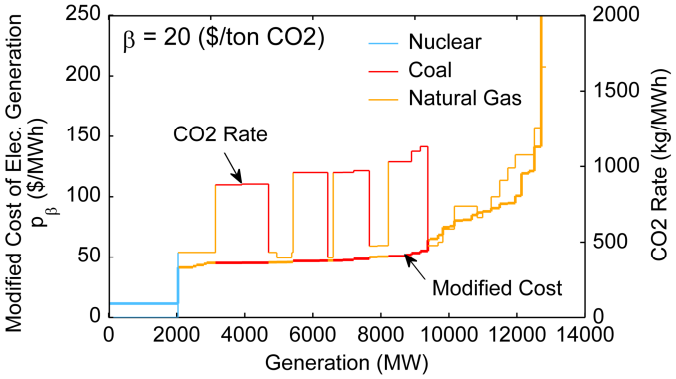

Figure 5.10 The modified price curve and CO_2 rate with β = \$20/ton CO_2

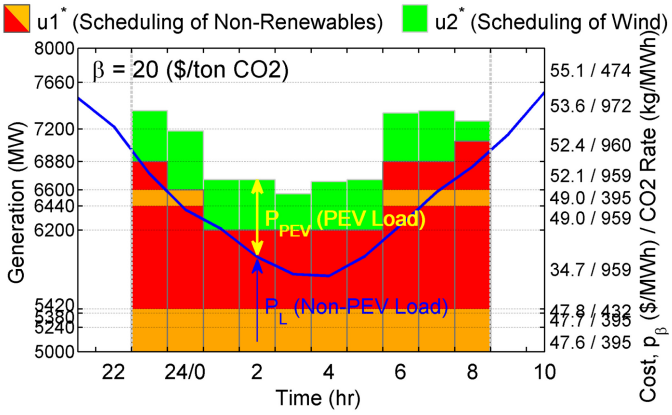

Figure 5.11 The optimal scheduling with β = \$20/ton CO_2

Besides better utilization of the generation capacities in the middle of the valley hours, this optimization formulation is more effective in reducing the CO_2 emissions compared to the scheduling optimization presented in the previous section, which penalizes CO_2 directly in the objective function. The solution in Figure 5.11 achieves a 24.5% CO_2 reduction, better than the 9.8% reduction achieved in Figure 5.7. In this

optimization formulation, *both* the supply and demand are manipulated, rather than only the demand, which is the key for achieving both CO_2 reduction and costs reduction in electricity generation.

5.4 Impacts of the Carbon Disincentive Policy

As mentioned earlier, the grid operator can view the parameter β as a tuning knob to weigh the electricity generation costs and the grid CO_2 emissions. The optimal Pareto fronts are used to show the tradeoff between the CO_2 emissions and cost of electricity generation when the carbon disincentive varies. Impacts of the carbon disincentive on the mix of electricity generation and the profits to power plants are also discussed.

5.4.1 Tradeoff between Electricity Generation Costs and CO_2 Emission

Figure 5.12 shows the optimal Pareto fronts with the carbon disincentive, β, varying from zero to \$20/ton CO_2. It is clear that, to reduce the CO_2 emissions, the cost of electricity generation has to increase because the low-CO_2 natural gas power plants are more expensive. As stated in the previous section, the emission-conscientious instance (β = 20) has 24.5% less CO_2 emissions but 19.5% higher costs than the cost-conscientious instance (β = 0).

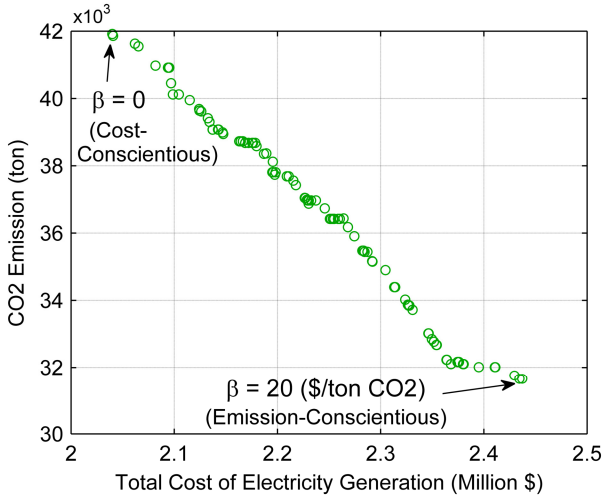

Figure 5.12 Optimal Pareto Front with β varying from 0 to \$20/ton CO_2

Figure 5.13 further shows, when the carbon disincentive is imposed, that significant amounts of electricity generation are shifted from high-CO_2 coal power plants to low-CO_2 natural gas power plants. However, the amount of electricity generated by nuclear plants is not affected. This is because nuclear power is assumed to produce no emissions; therefore, nuclear power is still the cheapest capacity after the carbon disincentive policy is imposed and will be dispatched first by the grid operator.

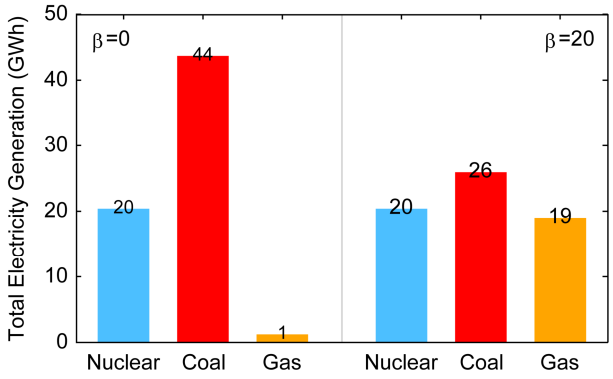

Figure 5.13 Electricity generation by different types of power plants

Furthermore, the carbon disincentive policy, although not intentionally planned, impacts profits distributions of the power plants: profits to high-CO_2 power plants are reduced and profits to low-CO_2 power plants are increased. The changes in the net profits among different types of power plants are shown in Figure 5.14. Notice that the carbon revenue is only shown for the sake of completeness but is not actually charged to the consumers. The profit change in different types of power plants can be explained by Eq.(5.7).

$$q = MC - p - \beta \cdot (\mathrm{CO}_2 \text{ rate}) \tag{5.7}$$

where q is the net profit to a power plant, MC is the market clearing price, p is generation cost, and β·(CO_2 rate) is the (virtual) carbon revenue. The presence of β increases MC, but the increased MC may not guarantee a higher net profit because β also increases the carbon revenue that has to be returned to consumers. The total revenue received by all power plants is also shown in Figure 5.14, which will be the total costs paid by consumers.

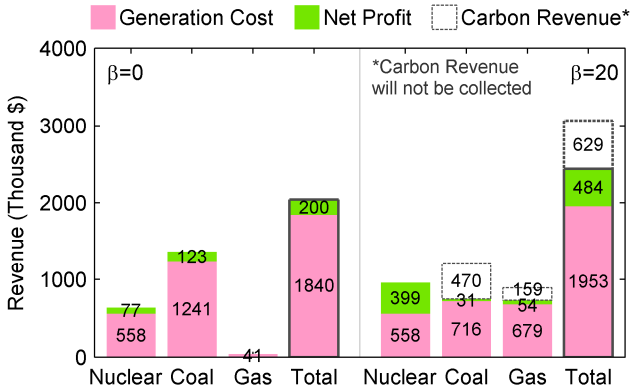

Figure 5.14 Revenue distributions of different types of power plants

5.4.2 Optimal Pareto Fronts of Various Scenarios

The Pareto Front can further provide insights into how aggressive a carbon disincentive should be to achieve a certain CO_2 reduction target. Three scenarios were investigated: Case 1 has only the non-PEV grid load and has no wind power; Case 2 has the non-PEV grid load and two million PEVs but no wind power; and, Case 3 is the case reported in the previous sub-sections with the grid load, PEVs, and wind power. These three scenarios are chosen based on the concept similar to that in the simulation study in Chapter 4: the three scenarios are set up to have PEVs and wind power included onto the electric grid progressively. Therefore, the comparison on the reduction of their CO_2 emissions and costs will allow us to understand not only the effectiveness of imposing the carbon disincentive policy, but also the effectiveness of introducing PEVs and wind power on the electric grid. Figure 5.15 shows the Pareto fronts of these three scenarios.

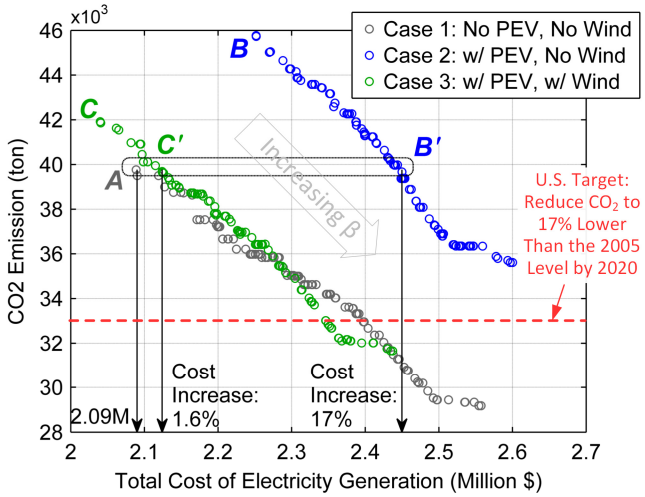

Figure 5.15 Pareto fronts of three different scenarios

The instances in the three cases with $\beta = 0$ are marked as *A*, *B*, and *C*, among which *B* has the highest cost and CO_2 emissions because it has more load due to the PEV charging but no wind power. However, it is unclear if *C* is better or worse than *A* because the former has lower CO_2 emissions but higher costs. In fact, it is more meaningful to compare *A*, *B*', and *C*' because they all have the same level of CO_2 emissions. Case *B*' has $\beta = 12.62$ and a cost 17% higher than *A*, whereas *C*' has $\beta = 5.38$ and a cost only 1.6% higher than *A*. The lower cost increase in Case *C*' is attributed to replacing non-renewable generation with wind energy. Note that the cost assessment is based on the assumption that the wind generation is free, although the wind generation may incur reserve costs if the reserves to cover wind intermittency are provided by non-renewable sources. Furthermore, the red dashed line in Figure 5.15 marks the U.S. target to reduce the greenhouse gas emissions to 17% lower than the 2005 level by 2020 [174]. For a grid with no PEVs and no wind power (Case 1), a carbon disincentive of \$15.36/ton CO_2 needs to be imposed and the electricity generation costs will increase by 15.3%. In contrast, with PEVs and wind on the grid (Case 3), a carbon disincentive of \$17.16/ton CO_2 should be imposed and the electricity generation costs will increase only by 12.8%. For Case 2, the carbon disincentive needs to be higher than \$20/ton CO_2.

Figure 5.16 shows the three Pareto fronts in normalized units; the normalized units provide a more fair comparison. The comparison in Figure 5.15 is not entirely fair because the demands in the three scenarios are not identical; two of the three scenarios

have the additional demand due to PEV charging and require more electricity generation. The normalized units render the CO_2 emissions and costs of electricity generation with the total demand served, and eliminate the inconsistency among the three scenarios. Therefore, the fact that Case 2 has higher total emissions and total costs in Figure 5.15 does not mean it is worse than Case 1. In the normalized units, Case 2 has lower per unit costs of electricity generation than Case 1 because the controllable PEV load helps to reduce the costs associated with conventional reserves and the charging is done strategically when cheap generation is available. However, given the same carbon disincentive, Case 2 still has higher per unit CO_2 emissions because this scenario dispatches relatively more coal generation in order to fulfill the PEV load. Furthermore, the fact that Case 3 outperforms Case 2 in both emissions and costs echoes the conclusion in Chapter 4 that PEVs and wind power should be deployed simultaneously.

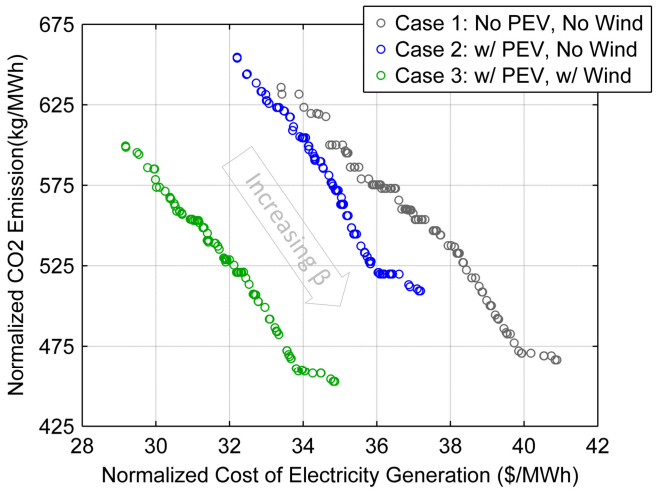

Figure 5.16 Normalized Pareto fronts

Notice that the above results are based on the data specific to the situation in Michigan; in particular, the generation mix is coal-dominant. However, the same analysis can be applied to other conditions with different generation mix, grid load, and wind conditions. For example, a gas-dominant grid, such as the Texas grid, will have a Pareto front with a flat slope (i.e. lower sensitivity) because the merit order of the power plants will not change much even if the carbon disincentive varies. A much higher load profile will also make the Pareto Front has a flat slope because, when the load is high, most

generation capacity will be dispatched no matter which dispatch order is in use. Imposing a carbon disincentive policy in this situation will not change the CO_2 emissions.

5.5 Conclusion

This chapter investigates the tradeoff between the costs of electricity generation and CO_2 emissions of an electric grid with substantial volumes of PEVs and wind power. The methodology is expanded from the optimization framework developed in the previous chapter, in that two approaches are proposed to reduce CO_2 emissions. The first approach directly penalizes the CO_2 emissions in the objective function, and the second approach introduces a carbon disincentive to alter the dispatch order of power plants. The difference between these two approaches is that the first approach only manipulates the demand, whereas the second approach controls both supply and demand and achieves more CO_2 reduction.

With the carbon disincentive policy proposed in the second approach, the grid operator can view the disincentive parameter as a tuning knob to weigh the electricity generation costs and the grid CO_2 emissions. The optimal Pareto fronts confirm that the costs of electricity generation and the CO_2 emissions are competing objectives due to the nature of the generation mix in Michigan: the generation mix has significant coal capacities that are cheaper but produce more emissions than natural gas capacities. However, the proposed carbon disincentive policy is assumed to have a revenue return mechanism, so that it is less costly to consumers although a cost increase is unavoidable. Further investigation shows that having both PEVs and wind power on the grid is helpful, in that CO_2 can be reduced with minimum increase in the costs of electricity generation. This finding echoes the conclusion in Chapter 4 that PEVs and wind power should be deployed *simultaneously*, so that the synergy between them can be fully utilized. Furthermore, analyses indicate that introducing renewable generation can significantly reduce the generation costs on the grid, but not the CO_2 emissions; manipulations in both the supply and demand on the grid are needed in order to address both the generation costs and CO_2 emissions.

The discussion covered in this chapter focuses solely on the grid operation and does not include costs or emissions during vehicle driving. A possible extension of this work is to cover aspects in both the grid and transportation sector, which should provide more insights into the tradeoff of CO_2 and cost in both sectors.

CHAPTER 6

Generation Planning for a Future Electric Grid

The previous chapters introduced various methodologies to address intra-day and hourly variations in the grid load due to PEV charging and wind power fluctuations. In this chapter, the generation planning, which is an even longer time-scale problem, will be investigated. In other words, this chapter will answer the question of *when* and *what type* of new power plants should be constructed in the next two decades.

The generating capacities evolve over time; new power plants are constructed and commissioned to keep up with the long-term demand increases in the grid load or to replace outdated power plants. In addition, increasing concerns about environmental protection and sustainability prompt the shift to renewable power sources. In this chapter, a systematic methodology is proposed to evaluate the overall cost of adding different types of generating capacities to the generation mix. Four representative types of generation technologies are investigated: nuclear, coal, natural gas, and wind power. The proposed methodology considers the costs of constructing new power plants, operating existing and new power plants, providing reserves to accommodate wind power intermittency, and the cost increase related to CO_2 tax if applicable. This methodology can serve as a tool to provide guidance to grid investors and decision makers; also, the results help to identify the obstacles that may prevent wind power from achieving the grid parity.

The remainder of this chapter is organized as follows: Section 6.2 presents models for describing the costs of existing and new generating capacities; Section 6.3 describes the process to add new generating capacities to the grid and the methodology to assess the overall costs of capacity construction and electricity generation; Section 6.4 presents results from sensitivity analyses; finally, Section 6.5 provides concluding remarks and recommendations.

6.1 Literature Review

The literature related to the generation planning can roughly be categorized into two groups; one is to use optimization techniques to find the exact generation mix, and the other is to calculate the levelized cost of energy for the new generating technologies that will be introduced on the electric grid. Figure 6.1 summarizes the two groups of literature, and their key features are highlighted blow.

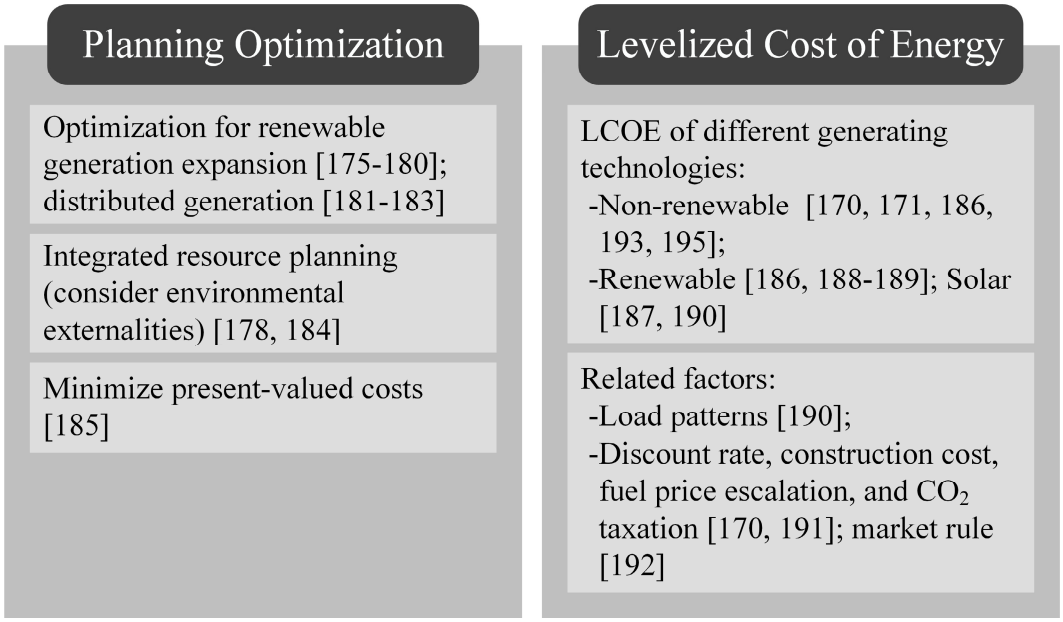

Figure 6.1 Summary of literature related to generation planning

To improve sustainability of the electric grid and to become less reliant on fossil fuel, several studies have applied optimization techniques to add large amounts of renewable generation to the energy system [175-180]. Investment in distributed generations also has been discussed, and many of them consider cogeneration to provide both heating and power services to improve overall efficiency and costs [181-183]. Integrated resource planning (IRP) organizes the use of natural resources and considers not only financial values but also environment externalities, such as greenhouse gas emissions [178, 184]. Different objective functions have been used in these planning studies, such as construction/installation costs of the project, energy generation costs, operation and maintenance (O&M) costs, or CO_2 emissions. The time horizon in these studies ranges from one to several years, while the time resolution is often one hour long,

and not shorter, to keep the problem size numerically tractable. These planning optimization problems are often solved using the linear programming or mixed-integer programming techniques, and the review in [185] provides a comprehensive summary of the different optimization formulations and solution methods adopted.

In addition to solving optimization problems for generation planning, the levelized cost of energy (LCOE), which is an estimate of the price of per unit energy, has been used to compare different generating technologies [170, 171, 186-190]. LCOE usually does not consider the hour-by-hour details in the generation dispatch; instead, it assumes that each type of power plant has a constant capacity factor, which is the annual average generation of the power plant. For example, nuclear power is often assumed to have a capacity factor higher than 85%, while the intermittent wind and solar power around 35% (see Appendix C). Using a constant capacity factor to approximate the operation of a power plant simplifies the calculation of generation dispatch. This simplification allows LCOE to cover a very long time horizon, such as 40 years, which is a feature the aforementioned planning optimization cannot grant. However, LCOE is known to be sensitive to the assumed values of the parameters, including geographical attributes (such as the local generation mix and load patterns) [190], and financial attributes (such as the discount rate, construction cost, fuel price escalation, and CO_2 taxation) [170, 191]. The electricity market rules also impact the LCOE [192], especially for renewable generating technologies because they require reserves to mitigate the intermittency. However, reserve costs have been ignored in most past studies. This may be justified when wind power is mandated and the reserve cost is absorbed by utility companies, but, in the long term, reserve costs to compensate for wind intermittency need to be considered when assessing the true cost of the grid power generation. Furthermore, because LCOE is vulnerable to uncertainties in input parameters, it is necessary to conduct sensitivity analyses [190] or perform Monte Carlo simulations [187] to give a range of results rather than a single future cost projection, in order to provide better guidance to grid investors and decision makers.

As increasing the share of renewable generation is a commonly-agreed objective in generation planning, the renewable intermittency and reserve-related costs should be included into the evaluation of new power plant construction. In addition, both the supply

and demand on the electric grid evolve over time. On the demand side, the grid load will increase every year, and more and more generation needs to be scheduled to satisfy the growing demand. On the supply side, the generation mix will change when new power plants are commissioned, and the grid operator will dispatch both existing and newly-commissioned power plant according to the new merit order. However, the existing planning optimizations do not comprehensively consider all of the above features; in particular, the reserve costs have been ignored in most studies. On a different note, the decision of constructing new generating capacities is assumed to be market driven as the ultimate goal of investigators will be to maximize profits (i.e. maximize costs). Thus, it is desirable to investigate all relevant financial factors seen in the LCOE related studies. A comprehensive generation planning should consider all of the aforementioned attributes, and a systematic methodology of cost evaluation is proposed in this chapter to achieve such a goal.

This study considers four types of representative generating technologies: nuclear, coal, natural gas, and wind power. Wind power is chosen over other type of renewable generation, as it is the technology that currently has the installation costs low enough to be comparable to coal-fired power plants [7, 8]. To make the planning problem tractable, instead of solving a large optimization problem to find the optimal generation mix, the methodology evaluates four separate scenarios. In each scenario, only one of the four generation technologies is chosen for all new constructions. Since each scenario will be a much simpler capacity planning problem, the long-term trends (annual increases in grid load), short-term dynamics (sub-hourly fluctuations in wind power generation), and changes in the merit order for power plant dispatch can all be included. To compare the different generating technologies, the proposed methodology considers costs of constructing new power plants, operating both new and existing power plants, reserves needed to accommodate intermittent wind generation, and the CO_2 tax if applicable. Therefore, a unique feature of this methodology is that it calculates the system-wide costs of electricity generation, rather than the technology-specific LCOE. This system-level perspective is important because adding new generating capacities to the grid will impact not only new capacities being introduced, but also existing capacities. Also, the four separate scenarios are still computationally affordable to conduct sensitivity analyses on

parameters with financial significance, such as the discount rate, construction cost deviation, natural gas price escalation, and CO_2 tax rate. A time span of 23 years (from 2012 to 2035) is considered when demonstrating the methodology in this chapter, and the goal of the generation planning is to maintain the generation adequacy, meaning to keep the total generating capacity 10% above the peak load at all time, at minimum costs.

6.2 Modeling of the Electric Grid

Several models are developed to calculate the costs of existing and new generating capacities on the electric grid. More specifically, the following models describe the construction costs of new capacities and the electricity generation costs of both new and existing capacities. The construction costs of existing capacities are irrelevant, as decisions of the generation planning will not impact them. In addition, wind power will have additional costs associated with reserve scheduling and dispatch due to its intermittency. CO_2 emissions produced by non-renewable power plants incur additional costs when the carbon tax is imposed. The statistics of the State of Michigan are again used to develop these grid models, although the proposed methodology is general and can be applied to other utility-scale power systems.

6.2.1 Generation Cost and CO_2 Emission of Existing Generating Capacity

The models to describe the costs of electricity generation and CO_2 emissions of existing capacities are largely based on the models previously developed in Section 4.2.3 and 5.2.3. Also, the generation costs and emissions of new capacities will be derived from these models. However, the cost model now includes more details. The electricity generation cost is assumed to consist of two components: fuel cost and O&M (operation and maintenance) cost. The reason of separating the fuel cost from the O&M is that the former will be updated annually according to the fuel price escalation, while the latter is assumed to be fixed. In reality, the O&M cost may increase slightly as power plant ages; however, such a phenomenon is ignored in this study. Figure 6.2 shows the existing generating capacities in Michigan in 2012, which totaled 14,540 MW. In general, the fuel cost is more substantial than the O&M cost for coal and natural gas power plants. On the contrary, the O&M cost of nuclear power is equally substantial as its fuel cost because

the nuclear fuel is much cheaper. Furthermore, the predicted wholesale fuel prices shown in Figure 6.3 will be used to update the fuel cost for electricity generation throughout the operation years. The data in Figure 6.3 is collected from two different sources. The nuclear fuel price is derived from [193], which increases about 0.5% annually. The prices of natural gas and coal are extracted from [158]; the former has an annual increase around 2% and the latter around 0.75%. Again, the grid operator is assumed to dispatch generating capacities based on the merit order, meaning that cheaper power plants will be dispatched before expensive ones. However, construction costs of existing capacities are not considered as they cannot be altered by the decision to add new capacities on the grid.

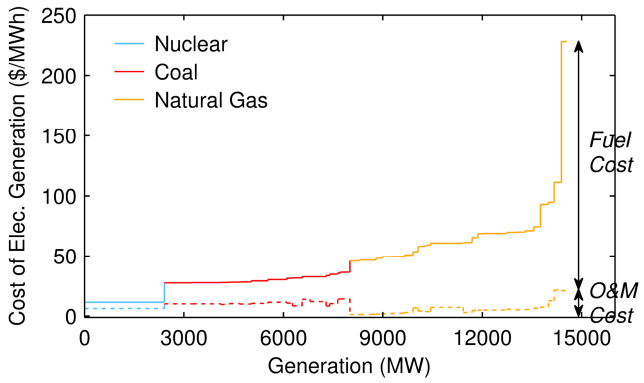

Figure 6.2 Generation cost of existing capacities in Michigan in 2012 [145]

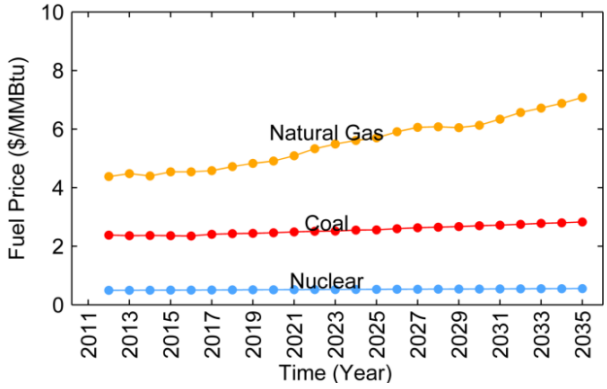

Figure 6.3 Long-term fuel price [158, 193]
(Annual fuel price escalation: nuclear ≈ 0.5%; coal ≈ 0.75%; natural gas ≈ 2%)

The assumptions on the reserve costs remain the same. There are two costs associated with reserves: 1) the reserve scheduling cost is about 3% more expensive than the electricity generation, based on the statistics in [127]; and, 2) the reserve dispatch cost

is assumed to be the same as the electricity generation cost and only occurs if the reserve is dispatched.

The CO_2 rate curve in Section 5.2.3 is again used to describe the grid CO_2 emissions, which incur costs if the carbon tax is imposed.

6.2.2 Cost Assumptions for New Generating Capacity

To build new generating capacities, both the construction costs and the generation costs incurred throughout the lifetime need to be considered.

The costs of power plant construction can be found in many references, and Figure 6.4 summarizes the ones that are more well-known. A complete summary can be found in Appendix C. The trend observed from the data indicates that natural gas is the least expensive technology to construct, and nuclear is the most expensive. As a matter of fact, nuclear power has an extra cost that will incur at the end of plant lifetime due to decommissioning. According to [194], the decommissioning cost is 300-400 million dollars per plant; however, this cost is not included in the construction cost, but included in the O&M throughout the plant lifetime as the decommissioning funds [195]. Furthermore, wind power appears to be competitive; its construction costs have been dropping since 1980 (see Figure 1.7) and now fall in between natural gas and coal. Eventually, the data reported in [53] and [196] are used in this study, because they are more relevant to the situations in the U.S.

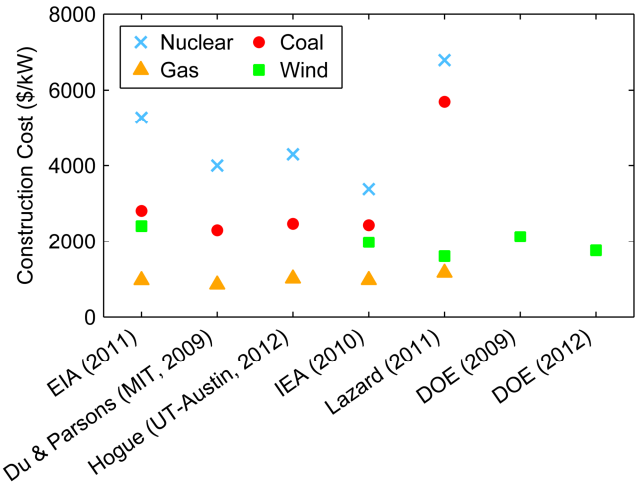

Figure 6.4 Construction cost summary [53, 170, 171, 186, 195-197]

In addition to the construction costs, Table 6.1 lists the other parameters related to constructing different types of power plants. The nameplate capacity of each type of generating technology is different; plants with a larger nameplate capacity usually have a longer lead time, which means the construction has to start years before the power plant is commissioned. The construction outlays are assumed to have a generic distribution as shown in Figure 6.5 with higher capital expenses in the middle of the construction [195]. The construction outlays will be used to calculate cash flows throughout the construction phase in Section 6.3.4.

Table 6.1 Parameters Related to Capacity Construction

	Nuclear	Coal	Natural Gas	Wind
Nameplate Capacity (MW) [a]	2409	1300	500	100
Plant Lifetime (yr) [a]	30	40	30	25
Overnight Cost ($/kW) [a, d]	5,275	2,809	967	1,750 [b]
Lead Time (yr) [a]	6	4	3	3
Discount Rate (-) [c]	7.68%			

[a] Adopted from [196]. [b] Adopted from [53]. [c] Adopted from [186].

[d] Overnight costs have a 3% annual increase rate [195]. The numbers shown in this table are for year 2012.

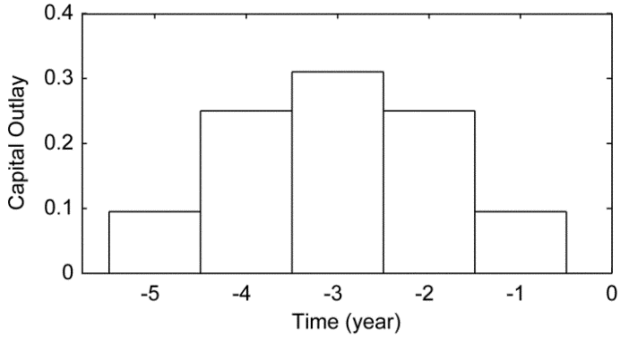

Figure 6.5 Capital outlays for power plant construction with a 5-year lead time [195] (Year 0 is the end of construction)

Once construction is completed and the power plant is commissioned, costs to generate electricity will incur whenever the power plant is dispatched throughout the

plant lifetime. New capacities are assumed to have the same generation costs as the cheapest existing capacity, assuming that new technologies are no more expensive or polluting than existing ones. CO_2 rates of new capacities are derived under similar assumptions. Furthermore, wind power will incur additional costs due to reserve scheduling/dispatch because of its intermittency. The reserves for wind power are discussed in the next section.

6.2.3 Costs due to Wind Power Intermittency

Wind intermittency impacts both the construction and operation of wind power. More specifically, higher nameplate capacities need to be constructed and more reserves need to be scheduled to ensure reliable grid operation.

The Eastern Wind Dataset from the National Renewable Energy Laboratory (NREL) [124] shows that the capacity factor of a typical wind power plant is about 32%; thus, it is assumed that the nameplate capacity of wind power needs to be tripled to meet the grid load increase.

The reserve requirement of wind power is calculated by the model developed in Section 3.2.1. However, some modifications are made so that the model can be scaled up or down when different amounts of wind power are added to the grid. The reserve scheduling and dispatch induce costs according to the assumptions on reserve costs mentioned in Section 6.2.1.

6.3 Planning of Generating Capacity for 2035

Generating capacities of the electric grid are designed to be higher than the peak grid load to ensure reliable grid operation. In this study, it is assumed that the total generating capacity should be kept 10% above the peak load at all times. In the following, a systematic methodology is developed to evaluate the overall costs of different strategies of adding new generating capacities to meet the increasing grid load in Michigan from 2012 to 2035. Four scenarios are created to investigate the four types of generation technologies of interests: nuclear, coal, natural gas, and wind. Each scenario deploys one and only one of the four technologies for new capacities. For simplicity, it is assumed that none of the existing power plants reaches retirement in the next 23 years.

6.3.1 New Generating Capacity to Meet Grid Load Increase

Unlike the daily load profile used in previous chapters, the whole-year load data in the Detroit Edison service area is used to model the base electric load on the Michigan grid; Figure 6.6 shows the annual load profile in 2012, which peaked at 12,573 MW. It is further assumed that the grid load will increase 1% annually [158]. Note that the PEV charging load is excluded from the load data. It is believe that the PEV load will not significantly impact the decisions of generation planning, because the PEV charging is unlikely to happen during peak hours on the grid. Therefore, for simplicity, the PEV load is not considered in this study. However, such a simplification also eliminates the possibility to use PEVs as an asset to facilitate grid operation in valley hours.

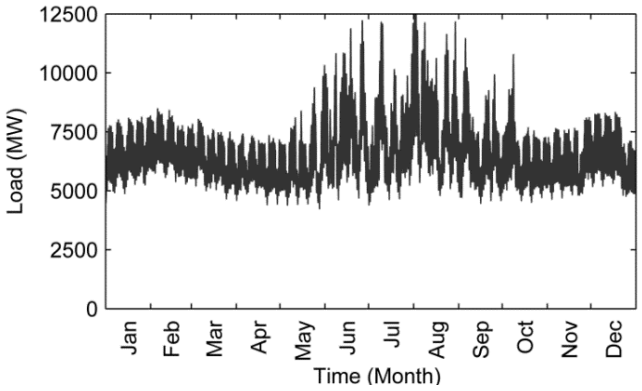

Figure 6.6 The annual grid load of Michigan in 2012 [90]
(time resolution: 1 hour)

For generation adequacy, it is assumed that the total generating capacity has to be kept 10% above the peak load at all times [178]. Figure 6.7 shows the projected peak load increments from 2012 to 2035 and the new generating capacity required to maintain the 10% margin. Notice that the total generating capacity in 2012 (14,540MW) has a 15.9% margin above the peak load (12,537MW). Figure 6.7 further shows that, if nuclear was the chosen technology, two new plants would have to be commissioned by 2035; one in 2017 and the other in 2032. Therefore, the construction of these two nuclear power plants will start in 2011 and 2026 due to the 6-year lead time, and the construction costs will spread throughout the construction period with outlays similar to that shown in Figure 6.5. The construction and commissioning year of other types of generating technologies were

found in similar ways. Note that the nameplate capacity of wind power needs to be tripled due to wind intermittency (as explained in Section 6.2.3).

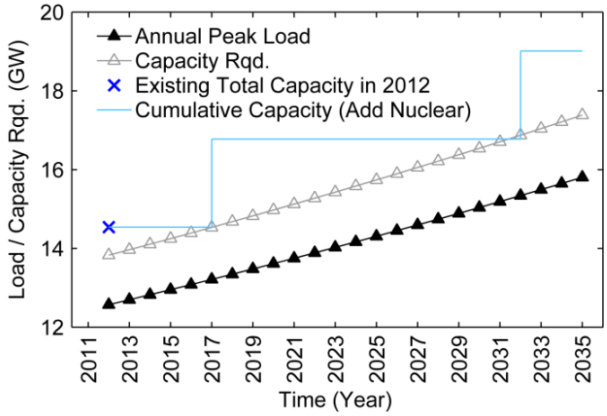

Figure 6.7 The peak load increase and new capacity requirements from 2012 to 2035

6.3.2 Economic Dispatch

The grid operator is assumed to dispatch generating capacities based on the merit order to meet the grid load on an hourly basis, meaning that the grid operator dispatches cheaper power plants before expensive ones. Figure 6.8 shows the merit orders of two different years; Year 2012 is the base year and 2017 is the year when a new nuclear power plant is commissioned. The merit order in 2017 is different from that in 2012 because of the increasing fuel costs (as shown in Figure 6.3). In addition, the new nuclear capacity, with the lowest O&M and fuel costs among its own kind, will be dispatched before existing capacities when the grid load calls for service.

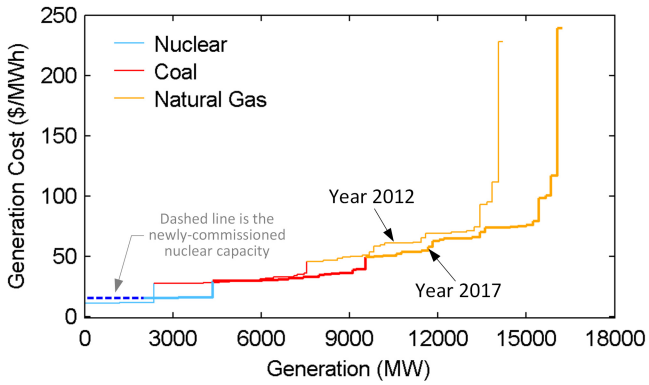

Figure 6.8 Merit order in 2012 and 2017 with additional nuclear power

To illustrate how the changes in the merit order affect the economic dispatch, Figure 6.9 and Figure 6.10 show the economic dispatch in August 2, 2012 and August 2, 2017. They are the dates when the peak load happens. Note that the electricity generation in 2017 is about 300MW higher than that in 2012 in order to satisfy the growing demand, which increases 1% every year. The electricity generation in Figure 6.9 matches the merit order of 2012 shown in Figure 6.8, in that the load below 2,405 MW is served by nuclear power, between 2,405-7,821MW by coal, and above 7,821MW by natural gas. On the other hand, the electricity generation in Figure 6.10 matches the merit order of 2017, in that load below 4,641 MW is served by nuclear power, between 4,641-10,057MW by coal, and above 10,057MW by natural gas. Furthermore, among the load served by nuclear power, the load below 2,236MW is served by the newly-commissioned nuclear capacity, and the load between 2,236-4,641MW is served by existing nuclear capacity.

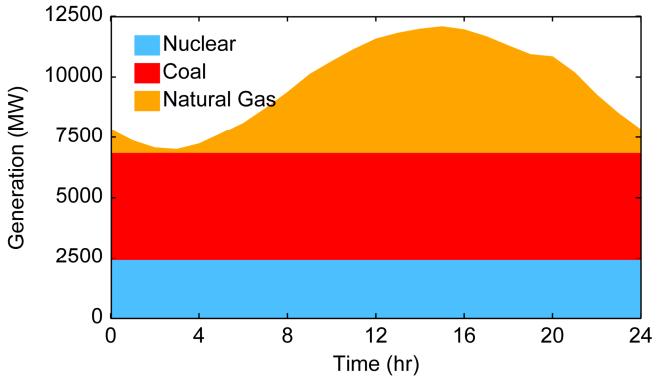

Figure 6.9 Hourly electricity generation in the peak load day in 2012

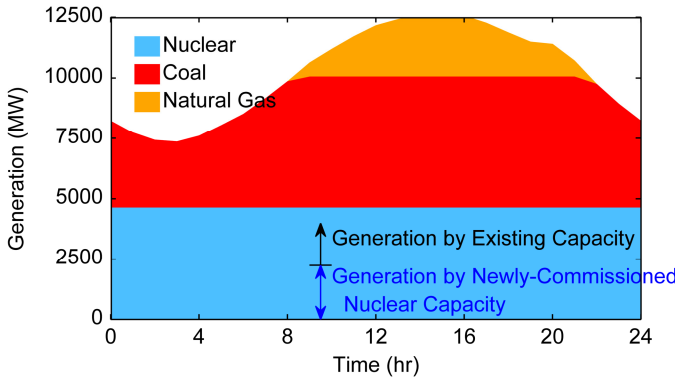

Figure 6.10 Hourly electricity generation in the peak load day in 2017

In terms of the 23-year long horizon of interests, Figure 6.11 shows the long-term evolution of electricity generation when the grid capacity is upgraded with nuclear power. It shows that, before the nuclear plant is commissioned in 2017, the existing nuclear power supplies about one-third of the electricity generation; the rest is contributed by coal and natural gas. Nuclear generation jumps in 2017 and 2032 due to the commissioning of new nuclear capacities. The same process is applied to two other scenarios when the grid is upgraded with coal and natural gas power plants.

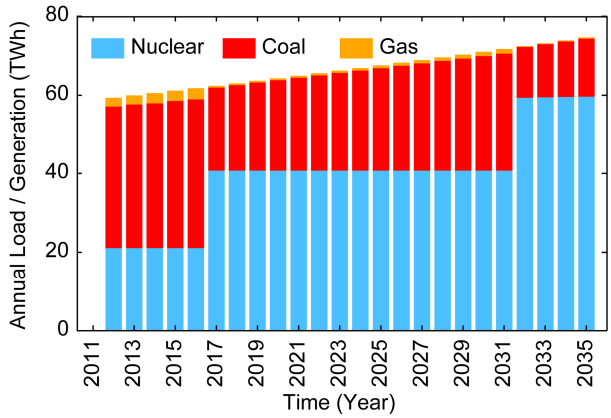

Figure 6.11 Evolution of annual electricity generation with additional nuclear power

6.3.3 Scheduling Optimization for Wind Power

The merit order dispatch needs modification when wind power is present, because reserves are needed to mitigate the wind intermittency. The scheduling optimization problem defined in Eq. (6.1) is solved every hour to find the optimal wind scheduling to minimize $J_{t,n}$, which is the total cost of electricity generation in hour t of year n. The objective function has three terms: costs of non-renewable electricity generation (C_g), reserve scheduling (C_{Rs}), and expected reserve dispatch (C_{Rd}). The objective function is minimized by one control variable, the wind power scheduling. The costs of non-renewable generation (C_g) can be read from the merit order, which may change when new generating capacity is commissioned, and the reserve scheduling costs (C_{Rs}) and the reserve dispatch costs (C_{Rd}) follow the assumptions described in Section 6.2.1.

$$\min_{u} : J_{t,n} = C_g(L_{t,n} - u) + C_{Rs}(R_s) + C_{Rd}(R_d) \tag{6.1}$$

where $L_{t,n}$ is the grid load in hour t of year n. The grid load ($L_{t,n}$) and wind forecast (w_f) are assumed to be known when solving this scheduling optimization. After the optimal wind scheduling is found, the non-renewable capacities follows the original economic dispatch to produce electricity in the amount of $L_{t,n} - u^*$, so that the grid loads are satisfied.

The scheduling optimization defined in Eq. (6.1) is actually a reduced problem of the horizon optimization problem in Section 4.3.1. Equation (6.1) is an instantaneous optimization problem and has only one control variable, but the optimization problem presented in Section 4.3.1 has two control variables, the scheduling of non-renewable generation and the scheduling of wind power. The problem in Section 4.3.1 has a higher problem dimension and is solved over a horizon because it has the PEV charging load. The new optimization problem in Eq. (6.1) does not have PEVs to act as an energy storage device to buffer the wind surplus or deficit; therefore, the non-renewable generation is not a degree of freedom but has to make up the remaining generation to serve the grid load after the wind power scheduling is determined. Figure 6.13 shows how the merit order in 2017 (the year when new wind power is first commissioned) differs from that in 2012 (the base year). This is an extraction of the whole merit order, which includes the generating capacities only up to 9,000MW. The costs of non-renewable generation in 2017 are more expensive than those in 2012 because of the fuel price escalation, and, in addition, the merit order in 2017 includes the newly-commissioned wind capacity, whose sorting position in the merit order is the found by solving the scheduling optimization defined in Eq. (6.1).

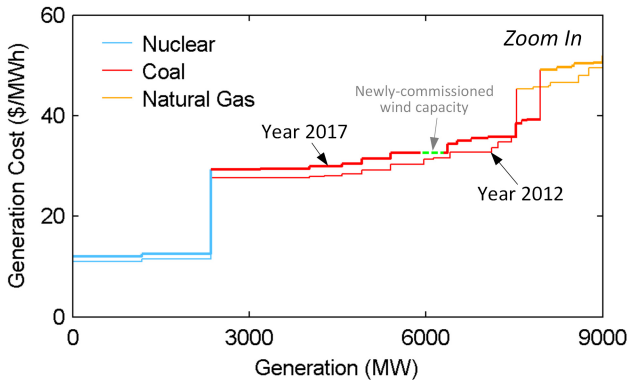

Figure 6.12 Merit order in 2012 and 2017 with additional wind power

Figure 6.13 shows the evolution of annual electricity generation when the grid is upgraded with wind power. Although the contribution of wind power increases gradually throughout the year as the wind capacity increases, not all wind power production is dispatched; some wind generation is curtailed as advised by the scheduling optimization in Eq. (6.1) to avoid paying for reserves.

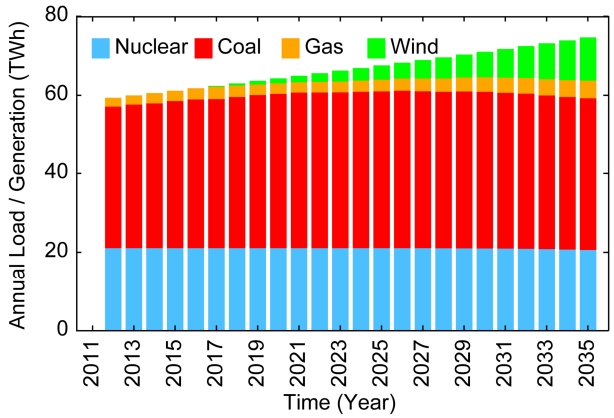

Figure 6.13 Evolution of annual electricity generation with wind power

6.3.4 Costs with Different Generating Capacity Upgrades

Once the construction and dispatch of new and existing generating capacities are known, a cash flow analysis is conducted to calculate the present value of all costs and LCOE for evaluating the investment choices of the grid upgrade.

Figure 6.14 shows the cash (out) flows of upgrading the grid with nuclear power; both costs of construction and electricity generation are considered. Construction costs only occur during construction periods. In this case, years 2011-2016 are the construction period of the first nuclear power plant, and construction outlays in those years follow a pattern similar to that in Figure 6.5; so do the construction outlays for the second nuclear power plant in 2026-2031. The construction costs of the second nuclear power plant are more expensive than the first one due to the 3% annual increase mentioned in Table 6.1. On the other hand, generation costs occurs every year due to the dispatch of *both* existing and new generating capacities (operation costs prior to the 2012 base year are irrelevant and excluded as the investment choices does not impact them). The generation costs are calculated based on the economic dispatch. For example, by cross referencing the cost

curves in Figure 6.8 and the hourly electricity generation in Figure 6.9, the grid operator will know which power plants are dispatched and how much costs are incurred in every operating hour throughout the years. Furthermore, Figure 6.14 shows that operating costs have large drops in 2017 and 2032. This is because the commissioning of new nuclear plants changes the merit order, as illustrated in Figure 6.8.

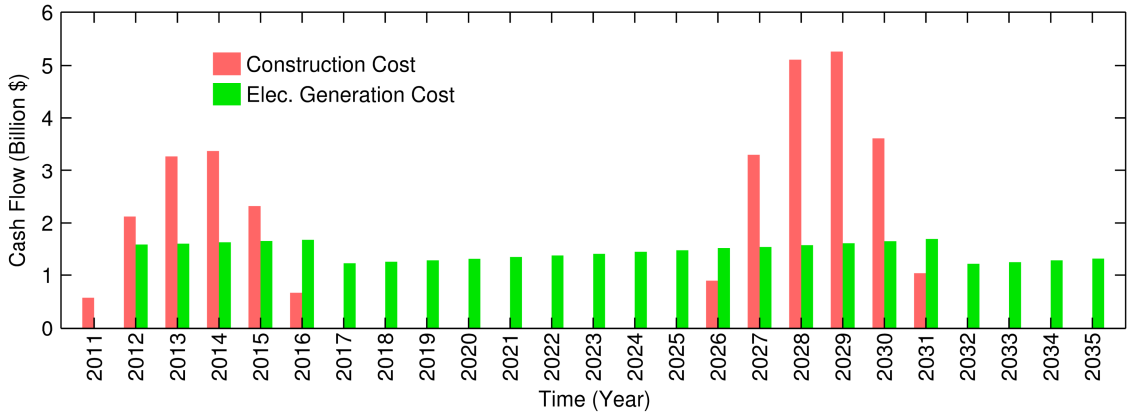

Figure 6.14 Cash flow of adding nuclear power to the grid

The cash flows shown in Figure 6.14 are discounted using Eq. (6.2), which renders costs in the past or future into a common unit of value [170].

$$DCF_n = \frac{CF_n}{(1+d)^n} \tag{6.2}$$

where CF_n is the cash flow in year n, d is the discount rate, and DCF_n is the discounted cash flow in year n. In this study, Year 2012 is chosen to be the base year and has n=0. In addition, Eq. (6.2) implies that, the further into the future a cost occurs, the less costly it is to the investor [170]. Figure 6.15 shows the discounted cash flows when the discount rate is 7.68% (see the assumptions of parameter values in Table 6.1). It can be seen that the construction costs of the second nuclear power plant are in fact cheaper than the first plant when the discount rate is considered. The cash flow analysis is conducted for all four types of generating technologies and is shown in Appendix D.

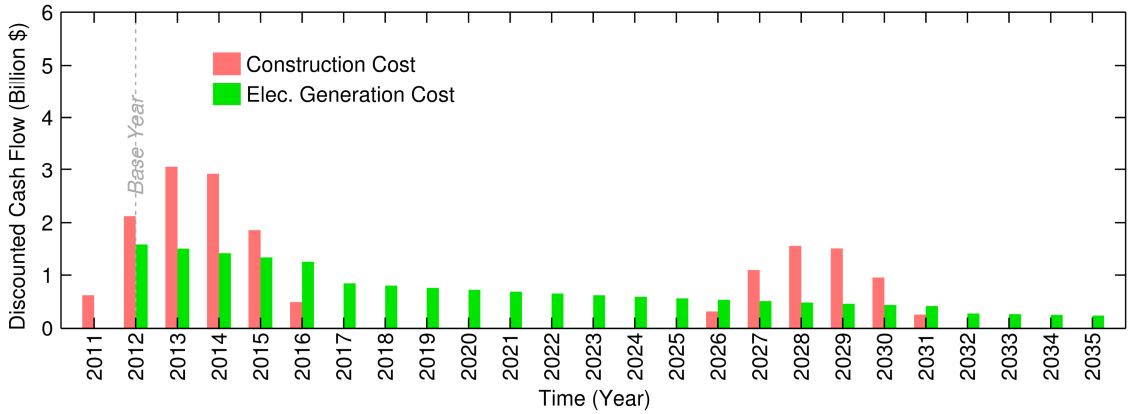

Figure 6.15 Discounted cash flow of adding nuclear power to the grid

To compare the several different investment choices, the total discounted cost, which is the sum of the discounted cash flows, is calculated. The total discounted cost is essentially the present value of all costs incurred throughout the years of interest. The significance of the total discounted cost lies in the fact that it consolidates all the costs to a unified value and provides a fair index to compare different investment choices. Furthermore, the total discounted cost can be interpreted as the amount of capital the investor needs to have (or borrow from the bank) in 2012 in order to cover all expenses throughout the years of interests. However, the amount of capital is not found by summing up the expenses in each operation year algebraically, but using Eq. (6.2), in which the discount rate is involved. In short, the investment choice with a lower total discounted cost is more cost-effective.

Figure 6.16 shows the total discounted costs of the four different investment choices, including the detailed makeups in the costs of electricity generation. The total discounted cost is further used in Eq. (6.3) to calculate the LCOE [190]. Notice that the LCOE shown in Table 6.2 is not specific to any type of generating technology, but the system-wide cost of using both existing and new generating capacities to produce electricity.

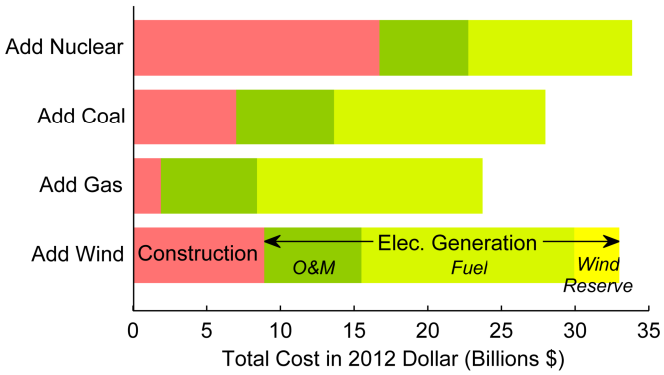

Figure 6.16 Total discounted costs (i.e. present value) over 23 years

$$LCOE = \frac{\sum_{n=0}^{N} \frac{CF_n}{(1+d)^n}}{\sum_{n=0}^{N} \frac{E_n}{(1+d)^n}} \tag{6.3}$$

where E_n is the annual electricity generation in year n (which is shown in Figure 6.11 and Figure 6.13), and, in this study, N is 23 for Year 2035.

Table 6.2 System-Wide LCOE

Scenario	**LCOE ($/MWh)**
Add Nuclear	45.08
Add Coal	37.24
Add Gas	31.57
Add Wind	43.92

To elaborate further on the information in Figure 6.16, it is clear that the makeup of the total discounted cost is different in each of the four different scenarios. Upgrading the grid with nuclear power will have the highest construction cost and the lowest fuel cost, whereas upgrading the grid with natural gas has the lowest construction cost and the highest fuel cost. O&M costs are similar in all four scenarios due to the similar O&M costs among different generating technologies (see the dash line in Figure 6.2). Both the total discounted cost and LCOE indicate that wind power is an expensive option due to the high construction cost for tripling the nameplate capacity and the operation cost for

reserve scheduling and dispatch. In other words, the costs to compensate for wind power intermittency greatly affect the wind power's ability to achieve grid parity.

6.4 Sensitivity Analyses

To better understand how uncertainties in input parameters impact the cost analysis of generation planning, sensitivity analyses are conducted. After reviewing the literature, four parameters are chosen to be further investigated: discount rate, construction (overnight) cost, natural gas price escalation, and CO_2 tax. The CO_2 tax is assumed to be the same as the carbon disincentive policy proposed in the previous chapter, in that the CO_2 tax will alter the merit order of power plants to promote the use of low-emission capacities, but no tax revenue will actual be collected. This revenue-neutral CO_2 taxation will be less costly to consumers. Table 6.3 summarizes the nominal and upper/lower bounds of these parameters.

Table 6.3 Parameters for Sensitivity Analyses

Parameter	Lower Bound	Nominal	Upper Bound
Discount Rate (-)	3%	7.68%	12%
Construction Cost Variation (-)	-20%	0	+20%
Gas Price Escalation(-) [e]	-2.5%	2%	5%
CO_2 Tax ($/ton CO_2) [f]	0	0	30

[e] The natural gas price shown in Figure 6.3 has an escalation of 2%, and the upper and lower bounds cover the 80% confidence intervals reported in [170].

[f] The CO_2 tax in [171] is used as the upper bound.

Figure 6.17 to Figure 6.20 show the sensitivities of the total discounted costs to the four chosen parameters. The discount rate impacts the cost in a way different than the other three parameters: a higher discount rate leads to cheaper costs when computing the present value, and all curves in Figure 6.17 have negative slopes. This is consistent with Eq. (6.2), in that a higher discount rate makes a future cost less costly in the present day. The other three parameters all have positive correlations with the cost. In addition, the discount rate has the most pronounced impact on the total cost (the curves in Figure 6.17

have steeper slopes than those in Figure 6.18 to Figure 6.21). This is because the discount rate affects both the construction and generation costs, whereas the other three parameters only affect either the construction or generation cost but not both.

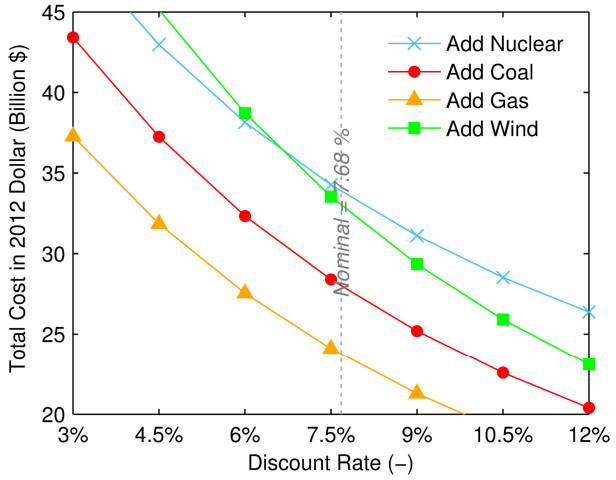

Figure 6.17 Sensitivity of total electricity generation cost to discount rate (all other three parameters are kept at nominal)

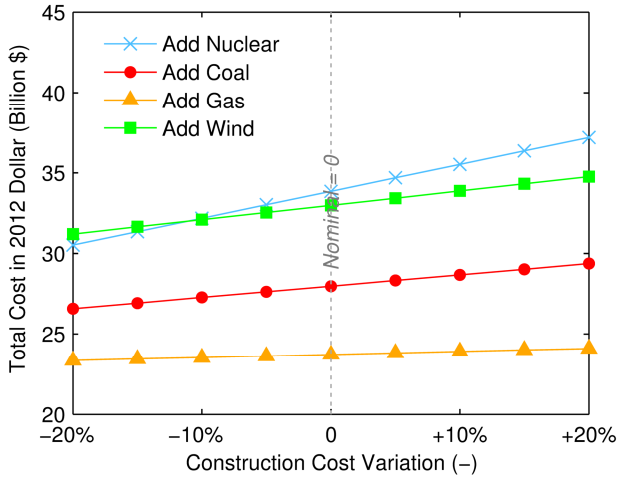

Figure 6.18 Sensitivity of total electricity generation cost to construction cost

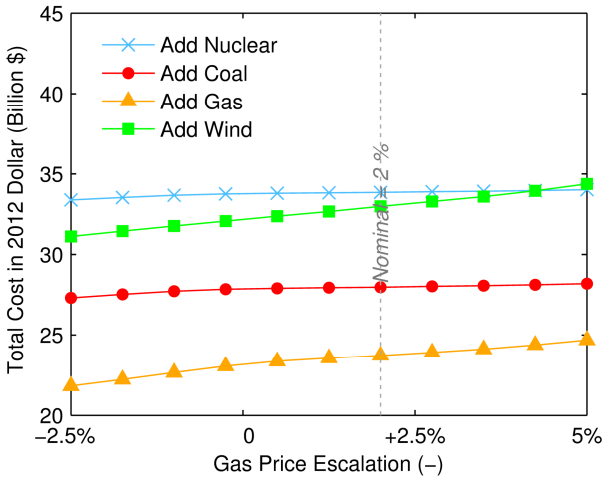

Figure 6.19 Sensitivity of total electricity generation cost to gas price

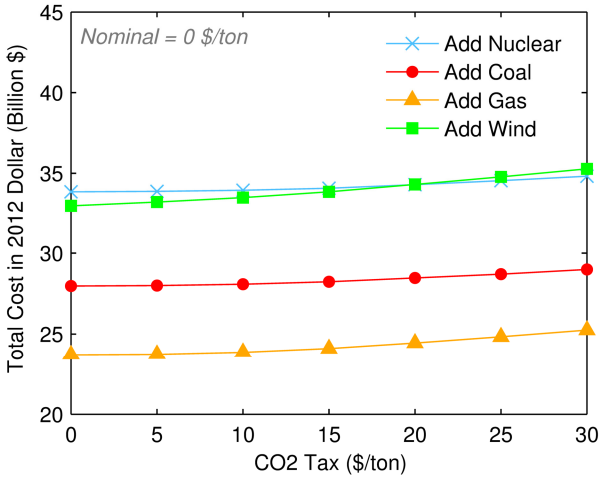

Figure 6.20 Sensitivity of total electricity generation cost to CO_2 tax

Figure 6.17 to Figure 6.20 conclude that nuclear and wind power are the most expensive options for upgrading the grid capacity in all possible parameter perturbations, and natural gas is the least expensive. In addition, it is rather surprising that neither the higher gas price nor CO_2 tax reduces the gap between wind power and non-renewable generating technologies. This is because reserves for wind power are provided by non-renewable capacities, and the reserve price is coupled with electricity generation cost (see assumptions of reserve prices in Section 6.2.1).

Despite the fact that the CO_2 tax cannot promote the dispatch of wind power on the grid, it is an effective means to reduce the grid CO_2 emission no matter what type of

technology is added to the grid. In Figure 6.21, even the scenario of upgrading the grid with nuclear power benefits from a decrease in CO_2 emissions with the CO_2 tax. However, in some instances, upgrading the grid with wind power results in slightly higher CO_2 emissions than natural gas. This is because the generation mixtures are different in these two scenarios—the former will use existing (old) natural gas plants to serve the grid load when wind fall shorts, whereas the latter will use new natural gas plants to serve the grid load. The new natural gas plants are assumed to have the lowest CO_2 rates among the existing natural gas plants (see assumptions of new generating capacity in Section 6.2.2).

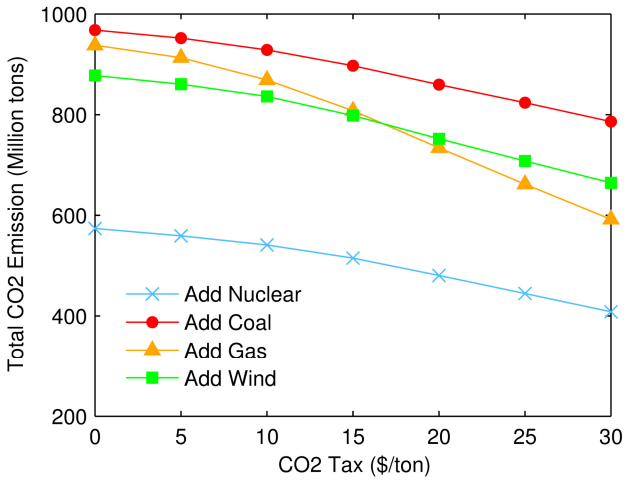

Figure 6.21 Sensitivity of total CO_2 emission to CO_2 tax.

The sensitivity analysis shows that adopting natural gas power plants is the most cost-effective choice to upgrade the grid capacity with all possible parameter perturbations, even when the natural gas price escalation is quite high. On the other hand, adopting wind power is expensive because of the costs to compensate for wind intermittency. Wind intermittency also reduces the effectiveness of wind power to reduce the grid CO_2 emission.

One potential solution to suppress costs associated with wind intermittency is to introduce energy storage devices to the grid. Although this will incur additional construction costs, the capacity of the storage can be small if a proper control algorithm is adopted, according to the findings in Chapter 3. A quick cost estimation of adding BESS

(battery energy storage system) and wind power together onto the grid is presented in Figure 6.22, in which BESS construction cost is assumed to be $350/kWh, according to [99]. The construction cost increases about 4.6% due to BESS, but significant cost reductions are seen in the fuel and reserve costs. With BESS deployed together with wind power, the overall cost will be 8.6% less than that without BESS. Furthermore, the reduction in the fuel and reserve costs with BESS can be understood as the best case scenario if significant PEVs are present on the gird and their charging is controlled to provide reserves. Controlling PEV charging to provide reserves is unlikely to outperform BESS because BESS can be available all day on the grid, whereas PEVs are not.

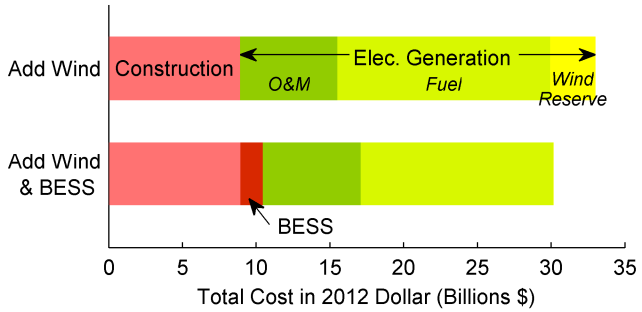

Figure 6.22 Wind power with energy storage system

However, deploying wind power with BESS is still not cheaper than the fossil fuel based generating technologies (coal and natural gas). This is because wind power on average has a capacity factor only at 32%, which leads to the need to construct more wind capacities. In this study, it is assumed that the wind capacity needs to be tripled to be comparable to the non-renewable generating technologies, whose capacity factors are usually above 85%. The data in [198] shows that offshore wind power can have a higher capacity factor, and the current-best value is 54%. Therefore, it is possible that the nameplate capacity of wind power may not have to be tripled in the future. In addition, a breakthrough in the construction costs of wind power may change the analysis results. The reduction in the construction costs of wind power will reduce the cost gap between wind power and other non-intermittent generating technologies.

6.5 Conclusion

This chapter presents a methodology to evaluate the costs of different investment choices to construct new power plants to meet the long-term demand increase on the electric grid. Four types of generating technologies were investigated: nuclear, coal, natural gas, and wind power. The proposed methodology considers the evolutions in both the supply and demand on the electric grid, including annual increases in the grid load and changes in the merit order when new power plants are commissioned. Furthermore, the renewable intermittency and reserve-related costs are considered, which has not been seen in the literature. To compare the different generating technologies, the methodology considers the costs of constructing new power plants and the costs of electricity generation using both new and existing power plants. Therefore, this methodology has a system-level perspective, which is important since the grid operation will dispatch both the new and existing capacities to meet the grid load. The discounted total cost of electricity generation and the system-wide LCOE are calculated to evaluate investment choices of adding different types of power plants on the grid. Sensitivity analyses were conducted on several parameters, including discount rate, construction (overnight) cost, natural gas price escalation, and CO_2 tax, to better understand how uncertainties in input parameters impact costs of grid upgrades.

The results show that the natural gas power plant is the most cost-effective option to upgrade the generation mix. Although natural gas power plants have the highest fuel cost among all generating technologies, when the construction costs are included in the cost evaluation, they become the cheapest option in the long run. This finding is consistent with the fact shown in Figure 1.5 that the new generating capacities constructed recently in the U.S. were mostly natural gas power plants. On the other hand, wind power is an expensive option as it incurs higher costs in both construction and operation in order to compensate for wind intermittency. In Chapter 3 and Chapter 4, it has been shown that incorporating wind power with BESS or PEV charging are effective ways to mitigate wind intermittency during the grid operation; however, the construction cost remains high because more wind capacities needs to be built to make up the low capacity factor.

The cost evaluation does not support wind power to be an economically sound choice of investment; however, the on-going improvement in the capacity factor of wind power is expected to lower its requirement of nameplate capacity in the future, which will lead to reductions in the construction costs. Furthermore, if the ultimate goal is to improve the sustainability and reduce the grid CO_2 emissions, the cost evaluation suggests that an economically viable strategy is to construct natural gas and wind power capacities alternately and to incorporate energy storage device in the grid operation.

CHAPTER 7
Conclusions and Future Work

7.1 Conclusions

This dissertation presents methodologies to incorporate large amounts of PEVs and wind power on the electric grid. Control and optimization schemes are developed to utilize the synergy between PEVs and the intermittent wind generation, which can lead to a win-win situation for both of the two new grid entities. Chapters 2-4 present control algorithms to charge PEVs and mitigate wind power intermittency. Chapters 5 and 6 investigate the grid CO_2 emissions and future generation planning (i.e. upgrade power plants).

A common theme of the simulation results in Chapters 2-4 is that PEVs and wind power are complementary to each other. The costs of electricity generation can be reduced if PEVs and wind power are deployed to the grid simultaneously and their operations are well-coordinated. In addition, the controlled PEV charging can also serve as reserves to regulate the grid frequency. Several simulations reveal the pitfalls if these two new grid entities are added onto the grid without coordination; therefore, it cannot be emphasized enough that a proper integration is needed to realize their full potentials.

Furthermore, to address the grid emissions, it is found in Chapters 5 that, not only should the demand be controlled (by controlling PEV charging), but also the interference in the electricity supply is needed. A carbon disincentive policy is proposed to promote the use low-CO_2 but more-expensive natural gas power plants over the high-CO_2 coal-fired power plants. The carbon disincentive policy is designed to be revenue-neutral to the grid operation, and therefore less burdensome to consumers.

However, bringing renewable generation onto the grid is still expensive in the next two decades, according to the cost evaluation for generation planning in Chapters 6. Wind power will not be as cost-effective as the non-intermittent natural gas power plants.

The wind intermittency can be well-addressed by PEVs or BESS using control or optimization schemes developed in the earlier chapters after the wind farm is built and commissioned for operation. However, the wind intermittency requires more wind capacities to be built, which keeps the construction costs high. In addition to integrating wind power with PEVs or BESS during the grid operations, a wide-spread adoption of wind power will require breakthroughs in the construction costs and continuous technology advancement to improve the capacity factor of wind generation.

7.2 Future Work

This dissertation has explored the various benefits of integrating PEV charging and renewable wind power into the grid operation; however, these two green technologies have more to be explored. The followings are several potential directions worth further study:

More sophisticated battery models to describe the battery inefficiencies and aging should be adopted. There has been a lot of development in modeling battery electrochemistry and model reduction in recent years; therefore, it is likely that a control-oriented model with proper fidelity will soon be available for the grid integration study. In addition, there is an interest to recycle used PEV batteries as backup power or energy storage devices on the grid. Therefore, battery models that can properly describe power fade and capacity fade is in need, so that analyses can be conducted more realistically to identify performance gains or limitations, and control algorithms can be developed accordingly.

More detailed models for wind power should be included. The wind power model used in this dissertation is developed based on the hourly data of one wind farm, and does not capture sub-hour fluctuations. The model does not capture the variations from different wind sources across state boundaries, either. Since the wind intermittency plays an important role in the study of grid integration, a model that can capture more details in wind power variation is desired.

Transmission limitations and inefficiencies should be considered. This dissertation makes the unspoken assumption that the power plants are connected to the

load by perfect transmission lines with no impedance or resistance. Therefore, it does not address congestion in transmission lines or voltage variations that may be caused by surplus wind generation. As these are dynamics in real grid operations, the physical phenomena in voltage changes and current flows due to transmission limitations and inefficiencies should be considered in future study. Several existing IEEE Distribution Test Feeders [199] or the Power System Test Case Archive [200] can be a good starting point for constructing transmission models for this study.

The coupling between the electric grid and ground transportation should be explored. PEVs are the intermediary between the electric grid and the transportation sector. Therefore, the benefits brought by integrating PEVs and wind power are not limited to the electric grid; PEVs and wind power also impact the costs and CO_2 emissions in the transportation sector. The coupling between these two energy sectors is worth studying to seek opportunities to integrate operations and improve sustainability in both sectors.

Last but not least, the modeling and optimization framework developed in this dissertation enables various studies to investigate the interactions between PEVs and wind power on the electric grid. The control and optimization schemes presented in each chapter show promising results in the ideal simulations, and yet each of them will require further studies, so that practicality issues, such as incorporating the proposed synergistic control algorithm for PEV charging and wind power scheduling with existing market rules or connecting far-flung renewable generation to the demand, can be resolved and real implementation can become possible in the future.

APPENDICES

APPENDIX A

Raw Data Used for PEV Fleet Modeling

The followings are the raw data used to identify the probability distributions of the plug-in time and plug-off time for modeling the PEV fleet in Chapters 2 and 4. Table A.1 and Table A.2 include the hourly traffic counts on the Interstate Highway 5 [95], which are used to develop the PEV fleet model in Chapter 2. Figure A.1 shows the temporal distributions of the real commute in Southeast Michigan [143], which are used to develop the PEV fleet model in Chapter 4.

Table A.1 Hourly Traffic Count on the Interstate Highway 5 (Hour 0-11) [95]

	Date	Day	t0	t1	t2	t3	t4	t5	t6	t7	t8	t9	t10	t11
1	9/1/2006	Fri	1232	1074	804	839	1298	2170	2843	3440	2940	3073	3385	3535
2	9/2/2006	Sat	3026	2082	1568	978	1027	1301	1736	2485	3250	4264	4621	4701
3	9/3/2006	Sun	869	637	495	390	415	555	760	1228	1889	2621	3230	3431
4	9/4/2006	Mon	1492	1053	683	630	529	623	824	1155	1841	2585	3610	3568
5	9/5/2006	Tue	1628	1032	838	868	1412	2610	3231	3508	2910	2816	2716	2755
6	9/6/2006	Wed	1132	733	583	735	1243	2251	3003	3345	2683	2495	2509	2424
7	9/7/2006	Thu	776	588	568	719	1182	2241	2995	3340	2735	2550	2410	2521
8	9/8/2006	Fri	894	749	596	746	1185	2174	2882	3340	2657	2604	2827	2869
9	9/9/2006	Sat	1148	877	629	637	713	1029	1466	2065	2736	3169	3536	3638
10	9/10/2006	Sun	704	547	453	336	397	504	737	1134	1739	2247	2827	2992
11	9/11/2006	Mon	927	846	636	643	1261	2417	3069	3316	2621	2408	2420	2494
12	9/12/2006	Tue	544	451	517	701	1113	2156	2910	3116	2641	2393	2303	2326
13	9/13/2006	Wed	585	533	491	622	1006	2042	2760	3103	2520	2391	2145	2250
14	9/14/2006	Thu	665	571	519	703	1177	2168	2946	3167	2661	2402	2348	2396
15	9/15/2006	Fri	863	708	623	716	1206	2158	2843	3223	2707	2601	2826	3075
16	9/16/2006	Sat	1281	978	657	608	671	1071	1464	2250	2910	3514	3869	3752
17	9/17/2006	Sun	793	593	418	342	361	435	797	1262	1773	2365	2864	3277
18	9/18/2006	Mon	1118	817	649	710	1297	2439	3006	3325	2703	2504	2547	2545
19	9/19/2006	Tue	670	573	480	684	1113	2276	2966	3406	2704	2433	2380	2499
20	9/20/2006	Wed	661	568	496	627	1132	2252	2902	3390	2742	2501	2410	2381
21	9/21/2006	Thu	700	610	546	679	1146	2312	2848	3360	2735	2466	2509	2516
22	9/22/2006	Fri	859	721	583	751	1120	2154	2950	3253	2770	2795	3033	3117
23	9/23/2006	Sat	1323	953	714	619	717	1010	1425	2148	2727	3419	3608	3878
24	9/24/2006	Sun	781	582	411	340	360	486	715	1090	1715	2347	2888	3255
25	9/25/2006	Mon	1124	784	679	721	1301	2495	3015	3228	2645	2361	2452	2591
26	9/26/2006	Tue	728	574	522	709	1165	2250	2922	3189	2684	2431	2322	2272
27	9/27/2006	Wed	732	545	512	643	1067	2213	2909	3122	2556	2467	2226	2348
28	9/28/2006	Thu	632	580	511	698	1129	2243	2879	3118	2703	2504	2479	2551
29	9/29/2006	Fri	944	640	614	729	1175	2140	2845	3190	2694	2829	2933	3104
30	9/30/2006	Sat	1418	952	687	555	838	1056	1434	2191	2870	3399	3699	3637

Table A.2 Hourly Traffic Count on the Interstate Highway 5 (Hour 11-23) [95]

	Date	Day	t12	t13	t14	t15	t16	t17	t18	t19	t20	t21	t22	t23
1	9/1/2006	Fri	3712	3521	3771	3835	3574	3769	3774	3852	3536	2926	2891	2800
2	9/2/2006	Sat	4595	4340	3883	3668	3519	3321	3135	2882	2308	2144	1793	1364
3	9/3/2006	Sun	3581	3426	3277	3492	4272	3990	4068	4221	3558	3406	2703	2082
4	9/4/2006	Mon	1231	2644	4405	5762	5416	5019	4755	4608	4660	4506	4255	2395
5	9/5/2006	Tue	3084	2965	3203	3232	2995	2799	2518	2351	1895	1538	1276	1012
6	9/6/2006	Wed	2348	2480	2734	2736	2548	2510	2437	2013	1730	1431	1172	903
7	9/7/2006	Thu	2527	2441	2734	2969	2726	2667	2463	2167	1832	1525	1298	1056
8	9/8/2006	Fri	2993	3029	3375	3429	3281	3214	3089	2966	2631	2384	1943	1571
9	9/9/2006	Sat	3393	3405	3108	3227	3172	3062	2497	2249	1891	1540	1382	945
10	9/10/2006	Sun	3306	3393	3737	4065	4339	4135	3938	3552	3158	2651	2127	1407
11	9/11/2006	Mon	2555	2407	3011	2858	1948	1450	1113	874	687	587	444	439
12	9/12/2006	Tue	2205	2427	1767	1546	1605	1378	1207	921	453	1441	922	754
13	9/13/2006	Wed	2215	2302	2481	2525	2376	2317	2217	1873	1670	1336	1106	842
14	9/14/2006	Thu	2500	2439	2657	2730	2674	2529	2441	2179	1841	1577	1435	1092
15	9/15/2006	Fri	3083	3290	3399	3542	3442	3332	3561	3272	2716	2619	1953	1751
16	9/16/2006	Sat	3678	3436	3423	3273	3168	3070	2634	2335	1926	1722	1399	1059
17	9/17/2006	Sun	3417	3607	3776	4022	4397	4230	4161	3887	3369	2912	2273	1635
18	9/18/2006	Mon	2613	2618	3063	2876	2714	2649	2477	2005	1554	1347	1154	917
19	9/19/2006	Tue	2383	2423	2539	2692	2638	2570	2305	1958	1609	1356	1092	831
20	9/20/2006	Wed	2542	2515	2655	2753	2599	2428	2354	2032	1569	1329	1141	877
21	9/21/2006	Thu	2355	2492	2843	2998	2845	2717	2598	2230	1899	1641	1310	1138
22	9/22/2006	Fri	2957	3139	3503	3562	3452	3360	3404	3122	2584	2232	2040	1706
23	9/23/2006	Sat	3477	3419	3431	3178	3281	3101	2590	2227	1867	1708	1371	1114
24	9/24/2006	Sun	3416	3604	3920	4169	4595	4428	4438	4087	3524	3013	2384	1725
25	9/25/2006	Mon	2569	2637	2830	3108	2718	2539	2455	1979	1664	1365	1072	834
26	9/26/2006	Tue	2389	2450	2642	2711	2589	2550	2408	2001	1551	1398	1200	990
27	9/27/2006	Wed	2389	2592	2707	2817	2560	2617	2355	2161	1637	1442	1096	970
28	9/28/2006	Thu	2501	2444	2721	2858	2837	2634	2583	2361	2033	1669	1371	1110
29	9/29/2006	Fri	3136	3115	3443	3366	3367	3109	3284	2616	2979	2273	1861	1731
30	9/30/2006	Sat	3422	3311	3327	3190	3227	2964	2698	2254	1758	1573	1306	1077

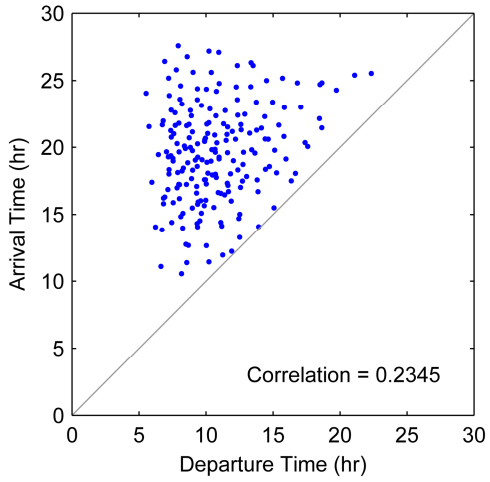

Figure A.1 Temporal distributions of real commute in the southeast Michigan [143]

APPENDIX B

Dynamic Programming

Dynamic Programming (DP) is a powerful tool to solve optimization problems with dynamics; it can handle constraints and nonlinearity in the problem and can guarantees global optimality. The DP technique is based on the Bellman's principle of optimality—"An optimal policy has the property that, whatever the initial state and optimal first decision may be, the remaining decisions constitute an optimal policy with regard to the state resulting from the first decision [201]." Based on the principle of optimality, DP converts the process of solving a horizon optimization problem into a recursive decision making process that progresses backward in time [202]. The recursive decision making process can be better explained by the generic optimization problem defined in Eq. (B.1), and its corresponding functional equations shown in Eqs. (B.2)-(B.3). The objective function defined in Eq. (B.1) has two terms: ψ_t is the instantaneous transitional cost at each step in the optimization horizon, and ϕ_T is the cost at final step T. The state dynamics are not shown, but are usually described by ordinary differential equations. Then, Eqs. (B.2)-(B.3) together provide a recipe to obtain the optimal solution to Eq. (B.1) recursively.

$$\min_{\boldsymbol{u}} : J = \sum_{t=1}^{T} \psi_t(x(t), u(t)) + \phi_T(x(T)) \tag{B.1}$$

$$J_T^* = \phi_T(x(T)) \tag{B.2}$$

$$J_t^*(x(t)) = \min_{u(t)} \left[\psi_t(x(t), u(t)) + J_{t+1}^*(x(t+1)) \right], \forall t < T \tag{B.3}$$

where x is the state, and u is the control variable.

To apply the DP technique, the terminal state penalty in Eq. (B.2) will be calculated first. Next, at the second last step (i.e. $t = T - 1$), the one-step sub-problem defined in Eq. (B.3) will be solved for all possible states. Equations (B.3) is also referred

as the optimal cost-to-go function, in that it represents the optimal cost if the system states with state $x(t)$ at step t and follows the optimal control policy thereafter until the final step. Once the optimal cost-to-go functions at $t = T - 1$ are found, Equations (B.3) will be reused to find the optimal cost-to-go functions for the instant one step ahead of time (i.e. $t = T - 2$). The iteration repeats until the initial step is reached. Therefore, it can be understood that DP can guarantee the global optimality because it exhaustively solves every one-stage sub-problem throughout the optimization horizon, which is also why DP is very computationally expensive.

APPENDIX C

Parameters Related to Costs of Power Plant Construction

The following is the collection of the parameters related to costs of power plant constructions from seven references.

Table C.1 Parameters Related to Capacity Construction [196]

	Nuclear	Coal	Natural Gas	Wind
Nameplate Capacity (MW)	2,236	1,300	540	100
Plant Lifetime (yr)	30	40	30	25
Overnight Cost ($/kW)	5,275	2,809	967	2,409
Lead Time (yr)	6	4	3	3
Discount Rate (-)	———	5.04%	———	

Table C.2 Parameters Related to Capacity Construction [193, 195, 197]

	Nuclear	Coal	Natural Gas	Wind
Nameplate Capacity (MW)	1,000	1,000	1,000	N/A
Plant Lifetime (yr)	———	40	———	N/A
Overnight Cost ($/kW)	4,000	2,300	850	N/A
Lead Time (yr)	5	4	2	N/A
Discount Rate (-)	11.5%	9.6%	9.6%	N/A
Capacity Factor (-)	———	85%	———	N/A

Table C.3 Parameters Related to Capacity Construction [170]

	Nuclear	Coal	Natural Gas	Wind
Nameplate Capacity (MW)	2,200	1,300	540	N/A
Plant Lifetime (yr)	40			N/A
Overnight Cost ($/kW)	4,295	2,471	1,008	N/A
Lead Time (yr)	5	4	2	N/A
Discount Rate (-)	7.86%	6.8%	6.8%	N/A
Capacity Factor (-)	90%	85%	85%	N/A

Table C.4 Parameters Related to Capacity Construction [171]

	Nuclear	Coal	Natural Gas	Wind
Nameplate Capacity (MW)	1,350	550	400	150
Plant Lifetime (yr)	60	40	30	20
Overnight Cost ($/kW)*	3,382	2,433	969	1,973
Lead Time (yr)	7	4	2	1
Discount Rate (-)	10%			
Capacity Factor (-)	85%			17-38%

* Listed are the medium values

Table C.5 Parameters Related to Capacity Construction [186]

	Nuclear	Coal	Natural Gas	Wind
Nameplate Capacity (MW)	1,100	600	580	100
Plant Lifetime (yr)	40			20
Overnight Cost ($/kW)	6,792	5,700	1,162	1,600
Lead Time (yr)	5.75	5	3	1
Discount Rate (-)	7.68%			8.09%
Capacity Factor (-)	93%	90%	75%	35%

Table C.6 Parameters Related to Wind Power Construction [53, 55]

	Wind (2010)	**Wind (2012)**
Nameplate Capacity (MW)	100	100
Plant Lifetime (yr)	N/A	N/A
Overnight Cost ($/kW)	2,120	1,750
Lead Time (yr)	N/A	N/A
Discount Rate (-)	N/A	N/A
Capacity Factor (-)	30%	33%

APPENDIX D

Discounted Cash Flow Analysis for Generation Planning

The following is the cash flow analysis on the four scenarios of generation planning with different types of generating technologies. The scenario of constructing nuclear power plants to upgrade the grid generation mix is shown in Figures D.1 to D.3; constructing coal power plants shown in Figures D.4 to D.6; constructing natural gas power plants shown in Figures D.7 to D.9; and, constructing wind power plants shown in Figures D.10 to D.12. In each scenario, the timing of *when* new capacity needs to be commissioned is shown first. Next, the cash (out) flows throughout the entire planning horizon are calculated, which are then used Eq. (D.1) to calculate the discounted cash flows. Equation (D.1) is identical to Eq. (6.2), whose implication has been explained in Section 6.3.1.

$$DCF_n = \frac{CF_n}{(1+d)^n} \tag{D.1}$$

where CF_n is the cash flow in year n, d is the discount rate, and DCF_n is the discounted cash flow in year n. In this study, Year 2012 is chosen to be the base year and has n=0.

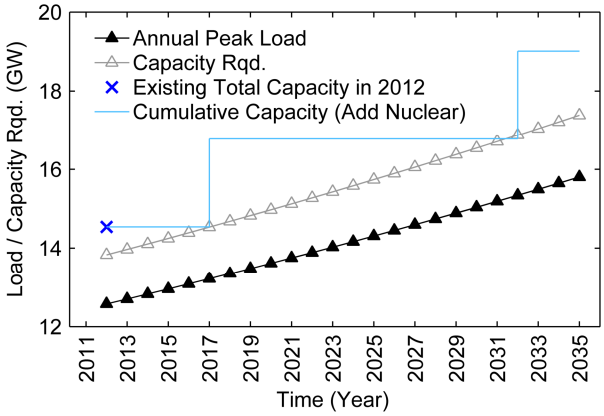

Figure D.1 Upgrade the generation mix with nuclear power plants

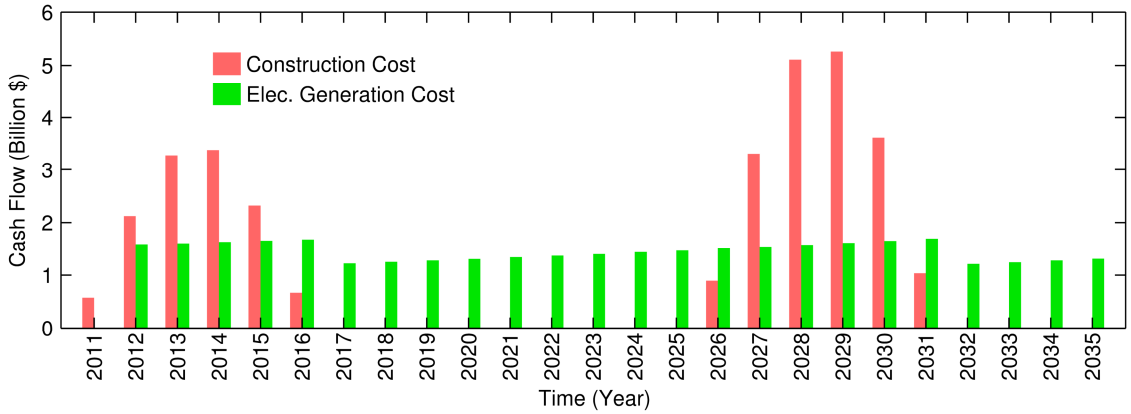

Figure D.2 Cash flow of adding nuclear power to the grid

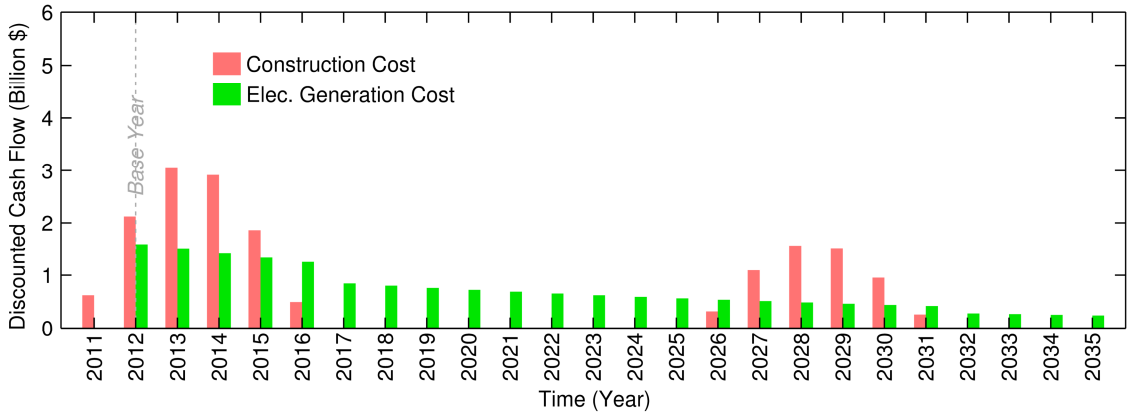

Figure D.3 Discounted cash flow of adding nuclear power to the grid

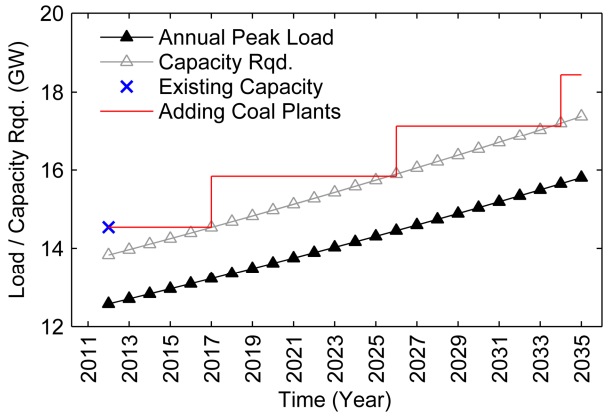

Figure D.4 Upgrade the generation mix with coal power plants

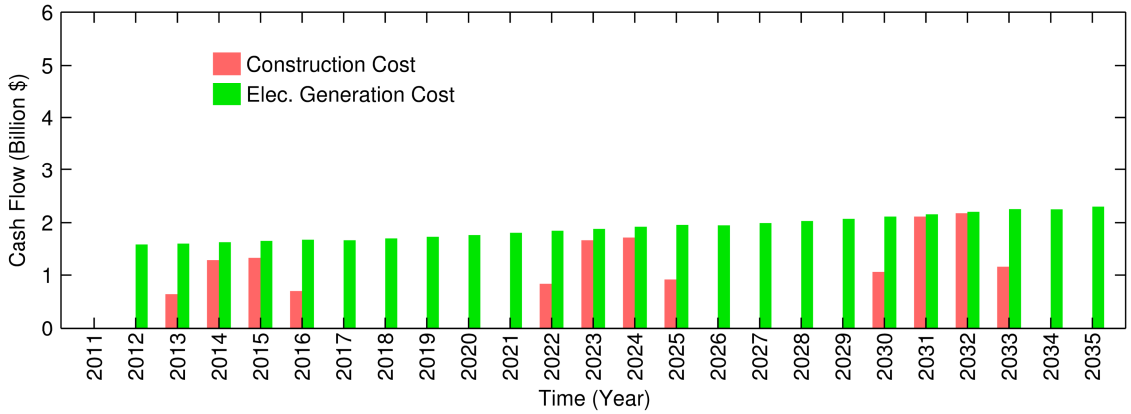

Figure D.5 Cash flow of adding coal power plants to the grid

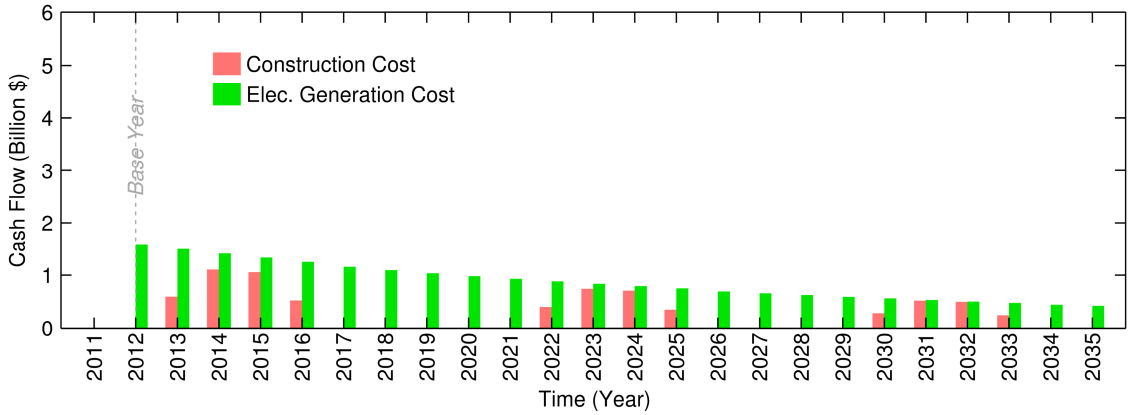

Figure D.6 Discounted cash flow of adding coal power plants to the grid

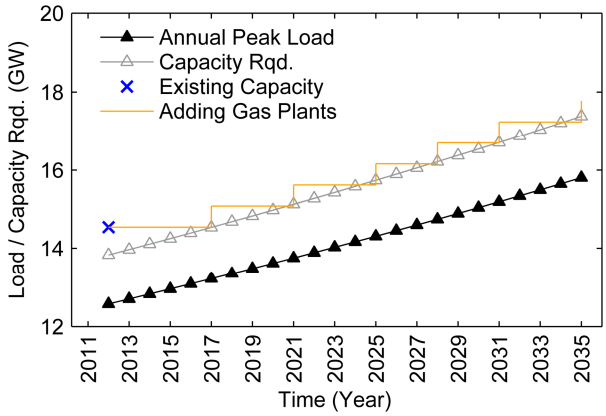

Figure D.7 Upgrade the generation mix with natural gas power plants

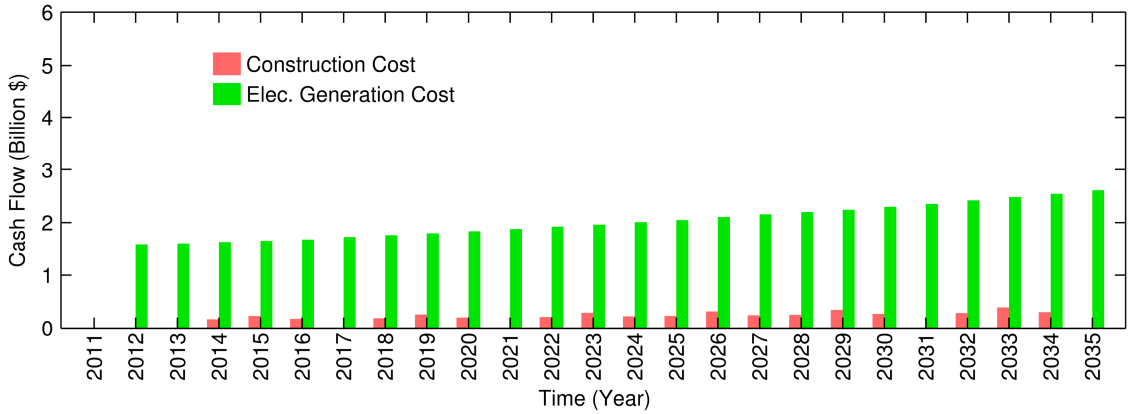

Figure D.8 Cash flow of adding gas power plants to the grid

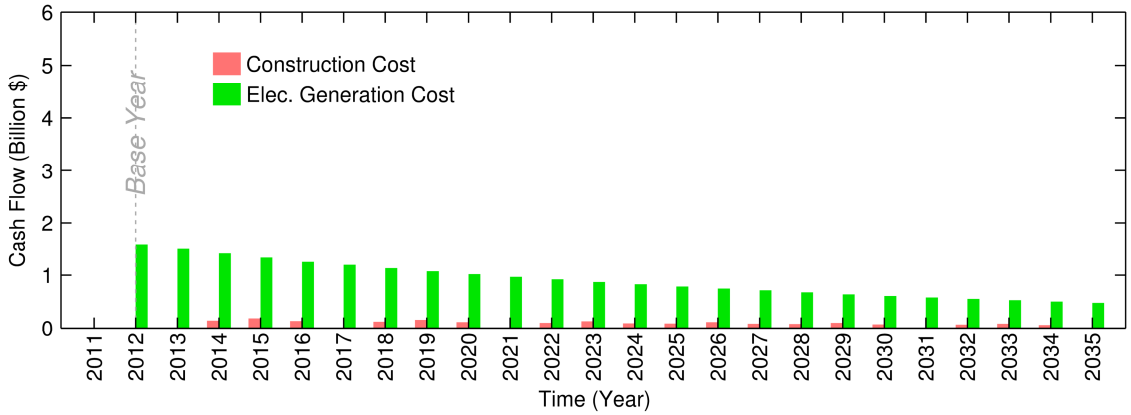

Figure D.9 Discounted cash flow of adding gas power plants to the grid

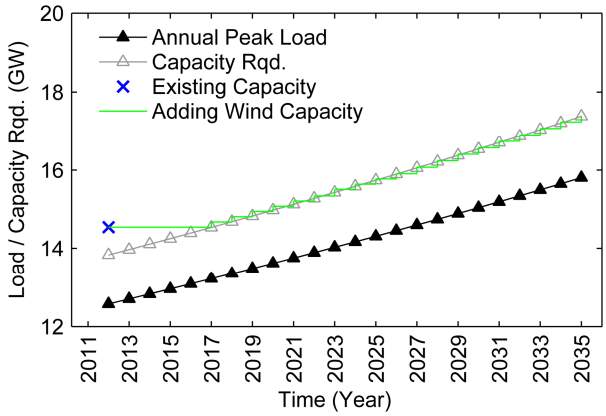

Figure D.10 Upgrade the generation mix with natural gas power plants

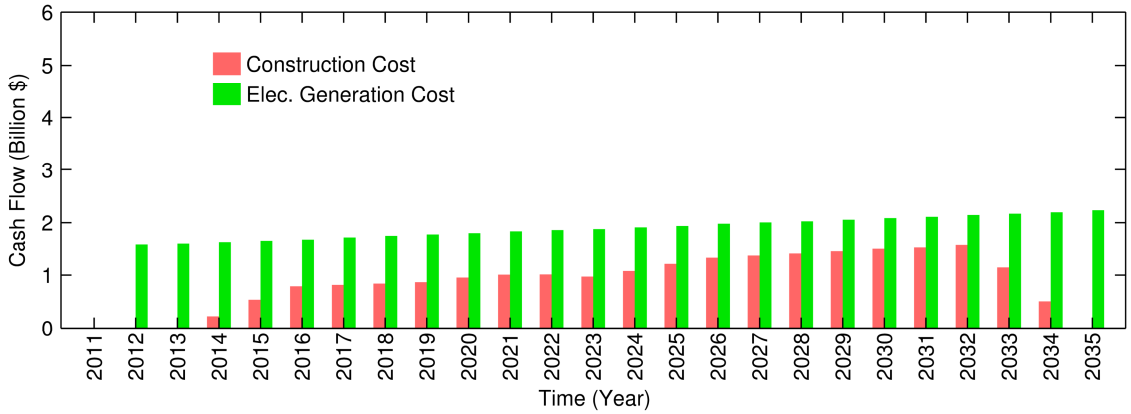

Figure D.11 Cash flow of adding gas power plants to the grid

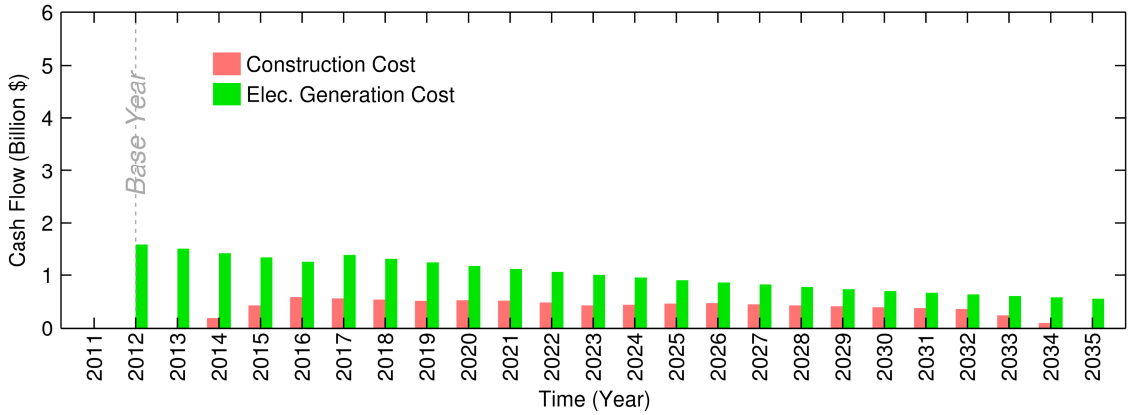

Figure D.12 Discounted cash flow of adding gas power plants to the grid

BIBLIOGRAPHY

[1] Lawrence Livermore National Laboratory, U.S. Energy Flow Charts, 2011, [Online]. Available: https://flowcharts.llnl.gov/index.html (Accessd: 1/12/2011).

[2] Lawrence Livermore National Laboratory, U.S. Carbon Flow Charts, 2010, [Online]. Available: https://flowcharts.llnl.gov/index.html (Accessd: 1/12/2011).

[3] Center for Climate and Energy Solutions, The American Clean Energy and Security Act (Waxman-Markey Bill), 2009, [Online]. Available: http://www.c2es.org/federal/congress/111/acesa (Accessd: 3/18/2013).

[4] The White House, President Obama Announces Historic 54.5 mpg Fuel Efficiency Standard, 2011, [Online]. Available: http://m.whitehouse.gov/the-press-office/2011/07/29/president-obama-announces-historic-545-mpg-fuel-efficiency-standard (Accessd: 2/20/2013).

[5] Federal Energy Regulatory Commission (FERC) Office of Energy Projects, "Energy Infrastructure Update," Report, 2012.

[6] Database of State Incentives for Renewables & Efficiency, 2013, [Online]. Available: http://www.dsireusa.org (Accessd: 2/15/2013).

[7] D. Schlissel, A. Smith, and R. Wilson, "Coal-Fired Power Plant Construction Costs," Synapse Energy Economics Inc., Report, 2008.

[8] D. Berry, "Investment Risk of New Coal-Fired Power Plants," Western Resource Advocates, Report, 2008.

[9] S. Moura, D. Callaway, H. Fathy, and J. Stein, "Impact of Battery Sizing on Stochastic Optimal Power Management in Plug-In Hybrid Electric Vehicles," in *IEEE International Conference on Vehicular Electronics and Safety*, Columbus, OH, 2008, pp. 96-102.

[10] D. Karbowski, C. Haliburton, and A. Rousseau, "Impact of Component Size on Plug-In Hybrid Vehicles Energy Consumption Using Global Optimization," in *EVS23 International Electric Vehicle Symposium*, Anaheim, CA, 2007.

[11] J. Axsen, A. Burke, and K. Kurani, "Batteries for Plug-In Hybrid Electric Vehicles (PHEVs): Goals and the State of Technology Circa 2008," Institute of Transportation Studies, University of California Davis, Report #UCD-ITS-RR-08-14, 2008.

[12] T. H. Bradley and A. A. Frank, "Design, Demonstrations and Sustainability Impact Assessments for Plug-In Hybrid Electric Vehicles," *Renewable and Sustainable Energy Reviews,* vol. 13, pp. 115-128, 2009.

[13] T. Markel, "Plug-In HEV Vehicle Design Options and Expectations," in *ZEV Technology Symposium*, Sacramento, CA, 2006.

[14] T. Markel and A. Simpson, "Plug-In Hybrid Electric Vehicle Energy Storage System Design," in *Advanced Automotive Battery Conference*, Baltimore, MD, 2006.

[15] J. Gonder and T. Markel, "Energy Management Strategies for Plug-In Hybrid Electric Vehicles," *SAE Paper,* 2007-01-0290.

[16] A. Rousseau, S. Pagerit, and D. W. Gao, "Plug-in Hybrid Electric Vehicle Control Strategy Parameter Optimization," *Journal of Asian Electric Vehicles,* vol. 6, pp. 1125-1133, 2008.

[17] S. J. Moura, H. K. Fathy, D. S. Callaway, and J. L. Stein, "A Stochastic Optimal Control Approach for Power Management in Plug-In Hybrid Electric Vehicles," *IEEE Transactions on Control Systems Technology,* vol. 19, pp. 545-555, 2011.

[18] S. Stockar, V. Marano, M. Canova, G. Rizzoni, and L. Guzzella, "Energy-Optimal Control of Plug-in Hybrid Electric Vehicles for Real-World Driving Cycles," *IEEE Transactions on Vehicular Technology,* vol. 60, pp. 2949-2962, 2011.

[19] S. Stockar, V. Marano, G. Rizzoni, and L. Guzzella, "Optimal control for plug-in hybrid electric vehicle applications," in *American Control Conference*, Baltimore, MD, 2010, pp. 5024-5030.

[20] The official U.S. government source for fuel economy information, New & Upcoming Plug-in Hybrids, 2013, [Online]. Available: http://www.fueleconomy.gov/feg/phevnews.shtml (Accessd: 3/13/2013).

[21] The official U.S. government source for fuel economy information, New & Upcoming Electric Vehicles, 2013, [Online]. Available: http://www.fueleconomy.gov/feg/evnews.shtml (Accessd: 3/13/2013).

[22] Alternative Fuels Data Center, Light-Duty Vehicle Search, 2013, [Online]. Available: http://www.afdc.energy.gov/vehicles/search/light/ (Accessd: 4/7/2013).

[23] University of Michigan Transportation Research Institute (UMTRI), Average sales-weighted fuel-economy rating (window sticker) of purchased new vehicles for October 2007 through February 2013, 2013, [Online]. Available: http://www.umich.edu/~umtriswt/EDI_sales-weighted-mpg.html (Accessd: 3/26/2013).

[24] SAE Electric Vehicle and Plug in Hybrid Electric Vehicle Conductive Charge Coupler, SAE Standard J1772, 2012.

[25] Plugs, socket-outlets, vehicle connectors and vehicle inlets - Conductive charging of electric vehicles - Part 1: General requirements, IEC 62196-1, 2011.

[26] K. Morrow, D. Karner, and J. Francfort, "Plug-in Hybrid Electric Vehicle Charging Infrastructure Review," Idaho National Laboratory, Report #INL/EXT-08-15058, 2008.

[27] F. Nemry, G. Leduc, and A. Muñoz, "Plug-in Hybrid and Battery-Electric Vehicles: State of the research and development and comparative analysis of energy and cost efficiency," Joint Research Centre, European Commision, Report #JRC 54699, 2009.

[28] W. Kempton and J. Tomic, "Vehicle-to-Grid Power Fundamentals: Calculating Capacity and Net Revenue," *Journal of Power Sources,* vol. 144, pp. 268-279, 2005.

[29] W. Kempton and J. Tomic, "Vehicle-to-Grid Power Implementation: From Stabilizing the Grid to Supporting Large-Scale Renewable Energy," *Journal of Power Sources,* vol. 144, pp. 280-294, 2005.

[30] S. L. Andersson, A. K. Elofsson, M. D. Galus, L. Göransson, S. Karlsson, F. Johnsson, and G. Andersson, "Plug-in hybrid electric vehicles as regulating power providers: Case studies of Sweden and Germany," *Energy Policy,* vol. 38, pp. 2751-2762, 2010.

[31] J. Lazar, J. Joyce, and X. Baldwin, "Plug-In Hybrid Vehicles, Wind Power, and the Smart Grid," presented at the EUEC Energy and Environment Conference, Tucson, AZ, 2008.

[32] J. D. Glover, M. S. Sarma, and J. O. Thomas, *Power system analysis and design*. CA: Pacific Grove, 2008.

[33] S. Stoft, *Power System Economics: Designing Markets for Electricity*. Piscataway, NJ: IEEE Press, 2002.

[34] D. Gan, R. J. Thomas, and R. D. Zimmerman, "Stability-Constrained Optimal Power Flow," *IEEE Transactions on Power Systems,* vol. 15, pp. 535-540, 2000.

[35] O. Alsac, J. Bright, M. Prais, and B. Stott, "Further Developments in LP-Based Optimal Power Flow," *IEEE Transactions on Power Systems,* vol. 5, pp. 697-711, 1990.

[36] Y. G. Rebours, D. S. Kirschen, M. Trotignon, and S. Rossignol, "A Survey of Frequency and Voltage Control Ancillary Services—Part I: Technical Features," *IEEE Transactions on Power Systems,* vol. 22, pp. 350-357, 2007.

[37] A. Isemonger, "The Evolving Design of RTO Ancillary Service Markets," *Energy Policy,* vol. 37, pp. 150-157, 2009.

[38] L. Cameron and P. Cramton, "The Role of the ISO in U.S. Electricity Markets: A Review of Restructuring in California and PJM," *The Electricity Journal,* vol. 12, pp. 71-81, 1999.

[39] M. Bhavaraju, B. Hobbs, and M.-C. Hu, "PJM Reliability Pricing Model - A Summary and Dynamic Analysis," in *IEEE Power Engineering Society General Meeting*, Tampa, FL, 2007, pp. 1-3.

[40] PJM Interconnection LLC., "PJM Manual 11: Energy & Ancillary Services Market Operations," Report, 2010.

[41] A. K. David and W. Fushuan, "Strategic bidding in competitive electricity markets: a literature survey," in *IEEE Power Engineering Society Summer Meeting*, Seattle, WA, 2000, pp. 2168-2173.

[42] S. Borenstein, "The Trouble with Electricity Markets: Understanding California's Restructuring Disaster," *Journal of Economic Perspectives,* vol. 16, pp. 191-211, 2002.

[43] P. Cramton, "Electricity Market Design: the Good, the Bad, and the Ugly," in *36th Hawaii International Conference on System Sciences*, Big Island, HI, 2003.

[44] C. Knittel, C. Wolfram, J. Bushnell, and S. Borenstein, "Inefficiencies and Market Power in Financial Arbitrage: A Study of California's Electricity Markets," Department of Economics, University of California Davis, Working Paper Series, Report #06-30, 2006.

[45] C. V. Atten, A. Saha, and L. Reynolds, "Benchmarking Air Emissions of the 100 Largest Electric Power Producers in the United States," M.J. Bradley & Associates, Report, 2012.

[46] U.S. Energy Information Administration, "Annual Energy Review 2011," Report #DOE/EIA-0384(2011), 2012.

[47] A. Pullen, K. Hays, and G. Knolle, "Wind Energy - The Facts, Part IV - Industry and Markets," The European Wind Energy Association, Report, 2009.

[48] B. C. Ummels, E. Pelgrum, and W. L. Kling, "Integration of large-scale wind power and use of energy storage in the netherlands' electricity supply," *IET Renewable Power Generation,* vol. 2, pp. 34-46, 2008.

[49] H. Holttinen, B. Lemström, P. Meibom, H. Bindner, A. Orths, F. v. Hulle, C. Ensslin, L. Hofmann, W. Winter, A. Tuohy, M. O'Malley, P. Smith, J. Pierik, J. Tande, A. Estanqueiro, J. Ricardo, E. Gomez, L. Söder, G. Strbac, A. Shakoor, J. Smith, B. Parsons, M. Milligan, and Y.-H. Wan, "Design and operation of power

systems with large amounts of wind power " International Energy Agency (IEA), VTT Working Papers 82, 2007.

[50] A. Smith, "Quantifying Exports and Minimising Curtailment: From 20% to 50% Wind Penetration in Denmark," in *BIEE Conference*, Oxford, UK, 2010.

[51] J. Garcia-Gonzalez, R. M. R. de la Muela, L. M. Santos, and A. M. Gonzalez, "Stochastic Joint Optimization of Wind Generation and Pumped-Storage Units in an Electricity Market," *IEEE Transactions on Power Systems,* vol. 23, pp. 460-468, 2008.

[52] H. Holttinen and S. Tuhkanen, "The effect of wind power on CO_2 abatement in the Nordic countries," *Energy Policy,* vol. 32, pp. 1639-1652, 2004.

[53] R. Wiser and M. Bolinger, "2011 Wind Technologies Market Report," Department of Energy, Report #DOE/GO-102012-3472, 2012.

[54] G. Barbose, N. Darghouth, R. Wiser, and J. Seel, "Tracking the Sun IV - An Historical Summary of the Installed Cost of Photovoltaics in the United States from 1998 to 2010," Lawrence Berkeley National Laboratory, Report, 2011.

[55] R. Wiser and M. Bolinger, "2009 Wind Technologies Market Report," Department of Energy, Report #DOE/GO-102010-3107, 2010.

[56] R. Piwko, D. Osborn, R. Gramlich, G. Jordan, D. Hawkins, and L. Porter. (2005 November/December) Wind Energy Delivery Issues - Transmission Planning and Competitive Electricity Market Operation. *IEEE Power & Energy Magazine*. 47-56.

[57] P. Morthorst, H. Auer, A. Garrad, and I. Blanco, "Wind Energy - The Facts, Part III - The Economics of Wind Power," European Wind Energy Association, Report, 2009.

[58] G. Sideratos and N. Hatziargyriou, "An Advanced Statistical Method for Wind Power Forecasting," *IEEE Transactions on Power Systems,* vol. 22, pp. 258-265, 2007.

[59] P. Pinson and G. Kariniotakis, "Wind Power Forecasting Using Fuzzy Neural Networks Enhanced with On-Line Prediction Risk Assessment," in *IEEE Power Tech Conference*, Bologna, Italy, 2003.

[60] G. Giebel, L. Landberg, G. Kariniotakis, and R. Brownsword, "State-of-the-Art on Methods and Software Tools for Short-Term Prediction of Wind Energy Production," in *European Wind Energy Conference & Exhibition*, Madrid, Spain, 2003.

[61] Department of Energy, "The Smart Grid: An Introduction," Report #DE-AC26-04NT41817, 2009.

[62] Department of Energy, "A Vision for the Modern Grid," Report, 2007.

[63] Smart Grid Basics, 2010, [Online]. Available: http://www.smartgrid.gov/basics (Accessd: 11/1/2011).

[64] A. Elgowainy, A. Burnham, M. Wang, J. Molburg, and A. Rousseau, "Well-to-Wheels Energy Use and Greenhouse Gas Emissions Analysis of Plug-in Hybrid Electric Vehicles," Center for Transportation Research, Argonne National Laboratory, Report #ANL/ESD/09-2, 2009.

[65] S. Hadley and A. Tsvetkova, "Potential Impacts of Plug-in Hybrid Electric Vehicles on Regional Power Generation," *The Electricity Journal,* vol. 22, pp. 56-68, 2009.

[66] M. Kintner-Meyer, K. Schneider, and R. Pratt, "Impacts Assessment of Plug-In Hybrid Vehicles on Electric Utilities and Regional U.S. Power Grids Part 1: Technical Analysis," Pacific Northwest National Laboratory, Report, 2007.

[67] T. Ibaraki and N. Katoh, *Resource Allocation Problems: Algorithmic Approaches*. Cambridge, MA: MIT Press, 1988.

[68] M. Pinedo, *Scheduling: Theory, Algorithms, and Systems*, 3 rd ed. New York: Springer, 2008.

[69] D. Gross, J. F. Shortle, and J. M. Thompson, *Fundamentals of Queueing Theory*, 4 th ed. Hoboken, N.J.: Wiley, 2008.

[70] I. Vermeulen, S. Bohte, S. Elkhuizen, H. Lameris, P. Bakker, and J. Poutré, "Adaptive Resource Allocation for Efficient Patient Scheduling," *Artificial Intelligence in Medicine,* vol. 46, pp. 67-80, 2009.

[71] M. Carter and S. Lapierre, "Scheduling Emergency Room Physicians," *Health Care Management Science,* vol. 4, pp. 347-360, 2001.

[72] M. Rossetti, G. Trzcinski, and S. Syverud, "Emergency Department Simulation and Determination of Optimal Attending Physician Staffing Schedules," in *31st Winter Simulation Conference*, Phoenix, AZ, 1999, pp. 1532-1540.

[73] D. Lemoine, D. Kammen, and A. Farrell, "An Innovation and Policy Agenda for Commercially Competitive Plug-In Hybrid Electric Vehicles," *Environmental Research Letters,* vol. 3, pp. 14003-14013, 2008.

[74] C. Ahn, C.-T. Li, and H. Peng, "Optimal Decentralized Charging Control Algorithm for Electrified Vehicles Connected to Smart Grid," *Journal of Power Sources,* vol. 196, pp. 10369-10379, 2011.

[75] M. Galus and G. Andersson, "Demand Management of Grid Connected Plug-In Hybrid Electric Vehicles (PHEV)," in *IEEE Energy 2030 Conference*, Atlanta, GA, 2008, pp. 1-8.

[76] S. Han, S. Han, and K. Sezaki, "Development of an Optimal Vehicle-to-Grid Aggregator for Frequency Regulation," *IEEE Transactions on Smart Grid,* vol. 1, pp. 65-72, 2010.

[77] J. M. Foster and M. C. Caramanis, "Energy reserves and clearing in stochastic power markets: The case of plug-in-hybrid electric vehicle battery charging," in *IEEE Conference on Decision and Control*, Atlanta, GA, 2010, pp. 1037-1044.

[78] W. Burke and D. Auslander, "Residential Electricity Auction with Uniform Pricing and Cost Constraints," in *North American Power Symposium*, Starkville, MS, 2009, pp. 1-6.

[79] Z. Ma, D. Callaway, and I. Hiskens, "Decentralized Charging Control for Large Populations of Plug-In Electric Vehicles: Application of the Nash Certainty Equivalence Principle," in *IEEE International Conference on Control Applications*, Yokohama, Japan, 2010, pp. 191-195.

[80] R. Maheswaran and T. Basar, "Decentralized Network Resource Allocation as A Repeated Noncooperative Market Game," in *40th IEEE Conference on Decision and Control*, Orlando, FL, 2001, pp. 4565-4570.

[81] DTE Energy, Plug-In Electric Vehicle Rates, 2010, [Online]. Available: http://www.dteenergy.com/residentialCustomers/productsPrograms/electricVehicles/pevRates.html (Accessd: 1/12/2011).

[82] Southern California Edison, Electric Car Rate Options, 2013, [Online]. Available: https://www.sce.com/wps/portal/home/business/electric-cars/electric-car-business-rates (Accessd: 4/2/2013).

[83] J. Lopes, F. Soares, and P. Almeida, "Identifying Management Procedures to Deal with Connection of Electric Vehicles in the Grid," in *IEEE Power Tech Conference*, Bucharest, Romania, 2009, pp. 1-8.

[84] J. Lopes, F. J. Soares, P. M. R. Almeida, and M. Moreira da Silva, "Smart Charging Strategies for Electric Vehicles: Enhancing Grid Performance and Maximizing the Use of Variable Renewable Energy Resources," in *EVS24 International Battery, Hybrid and Fuel Cell Electric Vehicle Symposium*, Stavanger, Norway, 2009.

[85] D. Callaway, "Tapping the Energy Storage Potential in Electric Loads to Deliver Load Following and Regulation, with Application to Wind Energy," *Energy Conversion and Management,* vol. 50, pp. 1389-1400, 2009.

[86] J. Short, D. Infield, and L. Freris, "Stabilization of Grid Frequency Through Dynamic Demand Control," *IEEE Transactions on Power Systems,* vol. 22, pp. 1284-1293, 2007.

[87] L. Goel, Q. Wu, and P. Wang, "Fuzzy logic-based direct load control of air conditioning loads considering nodal reliability characteristics in restructured power systems," *Electric Power Systems Research,* vol. 80, pp. 98-107, 2010.

[88] D. Callaway and I. Hiskens, "Achieving Controllability of Electric Loads," *Proceedings of the IEEE,* vol. 99, pp. 184-199, 2011.

[89] C.-T. Li, C. Ahn, H. Peng, and J. Sun, "Decentralized Charging of Plug-In Electric Vehicles," in *Dynamic System and Control Conference*, Arlington, VA, 2011, pp. 247-254.

[90] Federal Energy Regulatory Commission (FERC), Form 714-Annual Electric Control and Planning Area Report, 2009, [Online]. Available: http://www.ferc.gov/docs-filing/ferconline.asp (Accessd: 3/11/2011).

[91] H. Daneshi and A. Daneshi, "Real Time Load Forecast in Power System," in *3rd International Conference on Electric Utility Deregulation and Restructuring and Power Technologies*, Nanjing, China, 2008, pp. 689-695.

[92] U.S. Energy Information Administration, Market Trends -- Natural Gas, 2013, [Online]. Available: http://www.eia.gov/forecasts/aeo/MT_naturalgas.cfm#natgas_prices (Accessd: 4/23/2013).

[93] P. Kundur, N. J. Balu, and M. G. Lauby, *Power System Stability and Control*. New York: McGraw-Hill, 1994.

[94] F. Nemry and M. Brons, "Plug-in Hybrid and Battery Electric Vehicles: Market penetration scenarios of electric drive vehicles," Joint Research Centre, European Commision, Report #JRC58748, 2010.

[95] N. Buddhangkuranont, "Analysis of Interstate Highway 5 Hourly Traffic via Functional Linear Models," Master dissertation, Department of Statistics, University of California Los Angeles, Los Angeles, CA, 2007.

[96] R. Doherty and M. O'Malley, "A new approach to quantify reserve demand in systems with significant installed wind capacity," *IEEE Transactions on Power Systems,* vol. 20, pp. 587-595, 2005.

[97] Electric Reliability Council of Texas, "2010 Methodologies for Determining Ancillary Service Requirements," Report, , 2010.

[98] P. F. Ribeiro, B. K. Johnson, M. L. Crow, A. Arsoy, and Y. Liu, "Energy storage systems for advanced power applications," *Proceedings of the IEEE,* vol. 89, pp. 1744-1756, 2001.

[99] S. Schoenung, "Energy Storage Systems Cost Update," Sandia National Laboratory, Report, 2011.

[100] J. Eyer and G. Corey, "Energy Storage for the Electricity Grid: Benefits and Market Potential Assessment Guide," Sandia National Laboratory, Report, 2010.

[101] B. P. Roberts and C. Sandberg, "The Role of Energy Storage in Development of Smart Grids," Altair Nanotechnologies Inc., Report, 2012.

[102] S. O. Geurin, A. K. Barnes, and J. C. Balda, "Smart grid applications of selected energy storage technologies," in *IEEE PES Conference on Innovative Smart Grid Technologies*, Washington DC, 2012, pp. 1-8.

[103] S. Dutta and R. Sharma, "Optimal storage sizing for integrating wind and load forecast uncertainties," in *IEEE PES Conference on Innovative Smart Grid Technologies*, Washington DC, 2012, pp. 1-7.

[104] S. Bahramirad and H. Daneshi, "Optimal sizing of smart grid storage management system in a microgrid," in *IEEE PES Conference on Innovative Smart Grid Technologies*, Washington DC, 2012, pp. 1-7.

[105] M. Korpaas, A. T. Holen, and R. Hildrum, "Operation and sizing of energy storage for wind power plants in a market system," *International Journal of Electrical Power & Energy Systems,* vol. 25, pp. 599-606, 2003.

[106] T. K. A. Brekken, A. Yokochi, A. von Jouanne, Z. Z. Yen, H. M. Hapke, and D. A. Halamay, "Optimal Energy Storage Sizing and Control for Wind Power Applications," *IEEE Transactions on Sustainable Energy,* vol. 2, pp. 69-77, 2011.

[107] Y. Makarov, D. Pengwei, M. C. W. Kintner-Meyer, J. Chunlian, and H. Illian, "Optimal size of energy storage to accommodate high penetration of renewable resources in WECC system," in *IEEE PES Conference on Innovative Smart Grid Technologies*, Washington DC, 2010, pp. 1-5.

[108] P. Pinson, G. Papaefthymiou, B. Klockl, and J. Verboomen, "Dynamic sizing of energy storage for hedging wind power forecast uncertainty," in *IEEE PES General Meeting*, Alberta, Canada, 2009, pp. 1-8.

[109] X. Y. Wang, D. Mahinda Vilathgamuwa, and S. S. Choi, "Determination of Battery Storage Capacity in Energy Buffer for Wind Farm," *IEEE Transactions on Energy Conversion,* vol. 23, pp. 868-878, 2008.

[110] A. Arulampalam, M. Barnes, N. Jenkins, and J. B. Ekanayake, "Power quality and stability improvement of a wind farm using STATCOM supported with hybrid battery energy storage," *IEE Proceedings-Generation, Transmission and Distribution,* vol. 153, pp. 701-710, 2006.

[111] M. C. Such and C. Hill, "Battery energy storage and wind energy integrated into the Smart Grid," in *IEEE PES Conference on Innovative Smart Grid Technologies*, Washington DC, 2012, pp. 1-4.

[112] C. Banos, M. Aten, P. Cartwright, and T. C. Green, "Benefits and control of STATCOM with energy storage in wind power generation," in *8th IEE International Conference on AC and DC Power Transmission*, London, UK, 2006, pp. 230-235.

[113] M. Khalid and A. V. Savkin, "A model predictive control approach to the problem of wind power smoothing with controlled battery storage," *Renewable Energy,* vol. 35, pp. 1520-1526, 2010.

[114] S. Teleke, M. E. Baran, S. Bhattacharya, and A. Q. Huang, "Optimal Control of Battery Energy Storage for Wind Farm Dispatching," *IEEE Transactions on Energy Conversion,* vol. 25, pp. 787-794, 2010.

[115] X. Hu, K. J. Tseng, and M. Srinivasan, "Optimization of battery energy storage system with super-capacitor for renewable energy applications," in *8th IEEE International Conference on Power Electronics*, Jeju, Korea, 2011, pp. 1552-1557.

[116] W. Qi, J. Liu, X. Chen, and P. D. Christofides, "Supervisory Predictive Control of Standalone Wind/Solar Energy Generation Systems," *IEEE Transactions on Control Systems Technology,* vol. 19, pp. 199-207, 2011.

[117] H. Borhan, M. A. Rotea, and D. Viassolo, "Optimization-based power management of a wind farm with battery storage," *Wind Energy,* 2012, in press.

[118] J. Hill and C. Nwankpa, "System constraints effects on optimal dispatch schedule for battery storage systems," in *IEEE PES Conference on Innovative Smart Grid Technologies*, Washington DC, 2012, pp. 1-8.

[119] L. E. Benitez, P. C. Benitez, and G. C. van Kooten, "The economics of wind power with energy storage," *Energy Economics,* vol. 30, pp. 1973-1989, 2008.

[120] R. Dufo-López, J. L. Bernal-Agustín, and J. Contreras, "Optimization of control strategies for stand-alone renewable energy systems with hydrogen storage," *Renewable Energy,* vol. 32, pp. 1102-1126, 2007.

[121] G. Giebel, R. Brownsword, and G. Kariniotakis, "The State-Of-The-Art in Short-Term Prediction of Wind Power–A Literature Overview," Risø National Labratory, Report, 2003.

[122] G. Giebel, R. Brownsword, G. Kariniotakis, M. Denhard, and C. Draxl, "The State-Of-The-Art in Short-Term Prediction of Wind Power–A Literature Overview," Risø National Labratory, Report, 2011.

[123] C.-T. Li, H. Peng, and J. Sun, "MPC for Reducing Energy Storage Requirement of Wind Power Systems," in *American Control Conference*, 2013, accepted.

[124] National Renewable Energy Laboratory (NREL), Eastern Wind Dataset, 2010, [Online]. Available:

http://www.nrel.gov/wind/integrationdatasets/eastern/methodology.html (Accessd: 9/15/2010).

[125] J. Rogers, S. Fink, and K. Porter, "Examples of Wind Energy Curtailment Practices," National Renewable Energy Laboratory, Subcontract Report #NREL/SR-550-48737, 2010.

[126] E. Bitar, A. Giani, R. Rajagopal, D. Varagnolo, P. Khargonekar, K. Poolla, and P. Varaiya, "Optimal Contracts for Wind Power Producers in Electricity Markets," in *49th IEEE Conference on Decision and Control*, Atlanta, GA, 2010, pp. 1919-1926.

[127] Potomac Economics, "2010 State of the Market Report for the MISO Electricity Markets," Report, 2011.

[128] D. Q. Mayne, J. B. Rawlings, C. V. Rao, and P. O. M. Scokaert, "Constrained model predictive control: stability and optimality," *Automatica,* vol. 36, pp. 789-814, 2000.

[129] A. J. Lamadrid and T. D. Mount, "Integrating Wind Power: A Potential Role for Controllable Demand," in *7th Annual Carnegie Mellon Conference on the Electricity Industry*, Pittsburgh, PA, 2011.

[130]W. Katzenstein and J. Apt, "The cost of wind power variability," *Energy Policy,* vol. 51, pp. 233-243, 2012.

[131] J. Hetzer, D. Yu, and K. Bhattarai, "An Economic Dispatch Model Incorporating Wind Power," *IEEE Transactions on Energy Conversion,* vol. 23, pp. 603-611, 2008.

[132] F. Bouffard and F. Galiana, "Stochastic Security for Operations Planning With Significant Wind Power Generation," *IEEE Transactions on Power Systems,* vol. 23, pp. 306-316, 2008.

[133] V. Miranda and P. Hang, "Economic Dispatch Model with Fuzzy Wind Constraints and Attitudes of Dispatchers," *IEEE Transactions on Power Systems,* vol. 20, pp. 2143-2145, 2005.

[134] J. Matevosyan and L. Söder, "Minimization of imbalance cost trading wind power on the short-term power market," *IEEE Transactions on Power Systems,* vol. 21, pp. 1396-1404, 2006.

[135] P. Pinson, C. Chevallier, and G. Kariniotakis, "Trading wind generation from short-term probabilistic forecasts of wind power," *IEEE Transactions on Power Systems,* vol. 22, pp. 1148-1156 2007.

[136] E. Y. Bitar, R. Rajagopal, P. P. Khargonekar, K. Poolla, and P. Varaiya, "Bringing Wind Energy to Market," *IEEE Transactions on Power Systems,* vol. 27, pp. 1225-1235, 2012.

[137] M. D. Galus, R. La Fauci, and G. Andersson, "Investigating PHEV wind balancing capabilities using heuristics and model predictive control," in *IEEE Power and Energy Society General Meeting*, Minneapolis, MN, 2010, pp. 1-8.

[138] L. Xie, Y. Gu, A. Eskandari, and M. Ehsani, "Fast MPC-Based Coordination of Wind Power and Battery Energy Storage Systems," *Journal of Energy Engineering,* vol. 138, pp. 43-53, 2012.

[139] C. K. Ekman, "On the synergy between large electric vehicle fleet and high wind penetration – An analysis of the Danish case," *Renewable Energy,* vol. 36, pp. 546-553, 2011.

[140] Y. Gu and L. Xie, "Look-ahead coordination of wind energy and electric vehicles: A market-based approach," in *North American Power Symposium*, Arlington, TX, 2010, pp. 1-8.

[141] C.-T. Li, C. Ahn, H. Peng, and J. Sun, "Integration of Plug-In Electric Vehicle Charging and Wind Energy Scheduling on Electricity Grid," in *IEEE PES Conference on Innovative Smart Grid Technologies*, Washington DC, 2012, pp. 1-7.

[142] C.-T. Li, C. Ahn, H. Peng, and J. Sun, "Synergistic Control of Plug-In Vehicle Charging and Wind Power Scheduling," *IEEE Transactions on Power Systems,* 2012, accepted.

[143] T.-K. Lee, Z. Baraket, T. Gordon, and Z. Filipi, "Stochastic modeling for studies of real-world PHEV usage: driving schedules and daily temporal distributions," *IEEE Transactions on Vehicular Technology,* vol. 61, pp. 1493-1502, 2011.

[144] GM-Volt Website, Latest Chevy Volt Battery Pack and Generator Details and Clarifications, 2007, [Online]. Available: http://gm-volt.com/2007/08/29/latest-chevy-volt-battery-pack-and-generator-details-and-clarifications/ (Accessd: 5/13/2010).

[145] S. Hadley, "The Oak Ridge Competitive Electricity Dispatch (ORCED) Model," Oak Ridge National Laboratory, Report #ORNL/TM-2007/230, 2008.

[146] Electric Power Research Institute, "Environmental Assessment of Plug-In Hybrid Electric Vehicles, Volume 1: Nationwide Greenhouse Gas Emissions," Report #1015325, 2007.

[147] P. Balducci, "Plug-in Hybrid Electric Vehicle Market Penetration Scenarios," Pacific Northwest National Laboratory, Report #PNNL-17441, 2008.

[148] The World Bank, Motor vehicles (per 1,000 people), 2012, [Online]. Available: http://data.worldbank.org/indicator/IS.VEH.NVEH.P3 (Accessd: 4/30/2013).

[149] The World Bank, Energy use (kg of oil equivalent per capita), 2012, [Online]. Available: http://data.worldbank.org/indicator/EG.USE.PCAP.KG.OE (Accessd: 4/30/2013).

[150] D. Weisser, "A guide to life-cycle greenhouse gas (GHG) emissions from electric supply technologies," *Energy,* vol. 32, pp. 1543-1559, 2007.

[151] B. Lane, "Life Cycle Assessment of Vehicle Fuels and Technologies," Ecolane Transport Consultancy, Report, 2006.

[152] C. Samaras and K. Meisterling, "Life Cycle Assessment of Greenhouse Gas Emissions from Plug-in Hybrid Vehicles: Implications for Policy," *Environmental Science & Technology,* vol. 42, pp. 3170-3176, 2008.

[153] A. Bandivadekar, K. Bodek, L. Cheah, C. Evans, T. Groode, J. Heywood, E. Kasseris, M. Kromer, and M. Weiss, "On the Road in 2035," Laboratory for Energy and the Environment, Massachusetts Institute of Technology, Report #LFEE 2008-05 RP, 2008.

[154] P. Baptista, M. Tomás, and C. Silva, "Plug-in hybrid fuel cell vehicles market penetration scenarios," *International Journal of Hydrogen Energy,* vol. 35, pp. 10024-10030, 2010.

[155] M. Kintner-Meyer, K. Schneider, and R. Pratt, "Impacts Assessment of Plug-In Hybrid Vehicles on Electric Utilities and Regional U.S. Power Grids—Part 1: Technical Analysis," Pacific Northwest National Laboratory (PNNL), Report, 2007.

[156] R. Sioshansi, R. Fagiani, and V. Marano, "Cost and emissions impacts of plug-in hybrid vehicles on the Ohio power system," *Energy Policy,* vol. 38, pp. 6703-6712, 2010.

[157] A. Y. Saber and G. K. Venayagamoorthy, "Plug-in Vehicles and Renewable Energy Sources for Cost and Emission Reductions," *IEEE Transactions on Industrial Electronics,* vol. 58, pp. 1229-1238, 2011.

[158] U.S. Energy Information Administration, "Annual Energy Outlook 2011," Report #DOE/EIA-0383, 2011.

[159] P. Ekins, "European environmental taxes and charges: recent experience, issues and trends," *Ecological Economics,* vol. 31, pp. 39-62, 1999.

[160] B. Bosquet, "Environmental tax reform: does it work? A survey of the empirical evidence," *Ecological Economics,* vol. 34, pp. 19-32, 2000.

[161] F. Scrimgeour, L. Oxley, and K. Fatai, "Reducing carbon emissions? The relative effectiveness of different types of environmental tax: the case of New Zealand," *Environmental Modelling & Software,* vol. 20, pp. 1439-1448, 2005.

[162] M. Wier, K. Birr-Pedersen, H. K. Jacobsen, and J. Klok, "Are CO2 taxes regressive? Evidence from the Danish experience," *Ecological Economics,* vol. 52, pp. 239-251, 2005.

[163] P. Ekins and T. Baker, "Carbon Taxes and Carbon Emissions Trading," *Journal of Economic Surveys,* vol. 15, pp. 325-376, 2001.

[164] G. Metcalf, "Designing a Carbon Tax to Reduce U.S. Greenhouse Gas Emissions," *Review of Environmental Economics and Policy,* vol. 3, pp. 63-83, January 1, 2009 2009.

[165] G. Metcalf, "A Proposal for a U.S. Carbon Tax Swap: An Equitable Tax Reform to Address Global Climate Change," Hamilton Project, Brookings Institute,, Discussion Paper 2007-12, 2007.

[166] P. Ekins, H. Pollitt, P. Summerton, and U. Chewpreecha, "Increasing carbon and material productivity through environmental tax reform," *Energy Policy,* vol. 42, pp. 365-376, 2012.

[167] W. Nordhaus, "An Optimal Transition Path for Controlling Greenhouse Gases," *Science,* vol. 258, pp. 1315-1319, November 20, 1992 1992.

[168] A. Ulph and D. Ulph, "The Optimal Time Path of a Carbon Tax," *Oxford Economic Papers,* vol. 46, pp. 857-68, 1994.

[169] A. Bovenberg and L. Goulder, "Optimal Environmental Taxation in the Presence of Other Taxes: General- Equilibrium Analyses," *The American Economic Review,* vol. 86, pp. 985-1000, 1996.

[170] M. T. Hogue, "A Review of the Costs of Nuclear Power Generation," Bureau of Economic and Business Research, University of Utah, Report, 2012.

[171] International Energy Agency (IEA)/OECD Nuclear Energy Agency (NEA), "Projected Costs of Generating Electricity - 2010 Edition," Report, 2010.

[172] C.-T. Li, H. Peng, and J. Sun, "Reducing CO_2 emissions on the electric grid through a carbon disincentive policy," *Energy Policy,* 2013, accepted.

[173] J. Kelly, G. Keoleian, and I. Hiskens, "Comparison of economic and capacity factor electricity dispatch models to examine pollutant implications of changes in demand," *Journal of Cleaner Production,* under review.

[174] The White House, Administration Announces U.S. Emission Target for Copenhagen, 2009, [Online]. Available: http://www.whitehouse.gov/the-press-office/president-attend-copenhagen-climate-talks (Accessd: 1/4/2012).

[175] H. Lund, "Large-scale integration of wind power into different energy systems," *Energy,* vol. 30, pp. 2402-2412, 2005.

[176] H. Lund, "Large-scale integration of optimal combinations of PV, wind and wave power into the electricity supply," *Renewable Energy,* vol. 31, pp. 503-515, 2006.

[177] H. Lund and B. V. Mathiesen, "Energy system analysis of 100% renewable energy systems—The case of Denmark in years 2030 and 2050," *Energy,* vol. 34, pp. 524-531, 2009.

[178] R. Doherty, H. Outhred, and M. O'Malley, "Establishing the role that wind generation may have in future generation portfolios," *IEEE Transactions on Power Systems,* vol. 21, pp. 1415-1422, 2006.

[179] K. Karlsson and P. Meibom, "Optimal investment paths for future renewable based energy systems—Using the optimisation model Balmorel," *International Journal of Hydrogen Energy,* vol. 33, pp. 1777-1787, 2008.

[180] J. Kiviluoma and P. Meibom, "Influence of wind power, plug-in electric vehicles, and heat storages on power system investments," *Energy,* vol. 35, pp. 1244-1255, 2010.

[181] W. El-Khattam, Y. G. Hegazy, and M. M. A. Salama, "An integrated distributed generation optimization model for distribution system planning," *IEEE Transactions on Power Systems,* vol. 20, pp. 1158-1165, 2005.

[182] H. Li, R. Nalim, and P. A. Haldi, "Thermal-economic optimization of a distributed multi-generation energy system—A case study of Beijing," *Applied Thermal Engineering,* vol. 26, pp. 709-719, 2006.

[183] J.-J. Wang, Y.-Y. Jing, and C.-F. Zhang, "Optimization of capacity and operation for CCHP system by genetic algorithm," *Applied Energy,* vol. 87, pp. 1325-1335, 2010.

[184] J. N. Swisher, G. d. M. Jannuzzi, and R. Y. Redlinger, *Tools and Methods for Integrated Resource Planning*. London: Earth Print, 1997.

[185] G. Chicco and P. Mancarella, "Distributed multi-generation: A comprehensive view," *Renewable and Sustainable Energy Reviews,* vol. 13, pp. 535-551, 2009.

[186] Lazard Ltd., "Levelized Cost of Energy Analysis - Version 5.0," Report, 2011.

[187] S. B. Darling, F. You, T. Veselka, and A. Velosa, "Assumptions and the levelized cost of energy for photovoltaics," *Energy & Environmental Science,* vol. 4, pp. 3133-3139, 2011.

[188] K. Cory and P. Schwabe, "Wind Levelized Cost of Energy: A Comparison of Technical and Financing Input Variables," National Renewable Energy Laboratory, Report #NREL/TP-6A2-46671, 2009.

[189] R. Wiser, E. Lantz, M. Bolinger, and M. Hand, "Recent Developments in the Levelized Cost of Energy from U.S. Wind Power Projects," National Renewable Energy Laboratory, Report, 2012.

[190] K. Branker, M. J. M. Pathak, and J. M. Pearce, "A review of solar photovoltaic levelized cost of electricity," *Renewable and Sustainable Energy Reviews,* vol. 15, pp. 4470-4482, 2011.

[191] I. F. Roth and L. L. Ambs, "Incorporating externalities into a full cost approach to electric power generation life-cycle costing," *Energy,* vol. 29, pp. 2125-2144, 2004.

[192] F. A. Roques, D. M. Newbery, and W. J. Nuttall, "Investment Incentives and Electricity Market Design: the British Experience," *Review of Network Economics,* vol. 4, pp. 93-128, 2005.

[193] Y. Du and J. E. Parsons, "Update on the Cost of Nuclear Power," Center for Energy and Environmental Policy Research (CEEPR), Report # 09-004, 2009.

[194] U.S. Nuclear Regulatory Commission, Backgrounder on Decommissioning Nuclear Power Plants, 2013, [Online]. Available: http://www.nrc.gov/reading-rm/doc-collections/fact-sheets/decommissioning.html (Accessd: 4/23/2013).

[195] J. M. Deutch, E. J. Moniz, S. Ansolabehere, E. M. Driscoll, P. E. Gray, J. P. Holdren, P. L. Joskow, R. K. Lester, N. E. Todreas, E. S. Beckjord, N. Hottle, C. Jones, and E. Parent, "The Future of Nuclear Power," Massachusetts Institute of Technology, Report, 2003.

[196] U.S. Energy Information Administration, "Assumptions to the Annual Energy Outlook 2011," Report #DOE/EIA-0554, 2011.

[197] J. M. Deutch, C. W. Forsberg, A. C. Kadak, M. S. Kazimi, E. J. Moniz, J. E. Parsons, Y. Du, and L. Pierpoint, "Update of the MIT 2003 Future of Nuclear Power," Massachusetts Institute of Technology, Report, 2009.

[198] Open Energy Information, Transparent Cost Database, 2013, [Online]. Available: http://en.openei.org/apps/TCDB/ (Accessd: 4/26/2013).

[199] IEEE PES Distribution Test Feeders, 2012, [Online]. Available: http://www.ewh.ieee.org/soc/pes/dsacom/testfeeders/index.html (Accessd: 4/20/2013).

[200] Power Systems Test Case Archive, 1999, [Online]. Available: http://www.ee.washington.edu/research/pstca/ (Accessd: 4/20/2013).

[201] R. E. Bellman, *Dynamic Programming*. New Jersey: Princeton University Press, 1957.

[202] D. E. Kirk, *Optimal Control Theory: An Indroduction*. New Jersy: Prentice-Hall, 1970.